

DESIGN, TESTING, AND VALIDATION OF AN LC/MS COMPATIBLE CELL  
FOR MEASURING TRANSDERMAL DIFFUSION

By

LUCAS JAMES UTLEY

A DISSERTATION PRESENTED TO THE GRADUATE SCHOOL  
OF THE UNIVERSITY OF FLORIDA IN PARTIAL FULFILLMENT  
OF THE REQUIREMENTS FOR THE DEGREE OF  
DOCTOR OF PHILOSOPHY

UNIVERSITY OF FLORIDA

2001

Copyright 2001

by

Lucas James Utley

This is dedicated to my parents, James and Dolores, who set me on my scientific journey so many years ago, and to my wife Kristen, for her unwavering support and love.

## ACKNOWLEDGMENTS

This work would not have been possible without the aid and support of a number of individuals. It goes without saying that lacking the assistance of Ian Tebbett, my major advisor, this work would not have reached completion. He has provided opportunities to me that are generally not available to most graduate students. I am also deeply indebted to Ken Sloan for his freely given advice and assistance on all things dermal. His expertise and knowledge in this field have proven to be invaluable. Nancy Szabo provided useful criticism throughout this project and lent valuable experience to a number of aspects. The diffusion cell manufacturers Permegear and Glassblowers.com have graciously permitted the use of several images in this document. The pictures of the MIMS probe and of the diffusion cell prototypes were produced by Shawn Toffolo. Finally I must thank my wife, Kristen, without whose support I would not have made it this far.

## TABLE OF CONTENTS

	<u>page</u>
ACKNOWLEDGMENTS .....	iv
LIST OF TABLES .....	vii
LIST OF FIGURES .....	viii
ABSTRACT .....	xi
INTRODUCTION .....	1
Background .....	4
Previous Diffusion Cells .....	4
Detection Methods .....	14
Predictive Models .....	21
Potential of LC/MS .....	33
Statement of the Problem .....	42
Hypothesis .....	43
Specific Aims and Rationale .....	43
MATERIALS AND METHODS .....	45
Specific Aim One: Prototype Design .....	45
Membranes and Chemicals .....	45
Instrumentation .....	45
MIMS Probe .....	46
First Prototype .....	49
Second Prototype .....	50
Third Prototype .....	53
Specific Aim Two: Validation Testing .....	54
Membranes and Chemicals .....	54
Instrument Setup .....	55
Effect of Ethanol on Permeability .....	58
LC/MS Diffusion Cell Validation .....	59
Franz Cell .....	60
Hairless Mouse Skin, LC/MS Cell .....	60
Specific Aim Three: Applications .....	61
Membranes and Chemicals .....	61
Mixture of Caffeine and Theophylline .....	62

DEET and Permethrin.....	62
Testosterone .....	63
RESULTS.....	64
Specific Aim 1 .....	64
MIMS Probe.....	64
First Prototype.....	64
Second Prototype .....	66
Specific Aim 2 .....	70
Solubility Values.....	70
Effect of Ethanol on Permeation.....	71
Validation Test: LC/MS Cell.....	73
Validation Test: Franz Cell.....	74
LC/MS Validation: Mouse Skin. ....	76
Specific Aim 3 .....	78
Chemical Mixture: Caffeine and Theophylline .....	78
Testosterone .....	79
Chemical Mixture: DEET and Permethrin .....	80
DISCUSSION.....	83
Specific Aim One: Cell Construction .....	83
Membranes and Probe Chemicals.....	83
Prototype Construction .....	85
MIMS probe .....	85
First Prototype.....	87
Second Prototype .....	90
Specific Aim Two: Validation Testing.....	92
PDMS.....	93
Hairless Mouse Skin .....	97
Specific Aim Three: Applications .....	98
Mixture of Caffeine and Theophylline .....	99
DEET and Permethrin.....	100
Testosterone .....	101
Shortcomings .....	103
Application Issues.....	105
Summary .....	106
APPENDIX A: STANDARD CURVES .....	108
APPENDIX B: ENLARGEMENT OF FIGURES .....	109
LIST OF REFERENCES.....	119
BIOGRAPHICAL SKETCH .....	126

## LIST OF TABLES

<u>Table</u>	<u>Page</u>
3-1: Solubility vs. carbon number for esters of 4-hydroxybenzoic acid. ....	70
3-2: Comparison of caffeine flux through PDMS membranes . ....	72
3-3: Flux values for members of the 4-hydroxybenzoate series. ....	74
3-4: Flux values: Franz vs. LC/MS. ....	75
3-5: Hairless mouse skin flux values. ....	78

## LIST OF FIGURES

<u>Figure</u>	<u>Page</u>
1:1: Ussing cell.....	5
1-2: Flynn cell.....	6
1-3: Horizontal diffusion cell.....	7
1-4: Franz diffusion cell.....	8
1-5: Bronaugh cell.....	12
1-6: Quadrupole stability diagram.....	35
1-7: Ion trap schematic.....	37
1-8: Ion trap stability diagram.....	37
1-9: ESI probe assembly.....	40
1-10: APCI probe assembly.....	40
2-1: MIMS probe.....	47
2-2: MIMS schematic. Original instrumentation schematic for the MIMS probe.....	48
2-3: MIMS diffusion cell. Schematic for using MIMS probe as a diffusion cell.....	48
2-4: Prototype diffusion cell.....	50
2-5: Second prototype sketch.....	51
2-6: Second prototype photograph.....	52
2-7: Second prototype schematic.....	53
2-8: Third prototype photograph.....	54
2-9: Third prototype schematic.....	56



2-10: Quantitation.....	58
2-11: Ester series.....	59
3-1: Representative flux chromatograms; first prototype.....	65
3-2: Flux chromatograms: second prototype.....	67
3-3: Chamber problem, second prototype.....	68
3-4: Testosterone flux chromatogram: second prototype.....	69
3-5: Nicotine flux chromatogram: second prototype.....	69
3-6: Water solubility of the 4-hydroxybenzoate ester series vs. carbon number.....	71
3-7: Vehicle solubility of the 4-hydroxybenzoate ester series vs. carbon number.....	71
3-8: Effect of water vs. ethanol/water pretreatment on caffeine flux through PDMS.....	73
3-9: Flux of the 4-hydroxybenzoate ester series through PDMS membranes.....	74
3-10: Plot of paraben series fluxes.....	75
3-11: Comparison of flux values from Franz (static) and LC/MS diffusion cells.....	76
3-12: Repeated applications of caffeine to hairless mouse skin.....	77
3-13: LC/MS diffusion cell, PDMS vs. hairless mouse skin.....	77
3-14: Flux of a caffeine/theophylline mixture.....	79
3-15: Testosterone flux through hairless mouse skin.....	80
3-16: Flux of DEET + m/z 383 molecule.....	81
3-17: Possible permethrin solvolysis mechanism.....	82
4-1: Melting points for 4-hydroxybenzoic acid esters.....	97
A-1: Methyl paraben standard curve generated on the LCQ.....	108
A-2: Ethyl paraben standard curve generated on the LCQ.....	108
B-1: Enlargement of figure 3-1 A.....	110
B-2: Enlargement of figure 3-1 B.....	111
B-3: Enlargement of figure 3-2 A. Methyl 4-hydroxybenzoate.....	112

B-4: Enlargement of figure 3-2 B. Ethyl 4-hydroxybenzoate.....	113
B-5: Enlargement of figure 3-4. Testosterone.....	114
B-6: Enlargement of figure 3-4. Nicotine.....	115
B-7: Enlargement of figure 3-14. Caffeine and theophylline.....	116
B-8: Enlargement of figure 3-15. Testosterone.....	117
B-9: Enlargement of figure 3-16. DEET and permethrin.....	118

Abstract of Dissertation Presented to the Graduate School  
of the University of Florida in Partial Fulfillment of the  
Requirements for the Degree of Doctor of Philosophy

DESIGN, TESTING, AND VALIDATION OF AN LC/MS COMPATIBLE CELL FOR  
MEASURING TRANSDERMAL DIFFUSION

By

Lucas James Utley

August 2001

Chairman: Ian Tebbett  
Major Department: Medicinal Chemistry

The transdermal diffusion of drugs and potential toxicants is presently measured using two compartment diffusion cells. Solutes are typically monitored by absorption spectroscopy. This method is unable to detect molecules that do not absorb strongly in the UV/visible region of the spectrum, nor is it able to simultaneously determine the flux of multiple, structurally related chemicals. A diffusion cell coupled to a liquid chromatography mass spectrometer (LC/MS) is described here that is capable of overcoming the shortcomings inherent in presently available devices.

A flow through diffusion cell compatible with a Finnigan/MAT LCQ was constructed and tested vs. a traditional Franz diffusion cell. The fluxes of four esters of 4-hydroxybenzoic acid (methyl through n-butyl) were measured through silicone membranes using the LC/MS and Franz diffusion cells. The LC/MS diffusion cell replicated the Franz cell values, demonstrating its equivalence to the traditional technique. The fluxes of the first three members of the series were determined across

hairless mouse skin using the LC/MS cell. Those values were greater than those for silicone membranes, but the compound rank order was preserved. The fluxes of an extended 4-hydroxybenzoate series through silicone membranes were measured to fully characterize the performance of the device. Flux values demonstrated a parabolic nature, peaking at the amyl ester, before declining.

The ability of the LC/MS cell to measure the transdermal flux of compounds and mixtures that have traditionally proven difficult to analyze using standard methods was also demonstrated. The flux of testosterone, a molecule difficult to detect by absorption spectroscopy, was easily measured when applied to mouse skin in an ethanol:water vehicle. The measured flux was  $0.16 \text{ mg/cm}^2 \text{ h}$ .

The fluxes through hairless mouse skin of caffeine and theophylline, mixed in solution, were also determined. The absorbance spectra of these two related chemicals are essentially identical, and it would not be possible to distinguish between the two using standard techniques. The fluxes of caffeine and theophylline were measured to be  $0.07$  and  $0.05 \text{ mg/cm}^2 \text{ h}$ , respectively.

Preliminary work investigating the enhancement of n-n diethyltoluamide (DEET) on the flux of the pesticide permethrin through skin highlighted the ability of the LC/MS diffusion cell to positively identify a molecular structure. Permethrin was co-applied with DEET in an alcohol vehicle to hairless mouse skin. It was found to undergo solvolysis prior to penetrating skin, with the loss of two chlorine atoms. The standard technique of radio-labeling one of the carbon atoms in permethrin's structure would not have detected this event.

The design, testing and operation of a LC/MS compatible diffusion cell has been described here. It is not intended to replace but rather supplement presently available diffusion cells. This device broadens the types of chemicals and situations to which transdermal studies may be applied, and enhances the quality of the data that can be generated.

## CHAPTER 1 INTRODUCTION

The field of trans-dermal research has typically been devoted to the study of cosmetics and of dermally applied pharmaceuticals. In both cases the aim has been to evaluate the penetration of skin by a single compound of interest. The transdermal route of delivery is presently utilized in the delivery of such various drugs as steroids, vasodilators, opiates, and anti-muscarinics. There is ongoing research into the possibility of applying transdermal delivery devices to other problems, such as the following: the delivery of non-steroidal anti-inflammatory drugs directly to the site of injury, thus avoiding gastric irritation; methods of providing insulin dependent diabetics a way of reducing the need for daily injections; the elimination of side effects associated with dosing spikes seen during hormone supplementation therapy.<sup>1,2</sup> This has led to the development of a number of new transdermal delivery devices, including patches and gels, as well as increased use of more traditional devices such as creams and ointments. The clinical advantages of transdermal delivery devices make them appealing for a number of reasons including prolonged delivery of a drug at a constant rate; avoidance of first pass metabolism; avoidance of problems with the gastrointestinal route, such as drug breakdown or gastric irritation; easy termination of delivery; non-invasiveness; suitability for unconscious patients, or for those who cannot take drugs orally.<sup>2</sup>

As the range of drugs being investigated for possible delivery across the skin increases, so too do the number and variety of delivery mechanisms being investigated. Present FDA guidelines require the testing of both new drugs and new commercial formulations. When the new formulation is a transdermal delivery device, it is often designed to increase the penetration of skin by the drug. This may involve the use of penetration enhancers such as DMSO, laurocapram, or fatty acid esters. These chemicals alter the nature of the skin so that a drug can cross more readily; however, they are far from selective and can increase the flux of unwanted chemicals. Several penetration enhancers, such as DMSO, short chain alcohols, or soaps,<sup>3</sup> (reviewed in Scheuplein and Blank<sup>4</sup>), permanently alter the skin while enhancing flux, often resulting in localized irritation, which limits their use. When the device is a patch, adhesives must be incorporated to attach the device to the skin, as well as a matrix in which to contain the drug and control its release. Gels, ointments and creams may contain preservatives, stabilizers or emollients to keep the drug in suspension. In these cases, there is a valid concern as to what other chemicals may be crossing the skin from the device or whether the device may increase the absorption of chemicals applied subsequent to or in conjunction with the use of the device.

There has also been renewed interest in transdermal research from the field of environmental risk analysis. Questions have arisen regarding the extent to which transdermal penetration of environmental contaminants contributes to whole body dosing of some toxicants.<sup>5,6</sup> Scenarios include flux of chemical from contaminated soil when applied to skin, especially in areas where children play; whole body

exposure to pesticides during spray application; repeated exposure to toxicants dissolved in organic or aqueous vehicles, particularly when applied to clothing. In contrast to cosmetics and pharmaceuticals, environmental contaminants may be present in matrices whose components, such as organic solvents, interact with and change the permeability of skin; they may also be present as a class of closely related compounds (i.e., PCBs, Aroclors, etc.) that can act as co-solvents, enhancing each other's fluxes. In some instances, several chemicals may exert a toxic effect, with one or more of them acting as both toxicant and penetration enhancer/solvent.

Theoretical models can describe transdermal flux fairly well and several have a good deal of predictive power when applied to new chemicals.<sup>7-10</sup> These models require data about the nature of the solvent that the chemical is dissolved in when it is applied to skin. In general the predictive power is strongest when the chemical/solvent system closely resembles those used in the construction of the model. In cases of environmental contamination, the composition of solvent and co-solute may be unique to a given geographical area and can pose problems for predictive models; the number of environmental variables affecting dermal penetration can rapidly exceed the predictive capacity of a model system.<sup>11</sup>

A need presently exists for methods to evaluate the transdermal flux of pharmaceuticals and environmental contaminants from real world matrices. There does not presently exist a device or method that can simultaneously evaluate the penetration of the compound of interest as well as possible co-diffusants in real time.



## Background

### Previous Diffusion Cells

The dermal permeability of chemicals has traditionally been evaluated using diffusion cells. Briefly, a diffusion cell consists of two compartments separated by a membrane, typically excised animal skin. A donor phase, composed of a solvent containing the chemical of interest, is applied to one compartment and a receptor phase of pure solvent, which may or may not be different from the donor phase, is placed in the other. The receptor and often the donor phases are stirred, while being maintained at a constant temperature; the orientation of the cell can be either vertical or horizontal. The receptor phase is sampled at either discrete intervals or may be continuously monitored via a detector. Flux is calculated by plotting the cumulative solute in the receptor phase vs. time and taking the slope of that line; this value is normalized to a single unit of surface area.

Horizontal cells. Perhaps the earliest transdermal diffusion device was described by Han Ussing in 1948.<sup>12</sup> Ussing investigated the nature of ion active transport in frogs. He described a diffusion cell for the purpose of measuring the flux of ions across excised frog skin. Ussing's cell, depicted in figure 1-1, consists of two glass half cells clamped onto a sheet of excised frog skin; the half cells feature ports for sampling and recirculation of the donor and receptor phases. It is designed to keep frog skin in a viable state since Ussing was studying active transport mechanisms; as such, there are provisions made for providing dissolved oxygen and nutrients, features not required when passive transport is studied. Changes in membrane potential, as well as Geiger counting of labeled species, were used to determine flux. Ussing's cell is the basis from which modern horizontal cells are derived.

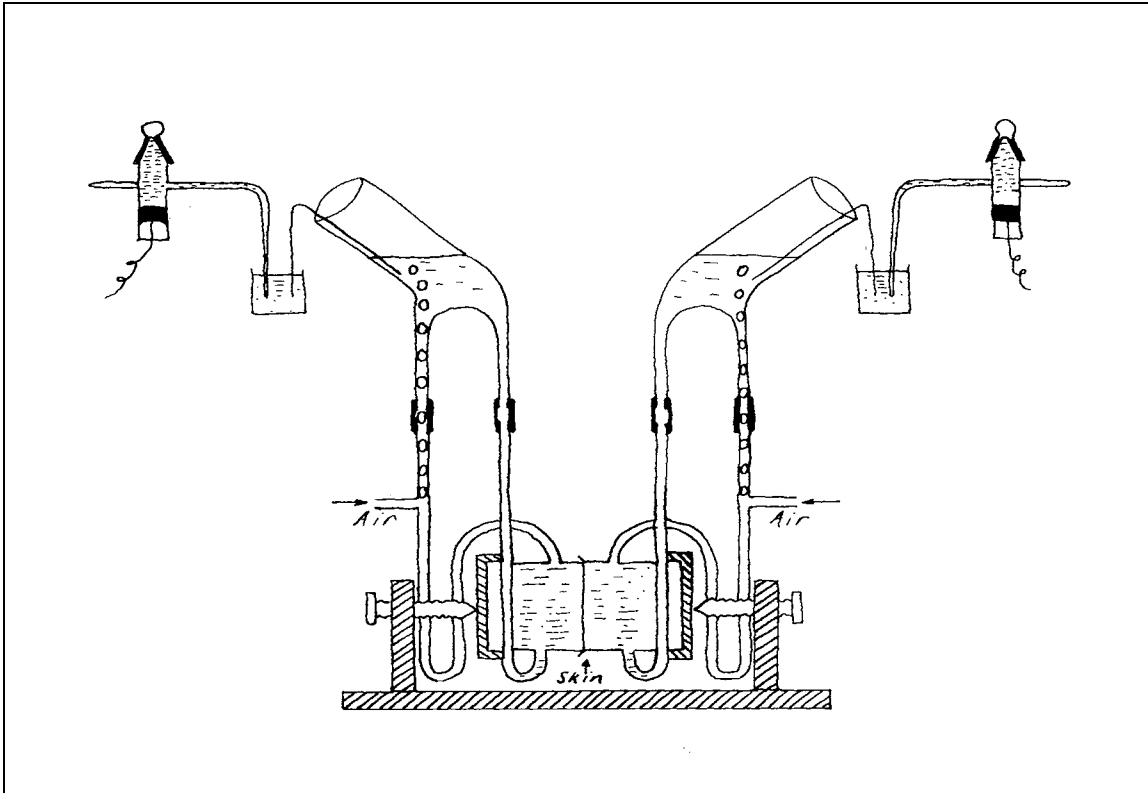


Figure 1:1: Ussing cell. Reproduced from Ussing.<sup>12</sup>

A variation of Ussing's design was described by Flynn and Smith,<sup>13</sup> in an attempt to improve on the available designs of the day. The original device, constructed of two stainless steel half-cells, is depicted in figure 1-2. The membrane is clamped vertically between the donor and receptor phase compartments; unlike Ussing's design, both compartments are thermo-regulated and stirred. The original device utilized a side-mounted impeller so that stirring is in the plane of, rather than perpendicular to, the membrane; this feature was later dispensed with, in favor of conventional magnetic stir-bars. A spectrophotometer equipped with a flow through absorbance cell was used for detection. The original device was validated using p-aminoacetophenone dissolved in distilled water.<sup>13</sup> Polydimethylsiloxane (PDMS)

membranes were used in place of skin. The device was evaluated over a range of temperatures, stirring speeds and membrane thickness.

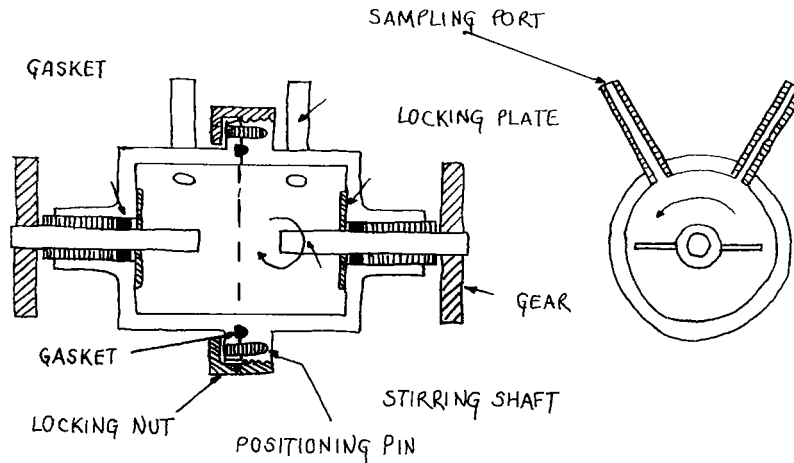


Figure 1-2: Flynn cell. Reproduced from Flynn and Smith.<sup>13</sup>

A horizontal cell fabricated of Pyrex glass (figure 1-3) was described by Chien and co-workers.<sup>14</sup> While similar to the Flynn design, it possesses several improvements. The donor and receptor phase chambers are independently thermostated using water jackets. This gives the experimenter greater flexibility in operating conditions, and is easier to manipulate than the external water bath used by Flynn. The Chien design can utilize smaller sections of skin; this is especially a concern when human skin is used, as only a small amount of tissue may be available.

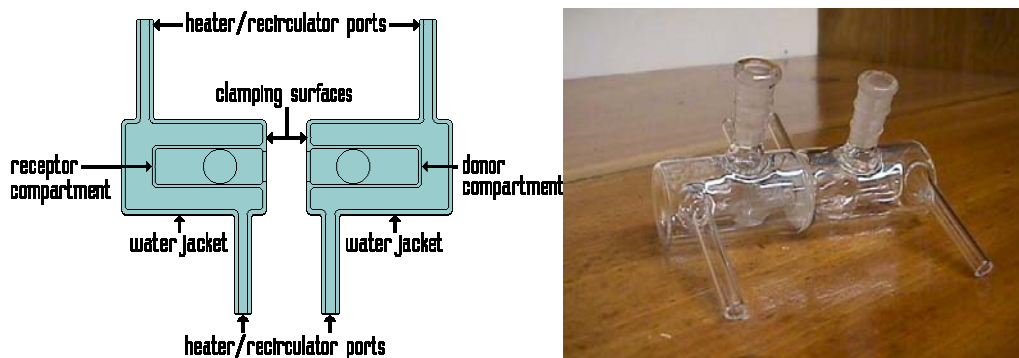


Figure 1-3: Horizontal diffusion cell. Illustration reproduced with permission from [www.permegear.com](http://www.permegear.com) (PermeGear Corp.). Photograph reproduced with permission from [GLASSBLOWERS.com](http://GLASSBLOWERS.com) Inc.

Horizontal cells can be cumbersome to manipulate during solvent changes, especially with regards to removing air bubbles from the solvent chambers. A problem that has been noted with this design, when mammalian skin is used as the membrane, is the excessive hydration that results from immersion in aqueous solvents. This is a state not normally seen in dermal applications and can result in the overestimation of dermal flux. The horizontal cell is difficult if not impossible to use with compounds that are applied as a thin layer, as opposed to a suspension.

Vertical cells. The cell that enjoys the widest present day use was designed by Thomas Franz,<sup>15</sup> in an attempt to correlate *in vitro* flux data with that from *in vivo* experiments. Franz chose to replicate earlier *in vivo* work by Feldman and Maibach,<sup>16</sup> in which  $^{14}\text{C}$  labeled chemicals were applied to the skin of human volunteers and flux was evaluated by the appearance of radio-label in the subject's urine. In his paper, Franz describes the construction of a vertical diffusion cell depicted in figure 1-4. The cell can be thermo-regulated by the use of a water-jacket, and the receptor phase is stirred by a Teflon coated stir-bar; the donor phase is left

unstirred. For determining diffusion kinetics, the entire receptor phase was removed at regular intervals (typically 1-2 hours) over the course of several days. Total absorption experiments were performed where the receptor phase was sampled only once at 24 hours after application. The receptor phases were gelled prior to scintillation counting. Franz reported good correlations between *in vivo* and *in vitro* experiments for 11 of 12 compounds examined; the one case of disagreement may have been due to an error in the *in vivo* experiment for that chemical.

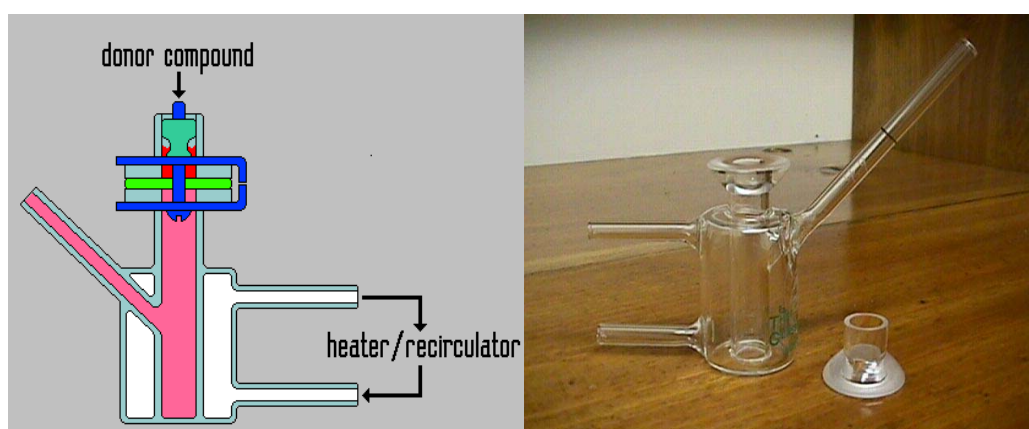


Figure 1-4: Franz diffusion cell. Illustration reproduced with permission from [www.permeagear.com](http://www.permeagear.com) (Permeagear Corp.). Photograph reproduced with permission from [GLASSBLOWERS.com](http://GLASSBLOWERS.com) Inc.

The Franz cell mimics dermal applications in its orientation and in the manner that chemicals may be applied to skin. The design lends itself well to applications such as determining the flux from ointments applied to skin in a thin layer and does not create the situation of over-hydrating the skin that can occur with horizontal designs. Skin may be left open to the air, or occluded. The design does possess some shortcomings, especially when kinetic data are being gathered. The vertical orientation, while easy to use, limits the ability to stir the donor phase without

evaporation from the upper chamber; this is problematic for rapidly settling suspensions and volatile solvents in the donor phase. There has been some suggestion that, for solutes which move rapidly within the membrane, the lack of stirring could result in the formation of boundary layers in the donor phase. Also, only the receptor phase is effectively thermostated, leading to the formation of a temperature gradient across the cell. An alternative design<sup>17</sup> purportedly improves the thermoregulation of the Franz cell, while maintaining its overall design.

Shortcomings of diffusion cells. A number of other researchers<sup>4,18</sup> have described the use of diffusion cells, often custom made for a given application, of varying design. Most follow a common theme: donor and receptor phase chambers are clamped onto a section of skin and the chambers are manually sampled. The chambers may or may not be stirred. While of good use, and providing valid, comparable data, these designs have not been widely used outside of a few research groups.

One of the major drawbacks of the available diffusion cell designs has been the need for manual sampling. For experiments involving slowly diffusing compounds, or those with a low solubility in the receptor phase, multiple sampling may be required over the course of several days. This can be taxing for a single researcher, to say the least. The most commonly used solution of splitting the sampling duties among several people introduces a potential source of error arising from differences in sample handling technique and is no more convenient when samples must be taken throughout the night. The delay inherent between the start of an experiment and the final data analysis means that problems early in the experiment

may not be detected until the experiment is complete. Also, with a sampling interval that is greater in time than the duration of some diffusion events (i.e., lag time), some events may be unobserved.

Two main approaches have been taken to overcome the difficulties with manual sampling. The first is to couple the cell to a fraction collector, substituting a machine for a human researcher; some mechanism for replenishing the receptor phase is usually added. This has the advantage that samples can be collected over a long period of time and with a short interval between sampling, thus allowing the observation of short duration events, such as the lag time to steady state. The second approach involves directing the cell's effluent directly into a detector, typically a UV absorbance device. Such an approach was first described by Flynn and Smith<sup>13</sup> in conjunction with their aforementioned cell design. Steady state was reported as absorbance units per minute. A hybrid of the two approaches is described by Flynn and Yalkowsky,<sup>19</sup> again using the previously described cell design. In their design, a horizontal diffusion cell's effluent is directed first through a spectrophotometer flow cell, and then to a fraction collector for analysis by GC. The donor phase is maintained close to saturated conditions by constantly recirculating it through a reservoir containing excess undissolved solute.

One problem with adapting classical cell designs, such as the Ussing and Franz cells, to flow through detection is the relatively large volume of the receptor chamber, especially compared to the sampling rate. The receptor phase must be well stirred so as to ensure rapid mixing and accurate sampling. The formation of concentration gradients may otherwise result in variations in measured concentration,

depending on where samples are taken in the chamber. In some instances, the receptor phase stream may end up separated from the diffusion layer by the formation of eddy currents. The receptor phase may move through the chamber with little interaction with the membrane; the transfer between the diffusion layer and the receptor solvent stream is then what is measured. Large receptor phase chambers also pose a problem of dilution, especially early in experiments as steady state is approached. If the receptor phase chamber is large compared to the sampling rate, the solute may be diluted below the limit of detection for the analytical method chosen. For these reasons new devices, with small volume receptor phase chambers, have been designed to allow operation in a flow through manner.

Flow-through cells. Bronaugh and Stewart<sup>20</sup> described a cell (figure 1-5) with a flow-through receptor phase chamber. Their device consisted of a Teflon block into which wells were milled. A lip machined into the edge of the well and just above its bottom supported the membrane and formed the receptor phase chamber. Receptor phase was channeled through the lower chamber via a side-arm inlet whose diameter was equal to the height of the chamber, in order to facilitate mixing; no other provision was made for the stirring of the chambers. A Teflon cap screwed into the holding block to secure the skin; a free turning ring in the cap prevented twisting of the skin. In their work, the receptor phase was collected as fractions before analysis via scintillation counting.<sup>20</sup>



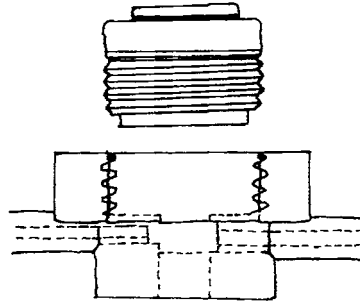


Figure 1-5: Bronaugh cell.

Bronaugh and Stewart performed a series of experiments to both define the operating parameters of their device and compare its performance against static designs in current use. The first parameter to be defined was the effect of flow rate on diffusion. This was determined by monitoring the flux of tritiated water through hairless rat skin. A lower limit of 1 ml/h was found with no difference seen at higher flow rates up to 40 ml/h; the flux values for 1, 5 and 40 ml/h were comparable, but there was higher variability seen in the 1 ml/h data. Total absorption values for tritiated water were comparable when measured with the Bronaugh and static cell designs. Flux values for [1,2-<sup>3</sup>H] cortisone and [7-<sup>14</sup>C] benzoic acid (applied in an acetone vehicle) were measured using flow-through and static cells; the values were found to be comparable for both chemicals. Finally, the flow-through cell was used to determine flux values for 3-[3-<sup>14</sup>C] phenyl-2-propenyl 2 aminobenzoate (cinnamyl anthranilate). Due to its low water solubility, cinnamyl anthranilate had proven difficult to measure using static cells; it had been found to be very difficult to maintain sink conditions in a static unit. The flow-through design was found to

significantly increase the flux of cinnamyl anthranilate compared to the static cell when normal saline was used as the receptor phase. The researchers speculated that this was due to increased partitioning of the solute from the skin as sink conditions were more readily maintained with the flow-through cell. When 6% PEG-20 was added to the receptor phase, the solubility of cinnamyl anthranilate increased and no difference in flux values could be seen between the two devices.

Squier *et al.*<sup>21</sup> recently produced a modification of the Bronaugh cell. This apparatus was designed to allow the use of small tissue biopsies ( $< 1 \text{ cm}^2$ ) and operates at low pressure. The cell body is machined out of KEL-F with a clear glass window located on the bottom of the receptor phase chamber for viewing. The donor phase block has a provision for the use of interchangeable spacers, allowing the use of different size tissues and receptor phase volumes. The device can utilize skin as well as more fragile membranes such as buccal mucosa; the cell can be adjusted to accommodate the differing thickness of these tissues. Effluent from the cell is directed into a fraction collector. As with the Bronaugh cell,<sup>20</sup> the flux of tritiated water was evaluated for the effect of flow rate, and a lower limit of 1 ml/h was found. Membrane size vs. flux was examined with no differences noted. When the flux values across oral mucosa measured by static vs. the flow-through cell were compared, greater variation about the mean was observed for the static device. Values from the static cell were also significantly lower ( $p < 0.001$ ); this difference was shown not to be due to receptor phase stasis in the static cell.

### Detection Methods

The various methods of detection utilized with previous diffusion cells have essentially been the same as those used in liquid chromatography. This is not surprising, since both involve the analysis of chemicals dissolved or suspended in a liquid. These detection methods have been the primary factor limiting the utility of diffusion cells. The most commonly used detection method is ultraviolet (UV) absorption, although fluorescence, potentiometry, and radiometric methods have been employed. The major drawback of these methods is their non-specific nature; none of them yields a signal that is unique to a given chemical structure. In experimental systems where single, pure compounds are studied, this is generally not a problem and a dynamic cell apparatus can be used. However, when mixtures of chemicals that have overlapping UV absorption spectra are examined, the above methods require some type of separation step to be employed before detection. In this case, fractions are collected from the cell and subjected to analysis after separation. This generally precludes using a dynamic cell with online monitoring, although an automatic fraction collector can be employed.

UV/Visible spectroscopy. Absorption spectroscopy in the ultraviolet to visible range (UV/VIS) is probably the most widely used detection method for diffusion studies. Among its advantages are low cost of instrumentation; relatively rugged nature; a large linear response range and ease of use. The major drawback to UV/VIS absorption is its lack of specificity; even chemicals that do not share common structural features can have qualitatively similar UV/VIS absorption spectra. The same functional group on two different molecules can give the same absorption. This is especially problematic when single wavelength instruments are used. Even

when diode array detectors, which are able to monitor an entire spectral range at once are employed, closely related compounds cannot be discerned by their absorption signals alone. Such cases generally require the use of post-experimental separation techniques, such as HPLC, thus negating many of the advantages gained by using a flow-through design. Molecules that lack a conjugated bond system are poorly detected (if at all) by UV absorption techniques. This includes chemicals being investigated for dermal delivery such as testosterone.

Absorption spectra are generated when a molecule undergoes an energetic state transition during exposure to light.<sup>22</sup> The wavelengths causing the transition are absorbed from the spectrum and do not exit the sample cell. The absorption spectrum is thus directly related to the structure of the molecule. The event responsible for absorption is the transition of an electron from the highest occupied molecular orbital (HOMO) to the lowest unoccupied molecular orbital (LUMO).<sup>23</sup> Possible transitions exist in every molecule; however most are energetically unfavorable to either induce or observe, as far as common laboratory instruments are concerned. Transitions that occur in the 190 to 800 nm wavelength region produce useful spectra that can be easily observed. These are mostly the  $n \rightarrow \pi^*$ ,  $n \rightarrow \sigma^*$  or  $\pi \rightarrow \pi^*$  state transitions. Thus, practical UV absorption detection is limited to molecules containing chromophores capable of undergoing these transitions. This essentially limits the usefulness of UV absorption to molecules containing nitrogen and oxygen, molecules with conjugated double bond systems, and molecules with halogen lone pair electrons.<sup>23</sup> Molecules possessing extensive conjugation absorb very strongly in the UV/VIS region.

Quantitation using the Beer-Lambert law  $A = ecl$  ( $A$  = absorbance,  $e$  = molar absorptivity,  $c$  = molar concentration and  $l$  = path-length) is affected by the nature of the solute.<sup>22</sup> The Beer-Lambert law is strictly observed for solutes existing as single species in solution but may not hold for molecules in equilibrium between two or more states. Needless to say, when more than one molecule in solution share an absorption maxima, the Beer-Lambert law cannot be used for quantitation. Absorption spectra are affected by the type of solvent used in the receptor phase. Solvents themselves have absorption spectra that can overlap with that of the solute and interfere with determining concentration. Solvents may interact with the solute in either the ground or excited state, thereby affecting the absorption spectrum even to the point of obliterating it.<sup>22</sup>

Fluorescence. Fluorescence detection shares a similar mechanism with UV/VIS absorption and is more specific with regards to identifying some chemicals. However, it shares many of the same shortcomings as UV devices. Closely related compounds, such as structural isomers, may have significantly overlapping spectra making the identification of solutes in a mixed solution impossible. Diode array instruments do have the advantage of being able to monitor several excitation/emission pairs, and thus increasing their specificity of detection; however they are still limited in the amount of structural information that is provided about a molecule.<sup>22</sup> From a purely mechanical point of view, these instruments are limited in the number of spectra that can be simultaneously monitored, with four or five excitation/emission pairs being the norm. Non-diode array instruments possess a

further shortcoming in being sensitive to mishandling and require a good deal more maintenance than either UV or diode array instruments.

Fluorescence is an excitation/emission process. A light source, typically a diffraction grated deuterium lamp or a laser, is used to deliver a single wavelength corresponding to a molecule's excitation maximum. Excitation occurs when a ground state electron is lifted to one of several excited energy levels in a quantum process.<sup>22</sup> Emission is the release of energy as light when the electron returns to the ground state. When excited, the electron can reside in a vibration level of the excited state. The electron can return to the base excited state by vibrational relaxation, a radiationless process. The electron may also cross from a higher excited state to a lower one if their vibration levels overlap; this is also a radiationless event. Excited molecules may also lose energy by external transitions such as intermolecular collisions or solvent interactions. These differences in excitation energy input and energy state before emission account for the differences in the two wavelengths.

Fluorescence spectra are dependent on molecular structure in a manner similar to that of UV/VIS absorption spectroscopy. Energy transitions of the  $n \rightarrow \pi^*$ ,  $n \rightarrow \sigma^*$  or  $\pi \rightarrow \pi^*$  nature are both inducible and observable with conventional instrumentation; thus detection is effectively limited to molecules possessing  $\pi$  bonded or lone pair electrons. Fluorescence is a great deal more specific in that it can isolate a particular functional group based on its electronic behavior. Excited state transitions and decay are affected both by the molecular structure of the group as well as its environment. Adjacent substituents can affect the stability of the ground and excited states, thereby changing the nature of the energetic transition and the resultant spectrum. Several

excitation/emission pairs can be monitored either to verify the identity of a molecule, or to monitor multiple solutes. The number of pairs that can be followed is physically limited by the light source and the detection optics. When a deuterium lamp is used as a source, the diffraction grating must be physically scanned through a series of wavelengths. The time spent between the desired wavelengths results in lost data and, depending on the nature of the analysis, can limit the number of wavelengths that can be scanned. The use of multiple gratings can reduce switch time, but the practical space in the detector is limited. Laser sources provide clean, narrow band excitation sources, but only one wavelength is available per source. Organic dye lasers whose output can be tuned are available, but are extremely expensive. Conventional detector optics share the same shortcomings as deuterium lamp sources, in that wavelength scanning must be physically done with diffraction gratings. Diode array detectors allow several wavelengths to be monitored simultaneously and are limited only in the slit width and the diode size.

In spite of its increased specificity over UV/VIS detectors, fluorescence possesses a number of shortcomings. The most obvious is when a molecule lacks functional groups capable of undergoing likely or observable energy state transitions. Any electron can be induced into an excited state given enough energy, however only those  $\pi$  bond or halogen lone pair electrons produce useful spectra with conventional equipment. Conjugation of  $\pi$  bond systems greatly increases the intensity and detail of emission spectra. Molecules lacking such features, or those with single  $\pi$  bond groups, are often not detectable with fluorescence spectroscopy.<sup>22</sup> Intersystem crossing can reduce or eliminate fluorescence depending on the energetic conditions

of the molecule. Intermolecular and solvent/solute collisions can also reduce fluorescence. Interactions between molecules that destabilize the excited state through radiationless energy transfer result in signal quenching. Finally, on a practical note, fluorescence detectors require more care in their operation and handling. The optical systems of fluorescence instruments are very sensitive to environmental changes and mishandling.

Radiolabeling. Radiolabeling of chemicals is a well-tested technique that possesses a great deal of inherent specificity. Correctly done, the researcher can attribute an observed signal to a single chemical with a great deal of certainty. Several chemicals can be monitored by using different isotope tags. However the number of possible tags that can be used in a single experiment is limited to three ( $\alpha$ ,  $\beta$ , and  $\gamma$  emitters). When static systems are used, detection is done via scintillation counting. Online detection is typically done either with either a Geiger counter ( $\alpha$  emission), photo multiplier tube ( $\beta$  emission) or a metal doped crystal such as NaI ( $\gamma$  emission). The number of chemicals that can be monitored simultaneously is limited to three; tags must be of differing emission particle types, since detectors cannot discriminate between source nuclei. Gamma rays emitters may be differentiated based on the ray's energy level.

The primary drawback of radio labeling methods is that the signal gives no information as to the identity of the labeled compound. Post labeling and post experimental structural determinations must be done to confirm the identity of the labeled structure. For a number of compounds this is a serious drawback. Molecules that can undergo hydrolysis or other metabolic processes may be altered during an



experiment; monitoring the appearance of the radio-label alone will not reveal this change. A second drawback to the use of radio-labels is the nature of the waste generated. The use of scintillation counting exacerbates the problem by adding organic solvent waste to the radioactivity. At a time when more institutions and researchers are moving away from the use of radioactivity due to the health risks and the increased fees for disposal, radiolabel methods are falling from favor. The increased testing of complex formulations is making radiometric methods unfeasible, especially when more than three chemicals are to be monitored simultaneously.

Potentiometry. Potentiometry based detectors are highly sensitive, but limited in their applications. A potentiometric probe compares the voltage between a solution and a reference electrode to record changes in the voltage potential. Changes in the number of charged molecules will affect this potential. Potentiometers are best suited to monitoring changes in ionic potential, such as the diffusion of charged species across membranes. They are also useful in evaluating membrane damage, since changes in membrane potential are often signals of degradation of its barrier properties (Mike Membrino, personal communication). Potentiometry is highly limited in its ability to positively identify chemicals in diffusion experiments.

Detector shortcomings. The one shortcoming common to all of the above detection methods is one of specificity. Multiple compounds are difficult, if not impossible, to monitor simultaneously using the previously mentioned detectors coupled to a flow through cell. When two or more compounds with differing absorbance or emission spectra are examined, the detector must be switched from one spectrum to another. The result is non-continuous monitoring, although the interval

may be very small. While signal switching is not an issue with photodiode array or radiometric detectors, the number of channels and chemicals that can be simultaneously monitored is practically limited. Data analysis and manipulation become difficult when full spectrum signals are acquired over a long period of time. Molecules with similar or overlapping spectra can be impossible to tell apart; signals from structural isomers are often identical in nature. None of the listed methods provide much information as to the structure of unknown compounds.

Nonspecific detection methods can be used in conjunction with a separation step, such as chromatography, however there are a number of reasons for desiring a flow-through device. Sampling is performed in separated intervals therefore, events of a duration less than the interval can be averaged out of the final measurement. For instance, the lag time (time between the beginning of diffusion and the achievement of steady state) for quickly diffusing molecules is often difficult to measure, since its duration may be small compared to the sampling interval (minutes vs. hours). This is important information for pharmacologists and toxicologists alike since it is a measure of how rapidly a drug or chemical can take effect.

### Predictive Models

Another approach to evaluating transdermal flux is via mathematical modeling. Transmembrane diffusion is a physical process governed by Fick's law:

$$J=(D/L) C K$$

where J is flux, D is the diffusivity of a chemical in the membrane, L is the diffusion length through the membrane, C is the concentration of chemical in the donor phase (assuming sink conditions in the receptor phase) and K is the partition coefficient

between the solvent and membrane. Since K is difficult to measure, it is usually approximated using an organic/aqueous partition coefficient such as octanol/water.

Scheuplein. Much of what is known about transdermal diffusion is derived from the work of Scheuplein and colleagues.<sup>3,4,24,25</sup> They helped establish the role of the stratum corneum as the principle barrier to diffusion across the skin<sup>24</sup> and as the major pathway for flux, as opposed to shunt venules.<sup>25</sup> Scheuplein *et al.* modeled skin diffusion as occurring in a Fickian process through a tri-laminate membrane consisting of the stratum corneum, epidermis and dermis. Solvent/vehicle partition coefficients were measured<sup>24</sup> or calculated<sup>3</sup> for a series of straight chain alcohols. Scheuplein *et al.*'s model could qualitatively predict the behavior of chemicals within his series as concentrations and vehicles were altered.

Michaels. Michaels *et al.* devised a model of transdermal penetration through human skin based upon the lipid and aqueous solubilities of a compound.<sup>18</sup> They modeled skin as a "bricks and mortar" structure with desiccated keratinocytes ("bricks") held together by lipid ("mortar"). Their model proposed that movement through both phases could be described by:

$$\frac{J_{s(Max)} t_s}{C_{Aq}^*} = k_p D_p \left[ \left[ \frac{\beta + 1}{\frac{\beta D_p}{\sigma D_l} + 1} \right] + \sigma \frac{D_l}{D_p} \left[ \frac{2\beta / \alpha}{1 + \frac{\alpha + \beta}{2(1 + \beta)}} \right] \right]$$

where  $J_{s(Max)}$  is the maximum flux through skin,  $t_s$  is the skin thickness,  $C_{Aq}^*$  is the aqueous concentration at saturation,  $k$  is partition coefficient,  $D$  is solute diffusivity,  $\alpha$  is the plate axis ratio,  $\beta$  is the interstitial layer thickness/plate element thickness,  $\sigma$  is the lipid phase/ protein phase partition coefficient. The subscripts l and p denote lipid

and protein, respectively. Using  $\alpha$  and  $\beta$  values estimated from electron micrographs of skin, the authors defined the reduced equation:

$$\bar{J} t_s \cong k_p D_p \left[ \frac{1.16}{0.16 \frac{D_p}{\sigma D_l} + 1} + 0.0017 \left( \frac{\sigma D_l}{D_p} \right) \right]$$

where

$$\bar{J} = \frac{J_{s(Max)}}{C_{Aq}^*}$$

A plot of the mineral oil/water partition coefficient vs. the permeability coefficient demonstrated a near linear relationship for the ten drugs tested; the plot plateaued for the more lipophilic compounds nitroglycerine, fentanyl and estradiol. Two solution plots to Michael *et al.*'s model were overlaid on the data. The values of  $10^{-2}$  and  $10^{-3}$  for  $D_l/D_p$  yielded curves that bound eight out of ten of the data points. Michael *et al.*'s data provided useful information as to the importance of water solubility in determining transdermal flux.

Kasting *et al.* Kasting, Smith and Cooper<sup>26</sup> derived one of the first reliably predictive models of transdermal diffusion. Their model assumed lipid solubility and molecular volume to be the two predominate factors affecting diffusion. The equation:

$$\log J_M = \log (D^\circ/L) + \log S_{OCT} - (\beta/2.303)V$$

described the maximum flux ( $J_M$ ) from saturated solutions of drug in polyethylene glycol across a membrane with thickness  $L$ . The term  $D^\circ$  is the diffusivity of an ideal molecule having zero volume,  $S_{OCT}$  is the solubility of the drug in octanol,  $\beta$  is a

constant describing the nature of the skin and  $V$  is the van der Waal's volume. This assumed that a measure of lipid solubility and molecular volume alone is sufficient to model the solubility and movement of solutes in skin. It was also assumed that flux is independent of the vehicle, as saturated solutions were used; thus the activity of the solute was the same regardless of donor solvent, so long as the solvent did not alter the barrier properties of the skin. The model had limited predictive power with a best fit of  $r^2=0.74$  when compared to their data set. Substitution of isopropyl myristate for octanol solubility decreased the fit of the model ( $r^2=0.60$ ) to the data set; substitution of molecular weight for  $V$  gave an equivalent fit.

Kasting *et al.*'s work provides a base upon which many authors have built. However, a number of shortcomings must be noted. First is the use of ethanol in the receptor phase;<sup>26</sup> skins were equilibrated overnight in a solution of ethanol/0.02% sodium azide 1:1. Kasting's model assumes  $D^0$  and  $\beta$  to represent properties of the skin independent of what solvent is used. The author notes that penetration is enhanced by the use of ethanol vs. aqueous receptor phases by a factor of 1.7. The fact that ethanol can penetrate skin<sup>3</sup> indicates that it is an interactive solvent, therefore the  $D^0$  and  $\beta$  terms described by Kasting are descriptors of skin saturated with ethanol, not of skin alone. A second problem lies with the value of  $L$ , the diffusion pathway. The author uses a value of 10  $\mu\text{m}$  based on physical measurements of the stratum corneum's thickness. This value does not account for the tortuosity of the path, and subsequently underestimates its length; by comparison  $L$  is typically estimated to be  $\sim 500 \mu\text{m}$ .<sup>9</sup> Finally, many of their octanol-water partition coefficients were calculated, as opposed to measured.

Anderson-Raykar. Anderson and Raykar refined the model of Kasting *et. al* and investigated the value of heptane/water vs. octanol/water partition coefficients for the prediction of flux.<sup>27</sup> Transport of a series of methyl substituted p-cresols through human stratum corneum was measured. Donor and receptor phases were pH 4 succinate buffer (0.01 ionic strength); donor phase solute concentrations were less than 0.1% to minimize skin damage. The difference between using heptane and octanol partition coefficients as a proxy for the skin partition coefficient was measured. They reported better correlation between  $PC_{\text{oct/water}}$  vs. permeability coefficient than for  $PC_{\text{hept/water}}$  (slope = 0.5 vs.0.4 respectively) for a series of substituted p-cresols and 21-esters of hydrocortisone. This indicated that skin is more polar than heptane. The permeability and partition coefficients of whole and de-lipidized stratum corneum were compared for two compounds; stratum corneum was de-lipidized using a chloroform/methanol mixture. The partition coefficient values showed no difference between whole and delipidized stratum corneum; this was surprising as both compounds have significant octanol/water partition coefficients. The permeability values were increased in the delipidized stratum corneum, and were in fact identical for all of the compounds measured.

The authors then included a molecular weight term in their diffusion model, based on their previous results from a series of 21-esters of hydrocortisone.<sup>28</sup> A combined plot of the permeability vs. octanol/water partition coefficients values for the two series gave two lines. The authors, in a similar manner to Kasting *et al*. hypothesized this was due to the difference in the molecular sizes of the two groups. Their derived model equation:

$$\log k_p = X + \psi \log PC_{(oct/water)} - n \log MW$$

where  $k_p$  is the permeability coefficient,  $X$  and  $\Psi$  are constants, and  $n$  is a mass selectivity term, resulted in both data series fitting a single line. The mass selectivity is a measure of how sensitive flux across a given membrane is to changes in molecular weight. Anderson and Raykar's calculated  $n$  value of 4.6 gave a reasonable fit to the test data set with a reported  $r^2 = 0.91$ . Kasting *et al.* tested a similar inverse power dependence of diffusivity on molecular volume and reported a decreased correlation to their data,<sup>26</sup> this may not be surprising given the points noted above regarding their data set.

Some points must be noted with regard to Anderson and Raykar's model. The first deals with the use of isolated stratum corneum. Many researchers eschew the use of isolated stratum corneum in favor of whole thickness skin because of the latter's increased physical strength and ease of handling. The role of the stratum corneum as the primary barrier to diffusion has been well established (reviewed in Sheuplein<sup>24</sup>). The use of organic solvents to remove stratum corneum lipids is questionable, as these may denature the protein structure that is allegedly being preserved for observation. In all likelihood, the lack difference in partition coefficients between whole and de-lipidized stratum corneum is likely due to there being holes in the membranes used. Finally, the use of pH 4 buffer is inappropriate, as many of the p-cresol compounds have pKa values in the range of 4-5. This would mean that a significant portion of the molecules in solution are ionized. Anderson and Raykar's model is intended to measure the diffusion of non-electrolytes, thus their data set is not entirely suitable. This is evident when the authors attempt to compare

their data to group contribution theory.<sup>27</sup> The contribution of substituting CH<sub>3</sub>-O for H-O is different than what would be expected, since in reality the hydroxyl is likely acting as a charged species.

Potts-Guy. Potts and Guy<sup>9</sup> refined Kasting *et al.*'s model to account for the difference between  $K_{MEM}$  and  $K_{OCT:AQ}$  and substituted the more readily measured term MW for V. Their equation:

$$\log P = \log (D^\circ/L) + f \log K_{OCT:AQ} - \beta^\circ MW$$

where  $K_{MEM} = (K_{OCT:AQ})^f$  and  $\beta^\circ$  is similar to Kasting's  $\beta$  but includes a conversion factor to account for the substitution of MW for V, demonstrated an  $r^2 = 0.83$  for the test data set (n= 61), but an  $r^2 = 0.67$  was found when applied to a Flynn's<sup>29</sup> data set (n= 93). The f exponent used to convert  $K_{OCT:AQ}$  to  $K_{MEM}$  accounts for the anisotropic nature of skin vs. octanol. The Potts/Guy model discounts the existence of an aqueous pore pathway for hydrophilic drugs. The data of Ackerman *et al.*<sup>30</sup> had been cited as evidence of a separate "aqueous pore" pathway, as separate P vs.  $K_{lipid}$  plots were observed for compounds of varying hydrophilicity. When the Potts-Guy equation was applied to these data, a plot of the predicted vs. measured P values gave a single line. While acknowledging the predictive ability of the Anderson and Raykar's MW power function model, Potts and Guy discounted this approach citing a lack of physiological correlation for the term. An upper limit on permeability for highly lipophilic molecules has been proposed. It has been assumed that the limiting mechanism for highly lipophilic molecules would be their transport into the more aqueous tissues underneath the stratum corneum. Potts and Guy tested this assumption using estimations of the permeability and path-length of the tissue



between the stratum corneum and the micro-vasculature. They found no support in their model system for an upper limit on permeability values for highly lipophilic molecules.

Abraham *et al.* Simple diffusional models base their permeability predictions on the molecular weight (or size) and lipid solubility of a molecule. While these can give good predictive power, they do not yield much information about the transdermal diffusion process. Abraham *et al.*<sup>7</sup> took the approach of modeling transdermal diffusion as a phase partitioning process. They applied a general solvation model:

$$\log SP = c + rR_2 + s\pi_2^H + a\Sigma\alpha_2^H + b\Sigma\beta_2^H + vVx$$

where SP is some property of a series of solutes in a given system.  $R_2$  is the excess molar refraction and represents the tendency of a solute to interact with a phase through  $\pi$  or n electrons. The symbols  $\Sigma\alpha_2^H$  and  $\Sigma\beta_2^H$  represent the effective solute hydrogen bond acidity and basicity, respectively, and  $\pi_2^H$  is a measure of solute dipolarity/polarizability while Vx is the characteristic volume calculated from the molecular structure. The coefficients r, s, a, b and v characterize the phase; r indicates the propensity of the phase to interact with  $\pi$  and n electrons of the solute, s describes phase dipolarity/polarizability, a is a measure of solvent hydrogen bonding basicity, b is a measure of solvent hydrogen bond acidity and v is a measure of lipophilicity. When their equation was regressed against a dataset of skin permeability coefficients, an  $r^2 = 0.98$  was obtained. Furthermore, the equation coefficients were instructive as to the nature of transdermal diffusion. Regression against Abraham *et al.*'s model showed two main factors influence permeability:

solute hydrogen bond basicity and solute size. Dipolarity of the solute played a smaller, though significant role. Solute acidity had little influence on permeability, according to Abraham *et al.*'s model. The authors interpreted this to be due to the hydration of skin by water which exerts an acidic effect.

Potts and Guy have published a solvchromatic refinement of their previously discussed diffusion model.<sup>8</sup> They described the equation:

$$\log P = [a_1 - \beta]MV + a_2\pi + a_3H_d + a_4H_a + a_5R_2 + \log(D_o / \delta)$$

where  $H_a$  and  $H_d$  are hydrogen bond acceptor and donor values, respectively. Closer inspection reveals this to be the same model as described by Abraham *et al.*,<sup>7</sup> but with a slightly different molecular volume term. The model was used to evaluate the partitioning of solutes from aqueous solutions into organic solvents. Doing so revealed an inverse relationship between  $H_a/H_b$  terms and partitioning into the organic phase. This phenomena was less pronounced in octanol, reflecting that solvent's ability to participate in hydrogen bond interactions. Comparison of this equation to their previously used dermal permeation dataset<sup>9</sup> gave a correlation of  $r^2 = 0.94$ , a significant improvement over the author's previous model. Potts and Guy dropped the  $R_2$  and  $\pi$  values from their epidermal permeation regression, finding that the model fit was significantly improved. Examination of the regression for permeation values showed molecular volume and  $H_a/H_d$  terms to have the greatest effect on permeation. The stratum corneum was shown to be a better acceptor of hydrogen bonds than octanol and to be more accommodating of polar species than alkane solvents.

Roberts-Sloan. The Potts-Guy equation only predicts the flux of drugs from aqueous vehicles and it also does not address the contribution of aqueous solubility to flux. Water solubility plays an important role in determining transdermal flux as evidenced by the fact that, for a series of compounds with similar lipid solubilities, the member with the highest water solubility generally has the highest transdermal flux.<sup>31</sup> Prediction of delivery rates from vehicles other than water is also desirable, as these are often used in pharmaceutical and cosmetic formulations. A revision of the Potts/Guy equation by Roberts and Sloan<sup>10</sup> addresses these shortcomings. Their equation was:

$$\log J_M = \log (D^\circ/L) + f \log S_{IPM} + (1-f) \log S_{AQ} - \beta^\circ MW$$

where  $S_{IPM}$  is solubility in isopropyl myristate and  $S_{AQ}$  is solubility in pH 4.0 buffer. This allows the use of IPM (or any other solvent) in the donor phase, as well as taking into account the effects of solute water solubility on flux. The inclusion of  $S_{AQ}$  is based on the influence of  $H_a$  and  $H_b$  coefficients  $a_3$  and  $a_4$  noted by Abraham *et al.*<sup>7</sup> and Potts and Guy.<sup>8</sup> The  $a_3$  and  $a_4$  coefficients terms are directly related to water solubility as they indicate the propensity of a solute to engage in hydrogen bond formation. Roberts and Sloan noted a positive correlation between  $a_3$  and  $a_4$  and flux, while Potts and Guy<sup>8</sup> and Abraham *et al.*<sup>7</sup> found a negative one. Comparisons to data sets of measured flux gave an  $r^2=0.94$  with the best performer in a series of drugs being correctly predicted six out of seven times.

Steroid molecules have traditionally posed a problem in transdermal diffusion modeling, even though they are typically included in model datasets. Work by Abraham *et al.*<sup>32</sup> demonstrates the nature of the problem. Using their previously

derived model equation,<sup>7</sup> the authors examined permeability coefficients from three sources: Anderson *et al.*,<sup>28</sup> Johnson *et al.*<sup>33</sup> and Scheuplein *et al.*<sup>34</sup> Application of their equation to the Johnson set resulted in a reasonable prediction of the permeability coefficients. This was not the case for the Scheuplein set; a plot of the predicted vs. observed values for both data sets shows the Johnson set grouping with the members of the test set, while the Scheuplein points cluster below the equation line. Inclusion of the Johnson set in a recalculation of coefficients results in only minor changes to the equation and no reduction in fit ( $r^2 = 0.956$  vs.  $0.957$ ). Plotting the predicted vs. observed values for the Anderson set shows them to lie above the equation line. It should be noted that Anderson used isolated stratum corneum, as opposed to the heat separated epidermis used by Scheuplein and Johnson. Abraham *et al.*'s experience demonstrates some of the difficulties in constructing a predictive model, especially when disparate datasets are utilized. Furthermore, even using a dataset that agreed well with their model, Abraham reported the presence of outliers whose permeation was not accurately predicted.

A number of attempts have been made to refine these models by correlating flux values with other physical parameters such as melting point or hydrogen bonding potential.<sup>35-38</sup> Melting point was used to address the contribution of the activity of the solute in solution. Hydrogen bonding potential, often broken into donor and acceptor terms, can be viewed as an indicator of aqueous solubility and solvent/solute interaction. Many of these equations invoke difficult to measure terms while failing to yield substantial improvements over previous models.

Shortcomings of models. Predictive models are useful for understanding what factors affect diffusion through skin. They are also useful for estimating how changes in molecular structure will modify a chemical's transport. As such, they are valuable guidelines for the design of new drugs and dermal delivery schemes. However, the predictive power of each of these models is limited to one degree or another by a number of factors. Saturated solutions are used in the donor phase so that the activity of the drug will always be unity. This assumes that the solvent used for the donor phase is non-interactive with human skin, meaning it does not enter the skin and alter its permeability. Many commonly used solvents, such as alcohols, have been shown to be interactive with human skin.<sup>39-42</sup> Assuming donor phase solvents to be non-interactive may severely underestimate flux from those solutions. Concomitant with the assumption of non-interaction is the assumption that solvent chemicals are not crossing the skin and behaving as drugs or toxicants.

Actual drug delivery systems may embody some or all of these exceptions. Saturated concentrations of the drug may not be present in a device, therefore calculation of the drug's activity coefficient is required in order to determine its partition coefficient between skin and the device. Sink conditions may not be present, altering the kinetics from predicted values. Chemicals present in the device as preservatives or penetration enhancers may enter the skin and affect its barrier properties. These chemicals may also cross the skin and exert a biological effect of their own. The majority of available models have limited veracity for chemicals whose properties lie far outside those used in the model dataset. The predictive value for extremely hydrophobic or hydrophilic chemicals tends to be low. Steroid

molecules are an example of a class of drugs whose penetration are not well predicted by the model systems in use.

Predictive models enjoy widespread use in the risk assessment community. They are used to estimate the delivery of potential toxicants through skin so as to calculate a safe exposure level. All of the previously listed short-comings apply when predictive models are used in this manner. The interactive nature of the solvent is of special concern, since predictive models may underestimate dermal penetration in these cases.

### Potential of LC/MS

Ion manipulation. Mass spectrometry (MS) is a detection method based on the separation of charged molecules, or ions. Ions are affected by the presence of an electromagnetic field in direct proportion to their mass to charge ratio (m/z).<sup>43</sup> When the charge on the molecule is one, this value represents the molecular weight of the ion. Differential electromagnetic fields can be used to separate ions in a manner that correspond to their m/z and allow for quantitation of those ions. Bench-top MS instruments are usually of either a quadrupole or ion trap configuration. Quadrupole instruments contain a set of metal rods to which is applied a DC potential as well as a radio frequency. The Rf/DC amplitude ratio is held constant as the range of both are scanned; the Rf frequency is held constant. For a given Rf/DC magnitude, there exists a single m/z whose trajectory is stable within the bounds of the quadrupole. The motion of ions in a quadrupole are described by:

$$\Phi_{(x,y)} = \Phi_o \frac{x^2 - y^2}{r_o^2}$$

$$\Phi_o = U - V \cos \omega t$$

where  $\Phi_o$  is the applied potential in terms of the DC voltage (U), and the Rf potential ( $V \cos \omega t$ ; V is amplitude,  $\omega$  is angular frequency and equals  $2\pi f$ , where f is frequency in Hz, t is time) and  $r_o$  is the inscribed radius between opposing rods; x and y are the distances from the center of the quadrupole field.<sup>43,44</sup> The velocity of an ion with respect to the z axis, parallel to the quadrupole, is determined by the energy imparted on it by the ionization source optics. A partial derivative with respect to one axis yields:

$$a_x = -a_y = \frac{4zeU}{m^2 r_o^2}$$

$$q_x = -q_y = \frac{2zeV}{m^2 r_o^2}$$

where e is the magnitude of the electronic charge, z is the number of charges and m is the mass of the ion.<sup>43,44</sup> The bounded solutions to a and q yield stable trajectories within the quadrupole. The stability diagram in figure 1-6 illustrates the region of stable trajectories in a-q space. The plot is overlaid with a typical quadrupole operating line representing the Rf/DC ratio. The slope of the line determines the width of a-q space it intersects, which is a measure of the instrumental resolving power. A typical quadrupole mass spectrometer utilizes an operating line with a slope of  $2 U/V$ .<sup>43</sup>

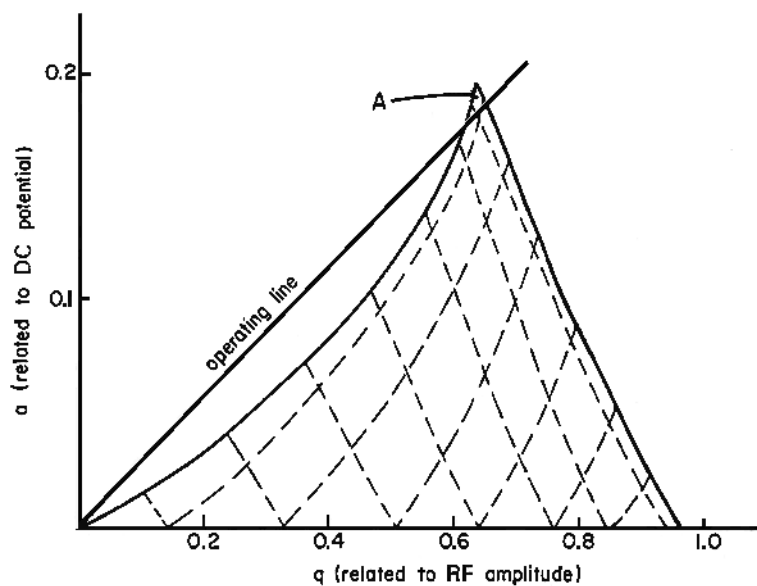


Figure 1-6: Quadrupole stability diagram from Watson.<sup>43</sup>

An ion trap mass spectrometer confines ions in three dimensional space. A schematic of a typical ion trap is shown in figure 1-7. The method of controlling ion motion within the trap is similar to that used in quadrupole instruments. Ion traps apply a DC potential to the end caps of a trap, and a Rf potential of the nature  $\Phi_o = U - V \cos \omega t$  to the ring electrode. The potential of an ion at any point in the trap can be described by:

$$\Phi_{r,z} = \Phi_o \frac{r^2 - 2z^2}{r_o^2} + \frac{\Phi_o}{2}$$

where  $r^2 = x^2 - y^2$  is the radial dimension,  $z$  is the axial dimension within the trap and  $r_o$  is the radius of the ring electrode.<sup>43,44</sup> This differentiates to:

$$a_z = -2a_r = -16 \frac{eU}{mr_o^2 \omega^2}$$



$$q_z = -2q_r = -8 \frac{eV}{mr_o^2 \omega^2}$$

Most ion trap mass spectrometers are operated by changing the Rf only while holding the DC potential constant. In that case:

$$\frac{m}{z} = \frac{4V}{q_{\max} \omega^2 r_o^2}$$

so that the ejected mass is directly proportional to the Rf  $V$  placed on the ring electrode.<sup>44</sup> The stability diagram for an ion trap is shown in figure 1-8. Ion traps can be used to isolate a single ion of interest through the use of resonance mass ejection. Ions in a field naturally tend to oscillate at a frequency characteristic of their mass; this is called the secular frequency. If an Rf field corresponding to the secular frequency is applied, the ion will absorb energy. The radius of its oscillations will increase until the ion is ejected from the trap. A broad-band Rf field can be applied to a population of trapped ions such that all species are ejected except for a selected  $m/z$ . The broad-band signal lacks the frequency corresponding to the ion of interest, and so that member is retained. Sequential mass spectrometry (MS/MS) can be performed in ion traps by applying a collisional waveform to an isolated mass. This waveform induces fragmentation of the molecule and the products are scanned out of the trap. This technique is extremely useful in the determination of unknown structures.

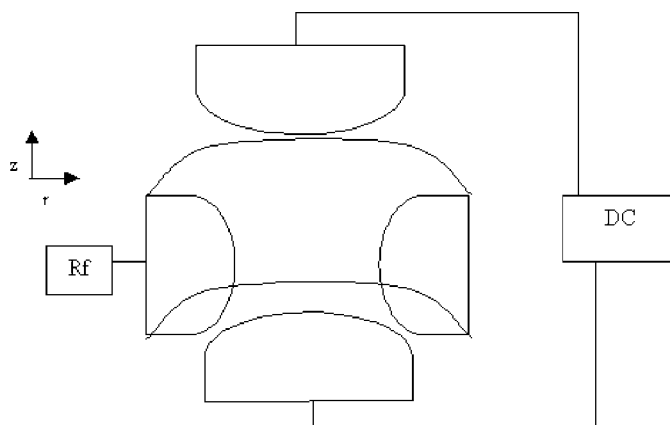


Figure 1-7: Ion trap schematic.

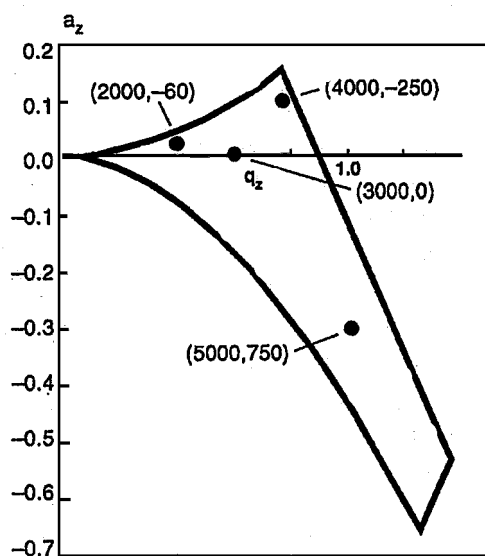


Figure 1-8: Ion trap stability diagram from Dass.<sup>44</sup>

A range of masses can be scanned many times per second with both devices. Mass scanning is done continuously throughout an experiment and allows several chemicals to be monitored simultaneously. The total ion chromatogram represents the signal produced by all species entering the instrument over a given timeframe.

This signal can be filtered to reveal the signal generated by a particular  $m/z$ .

Alternatively, the instrument can scan only a selected number of masses, increasing the sensitivity. Thus several chemicals can be monitored in a single experiment.

Mass spectrometry possesses none of the shortcomings inherent to other detection methods and would be an ideal detector for a diffusion cell system. The use of gas chromatography (GC) subsequent to collecting fractions from diffusion cells for analysis has been reported.<sup>19</sup> Presumably this method could employ gas chromatography/mass spectrometry (GC/MS) as opposed to GC alone. This approach does not allow for online monitoring of the diffusion process and is not amenable to some types of chemicals. The GC/MS is very effective at separating molecules that are volatile, fairly non-polar and thermally stable. Molecules that are non volatile or are polar in nature must be derivatized before GC/MS analysis. In addition to increasing the time required to complete an experiment, many compounds do not derivatize well and related chemicals can derivatize to yield the same end structure. The derivatized compounds must also be thermally stable to remain intact during the GC separation step. Solvents for GC/MS analysis must be of a volatile nature. Since most diffusion experiments are done using aqueous solvent systems, this generally means that samples must be transferred to a more suitable solvent prior to GC/MS analysis.

LC/MS. Liquid chromatography mass spectrometers (LC/MS) have recently become available in a practical instrumentation form. Most LC/MS instruments available can accommodate a wide range of solvents, regardless of volatility. The LC/MS separates a solute from its solvent by a combination of nebulization and

evaporation of the solvent stream. The two main ion production sources in LC/MS are electrospray ionization (ESI) and atmospheric pressure chemical ionization (APCI). In an ESI source, liquid effluent is directed into the source through a fused silica capillary (figure 1-9) that is in turn inserted inside of a hollow metal needle. The needle is held at a high electric potential (typically 3-8 kV), so that when a droplet of liquid formed at the end of the capillary comes close to the surface of the needle an electric discharge occurs and the droplet is dispersed. Nitrogen flowing through the needle nebulizes the charged droplets and propels them into the MS. ESI is a “soft” ionization source and typically results in the formation of singly charged molecules. Some species, especially those with hydrogen bonding groups, do not ionize well in this source and require the addition of a dilute acid or base to reliably form ions. Liquid can be introduced into an ESI source at rate ranging from 1  $\mu\text{l}/\text{min}$  to 1 ml/min. APCI sources ionize molecules using a nitrogen plasma discharge (figure 1-10). Liquid entering the source is flash vaporized at a temperature of 300-600  $^{\circ}\text{C}$  and then carried in a nitrogen stream over a corona discharge needle. This needle is held at a high enough voltage to induce the formation of a corona discharge, which produces a nitrogen plasma. Nitrogen gas participates in an electron transfer within the plasma to produce a single charge on the molecule of interest. Typical flow rates for an APCI source range from 0.1 to 2 ml/min. Although it can result in more fragmentation than an ESI source, APCI is considered a soft ionization method since molecular ions are the primary species produced.

### ESI Probe Assembly

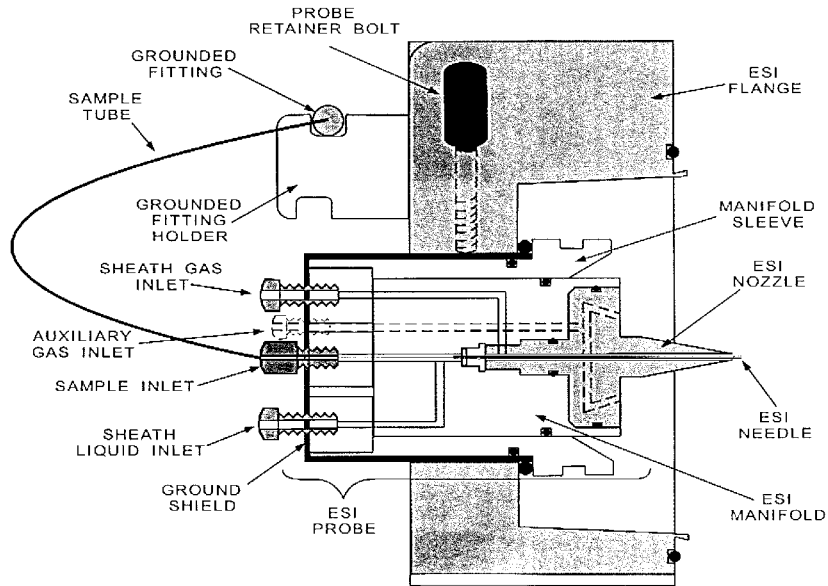


Figure 1-9: ESI probe assembly. Reproduced from Finnigan/MAT.<sup>45</sup>

### APCI Probe Assembly

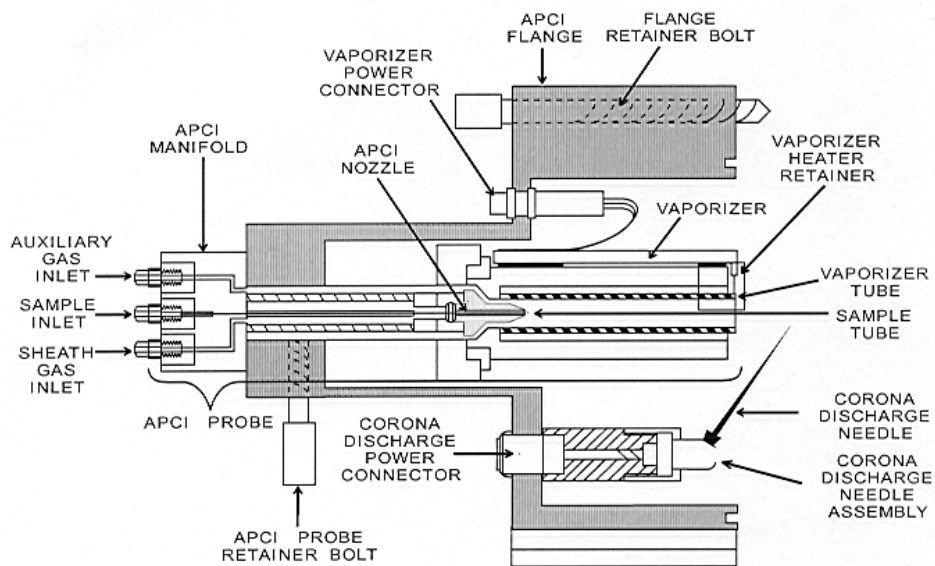


Figure 1-10: APCI probe assembly. Reproduced from Finnigan/MAT.<sup>45</sup>

The molecular weight alone of a molecule can often determine its identity. However with closely related chemicals, or those with the same mass, molecular weight is not sufficient. Molecular structures fragment along pathways of least resistance under a given set of energy conditions; in some cases, unique patterns can even be generated for structural isomers. These fragmentation patterns are reproducible if the energy levels applied are equivalent. The presence of three ions in the same relative abundance is sufficient for positive identification when compared to a known standard. Thus, mass spectrometry can identify chemical structures with a great deal of specificity. Sequential MS can be performed in ion trap instruments, where a particular  $m/z$  is isolated, then fragmented by the application of a high-energy waveform. Fragmentation analysis can then be used to deduce the identity of the parent compound. This process can yield information about the structure of an unknown molecule.

The LC/MS has excellent potential as an optimal detector for a transdermal cell. The LC/MS allows for online monitoring of trans-membrane flux, as well as post-experimental data manipulation. Solvent flow can be introduced directly from the diffusion cell into the instrument without the need for derivatization. Since detection in the MS is based on the mass to charge ratio of a molecule, mixtures of chemicals can be analyzed; photometric detectors cannot resolve mixtures of related chemicals that absorb at the same wavelength. Structural information can also be elucidated from MS data, facilitating the analysis of unknown compounds.

### Statement of the Problem

The presently available diffusion cell technologies are inappropriate for the evaluation of flux from complex matrices. They are adequate for measuring the delivery of a single compound from a donor phase where the solvent is neither a co-diffusant or a potential toxicant. A number of situations exist where traditional devices are not appropriate tools. An example would be when the time to induction and duration of effect needs to be known for a dermally delivered drug. The induction time to steady state delivery is difficult to accurately measure with a static cell; chemicals without useful UV/VIS or fluorescence spectrum would not be possible to evaluate using a flow-through cell. Drug delivery devices such as patches or creams, especially when penetration enhancers are used, present the possibility of co-diffusion of one or more device components along with the drug; if these components have spectra that overlap, then online devices could not be used to evaluate flux. Post experimental separation techniques allow for flux to be evaluated, but short term events (such as the lag time for some chemicals) may be missed.

Environmental toxicants are often present in matrices whose components act both as solvents and potential toxicants. The insect repellent DEET behaves in such a manner. DEET has been shown to enhance the dermal penetration of a number of chemicals<sup>46</sup> and has been shown to be capable of crossing human skin. The lag time for DEET would be expected to be short, given its physical properties, so an online cell would be desirable. However DEET does not have a useful UV/VIS or fluorescence spectrum. Pesticides are often applied in conjunction with DEET use. Many of these are employed as mixtures of closely related compounds (i.e., pyrethroids) that often share similar absorption spectra. Several formulations

combining DEET with insect repellent synergists or sunscreens are presently available. Evaluating the effect of DEET on the flux of these chemicals would not be practical with presently available flow-through cells as each are multi-component mixtures.

The ideal diffusion cell would operate as an online unit and would utilize a universal detection system. The detector would be compatible with a wide array of solvents and would be highly specific, to the point of being able to discern between closely related chemicals. Liquid inlet mass spectrometry is the method that most closely fits this description. In addition, the presently available flow through diffusion cells possess design flaws in their receptor phase chamber design. They utilize receptor phase chambers whose shape and volume dictate the need for vigorous stirring in order to avoid the creation of stagnant areas in the solvent stream.

### Hypothesis

Mass spectrometry would be an ideal detector for monitoring transdermal flux. It is hypothesized that a well designed diffusion cell operating in a flow-through manner would allow for the real time monitoring of transdermal diffusion. Such a device would be uniquely useful for simultaneously monitoring the flux of multiple chemicals across skin as well as the penetration of molecules that have previously required radio-labeling for observation.

### Specific Aims and Rationale

The purpose of this work is to demonstrate the superiority of mass spectrometry as a detection device in transdermal studies versus presently available



instruments. Three specific aims that must be met in order to satisfy the validity of this hypothesis have been identified.

Specific aim one was to physically couple a diffusion cell to a LC/MS device so that the cell can be operated in a flow through manner. Available LC/MS instruments have physical requirements of flow rate that must be accommodated in a cell design. Many of the chemicals of interest for transdermal evaluation have low flux values, therefore a large surface area for diffusion was a desirable feature.

Specific aim two was to validate the performance of the device designed in aim one against accepted methods. This required measuring the flux of chemicals using both the LC/MS design and static Franz cells. It was decided to use a series of benzoic acid esters differing in alkyl chain length to minimize the effects of structural differences. The transdermal fluxes of analogous series have been extensively described in the literature,<sup>39,47-54</sup> providing an additional point of reference. Validation experiments were performed using synthetic membranes and hairless mouse skin.

Specific aim three was to demonstrate several applications of this device using both chemical mixtures as well as molecules that have proven difficult to assess using presently available methods. The simultaneous diffusion of chemical mixtures as well as the fluxes of compounds such as steroids have been difficult to measure without resorting to the use of radio-labels. The simultaneous measurement of flux values for several chemicals and for steroid molecules without the requirement for radio-labeling will be demonstrated.

## CHAPTER 2 MATERIALS AND METHODS

### Specific Aim One: Prototype Design

#### Membranes and Chemicals

Prolastic polydimethyl siloxane (PDMS) membranes were obtained (0.01" thickness) from Pillar Surgical Corporation (La Jolla, CA) with all of the membranes coming from a single production lot. Membranes were soaked overnight in 50% ethanol/water prior to use to remove extractables. Skins from female hairless mice (SKH-hr-1, Charles River) were a gift from Dr .Ken Sloan (Department of Medicinal Chemistry, College of Pharmacy, University of Florida). The ethyl, and n-butyl 4-hydroxybenzoate esters, n-butyl 4-aminobenzoate and theophylline were obtained from Sigma/Aldrich (St. Louis, MO). Ethanol was purchased from AAPER Chemical Company (Shelbyville, KY) and distilled water was produced in house using a Megapure MP-1 still (Barnstead/Thermolyne Dubuque, IA). Saturated solutions of each permeant were prepared two days before use by adding an excess of chemical to 50% ethanol/water and leaving it to stir for at least 24 hours after saturation was reached. The solutions were centrifuged and/or filtered before use.

#### Instrumentation

The mass spectrometer used was a Finnigan/MAT LCQ (Thermoquest, San Diego, CA) and equipped with ESI and APCI sources. The LCQ was tuned for each of the probe chemicals by infusing a 100 µg/ml standard into a solvent stream

entering the instrument. The solvent used was 50% ethanol/water and was introduced at the same rate used for each cell design. The instrument's ion optic parameters and gas flow were adjusted to maximize the signal for the probe compound; these parameters are concentration independent over standard operating ranges ( $< 1$  mg/ml). The HPLC system (model 1100) was purchased from Hewlett- Packard (Palo Alto, CA). A Waters 996 photodiode array detector (Milford, MA) was used for some concentration measurements.

### MIMS Probe

The Membrane Inlet Mass Spectrometer (MIMS) probe (MIMS Technology Inc., Palm Bay, FL) (figure 2-1) was originally designed to separate volatile chemicals from aqueous fluids prior to analysis by mass spectrometry, as shown in figure 2-2. Modifications to the MIMS unit (figure 2-3) were considered as a possible way to construct a diffusion cell device. Receptor phase was introduced into the probe from a syringe pump at a rate of 10  $\mu$ l/min. Membranes were pierced using a hollow center punch and attached to the unit as shown. A number of materials, including latex, nitrile rubber, buna-n rubber and PDMS, were tested in an attempt to build a good seal between the membrane and the probe body. The tip of the probe was immersed in donor phase contained in a water jacketed beaker (ARS, Micanopy, FL). The donor phase, a saturated solution of theophylline in ethanol/water, was stirred and maintained at 32  $^{\circ}$ C. Effluent from the MIMS unit was introduced into the LC/MS using the ESI source. Data was acquired using tune parameters for theophylline. The nitrogen flow rate was set to 30 units, capillary voltage was V and the capillary temperature was 200  $^{\circ}$ C. As the chemical diffused from the donor

phase, through the membrane and into the receptor phase chamber, it was carried to the mass spectrometer for detection.

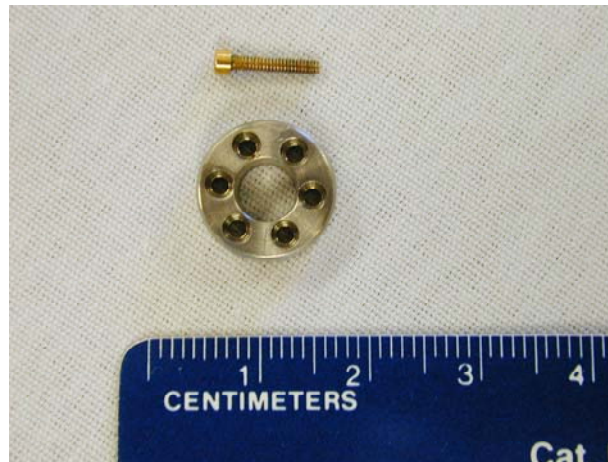
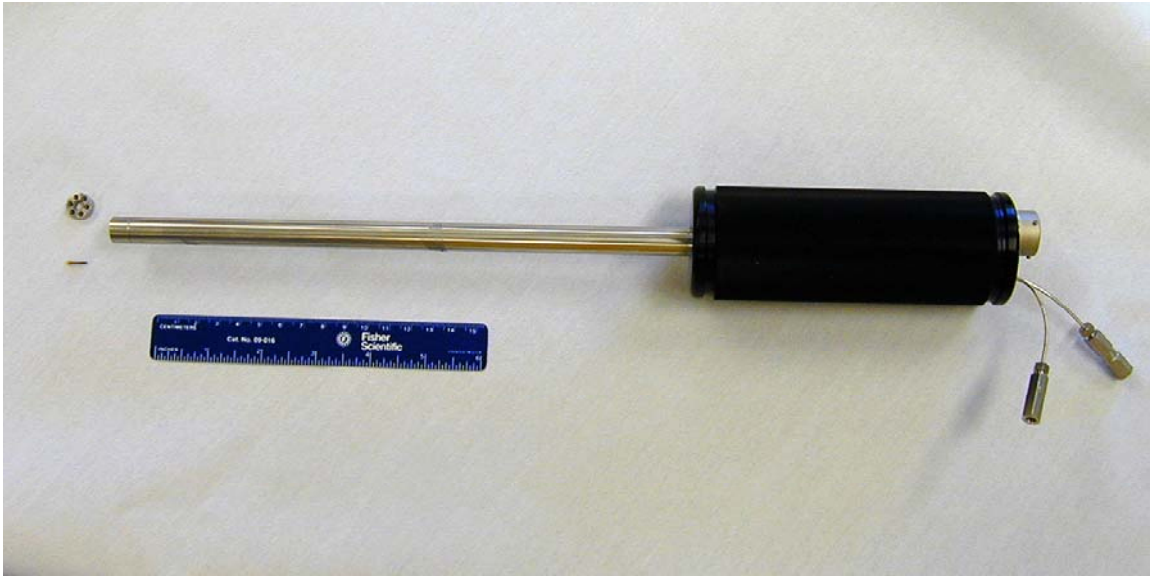


Figure 2-1: MIMS probe.

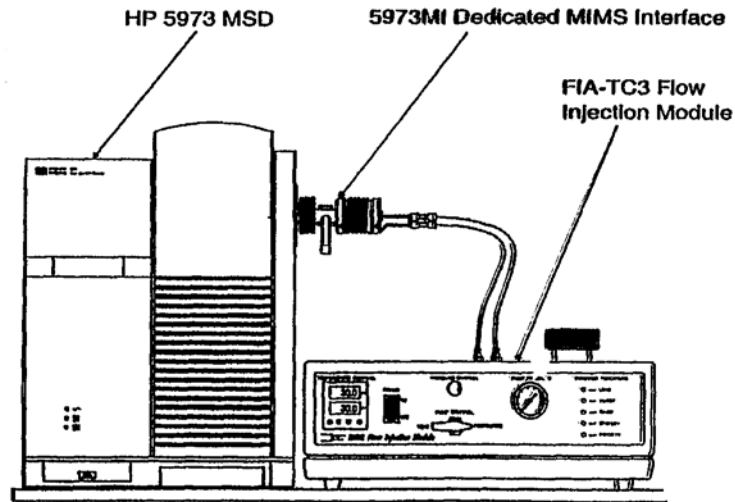


Figure 2-2: MIMS schematic. Original instrumentation schematic for the MIMS probe. Adapted from Lopez *et al.*<sup>55</sup>

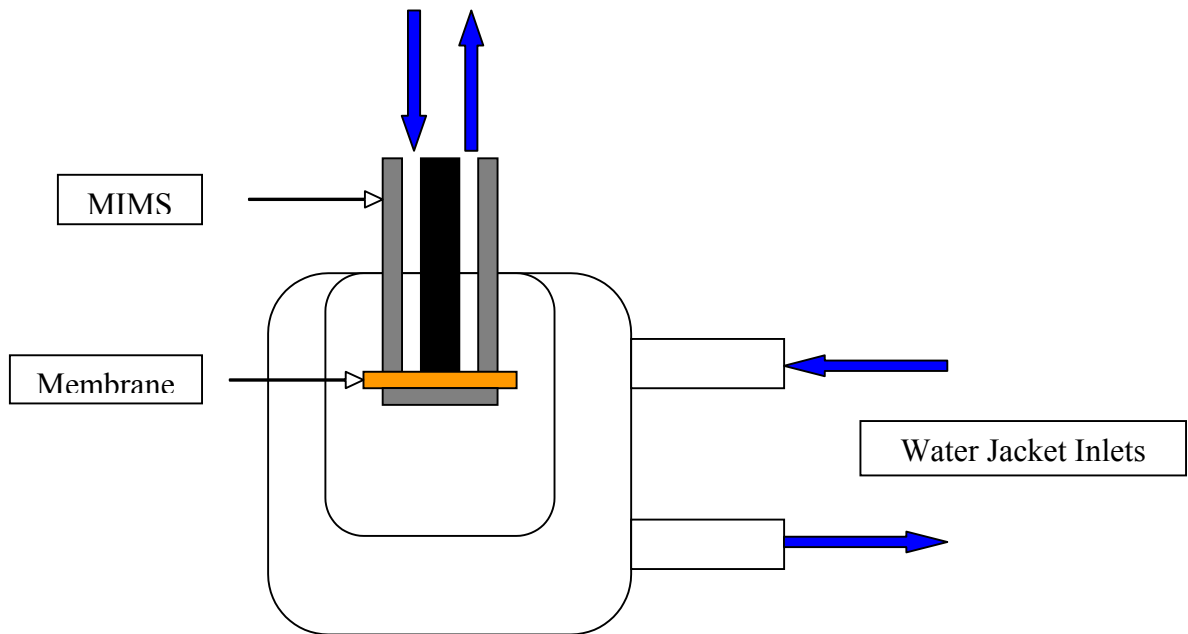


Figure 2-3: MIMS diffusion cell. Schematic for using MIMS probe as a diffusion cell.

### First Prototype

A prototype cell (figure 2-4) was designed to correct shortcomings evident in the MIMS device. The original prototype was constructed from microscope slide glass and marine silicone; it was intended to be a non-working model. The donor phase tank measured approximately 0.5" h x 1.0" w x 2.0" l (0.13 cm h x 2.54 cm w x 5.08 cm l). The glass was cut freehand, therefore the tank dimensions were not perfectly square. The receptor phase plate was constructed from a small square of glass. Two holes were drilled in the plate about 0.25" outside of the long axis of the donor phase tank. Inlets were constructed by cementing PEEK tubing into place on one side of the tank; the tubes were reinforced using sections of Pasteur pipettes and marine silicone. A receptor phase spacer was constructed from a piece of acetate sheeting cut to the same size as the donor and receptor phase plates. The unit was assembled as shown in figure 2-4 and held together using binder clamps. The model proved to be solid enough for an initial test.

After equilibrating in 50% ethanol/water, a section of PDMS membrane was placed in the device and the cell was connected to the HPLC and the LCQ as shown in figure 2-7. A saturated solution of test chemical was placed in the donor phase and data was acquired using that compound's tune parameters. Methyl, ethyl and n-butyl 4-hydroxybenzoate, theophylline, and n-butyl p-aminobenzoate were tested. Data were acquired in full scan.

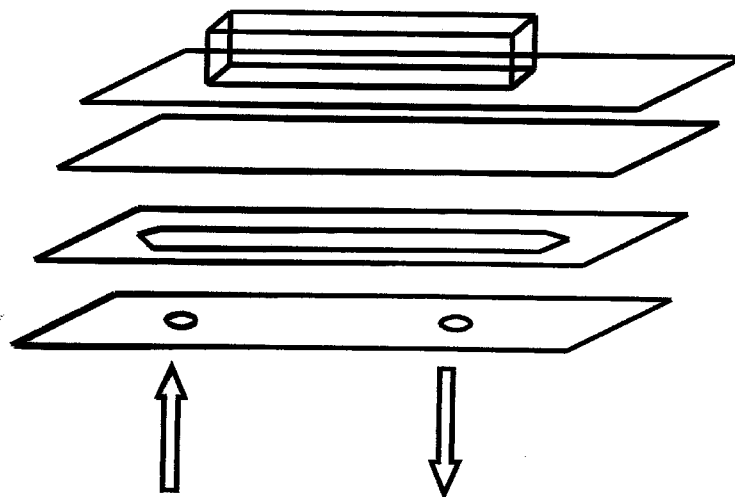


Figure 2-4: Prototype diffusion cell. Design concept for prototype diffusion cell. Components consist of, from top to bottom, a donor phase tank, membrane, receptor phase channel, and a receptor phase inlet plate.

### Second Prototype

A second prototype, based on the first design, was fabricated for more intensive testing. The services of Advanced Research Systems (ARS Micanopy, FL) were enlisted for this project. A diagram of the second cell is shown in figure 2-5. The donor phase chamber dimensions were kept at 0.5" h x 1.0" w x 2.0" l. The donor phase tank was machined from a block of Teflon measuring 1.25 "h x 3" w x 5" l. The receptor phase plate was machined from stainless steel. The inlet/outlet ports were drilled to accept standard tubing using a cone ferrule so that the tube could be installed then sliced flush with the plate surface. The ports were tapped for 10-32 threaded HPLC fittings. The receptor phase channel was fabricated in-house from

1mm latex sheeting (Small Parts Corp., Miami Lakes, FL). The cell components are shown in figure 2-6.

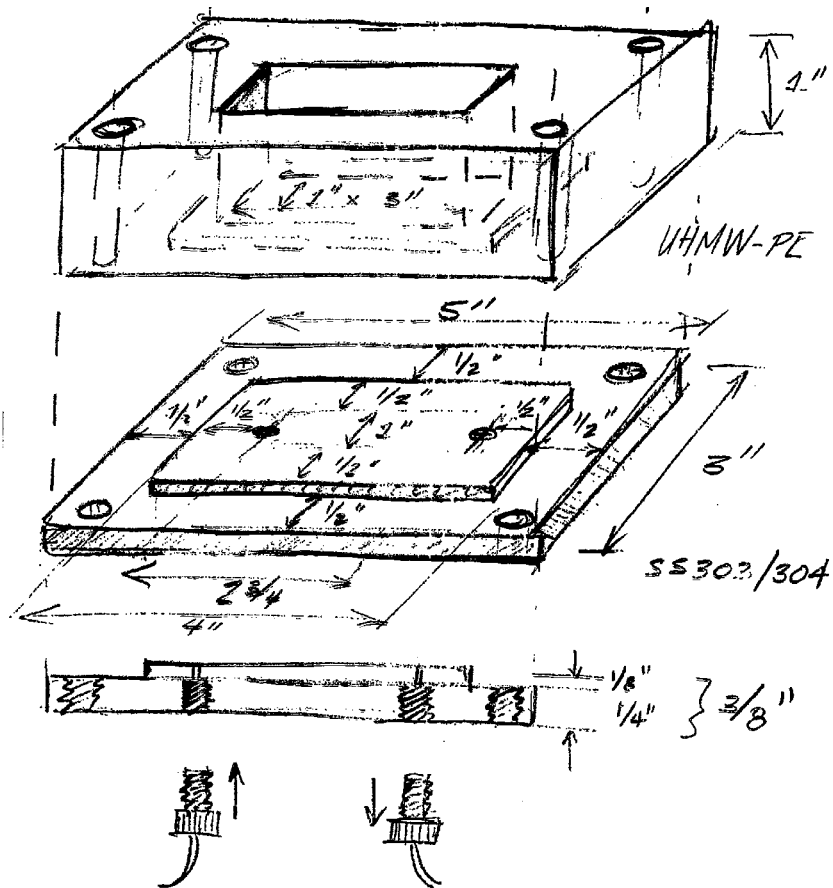


Figure 2-5: Second prototype sketch. Drawing made by ARS prior to fabricating the second prototype.



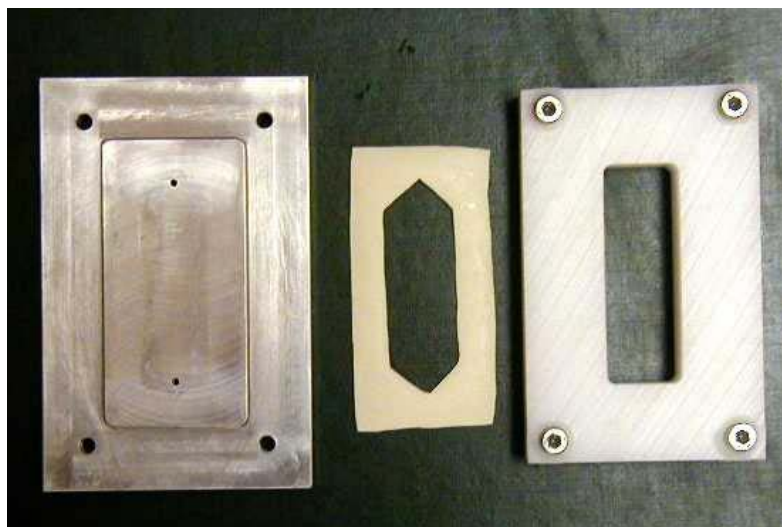


Figure 2-6: Second prototype photograph. Components of the second prototype from left to right: receptor phase inlet plate, receptor phase channel and donor phase tank. The membrane is not shown in this photograph.

The PDMS membranes were equilibrated overnight before placing them in the unit as shown in figure 2-4. The cell was attached to the HPLC pump and the LCQ as shown in figure 2-7. Saturated solutions of test chemicals were placed in the donor phase tank and the tank was sealed with parafilm to prevent evaporation. methyl and ethyl 4-hydroxybenzoate were tested. Data files were acquired using compound specific tune parameters in full scan mode.

Two experiments were performed using hairless mouse skin (SKH-hr-1, Charles River) obtained from Kenneth Sloan. The skin was equilibrated overnight in 50% ethanol/water before it was mounted in the cell. In the first experiment, a transdermal nicotine patch (Nicoderm CQ®, Bristol-Meyers) was applied to the skin. In the second experiment, a suspension of testosterone (Sigma, St. Louis, MO) in 50% ethanol/water was applied to a fresh piece of skin. Data files were acquired using compound specific tune parameters in full scan mode.

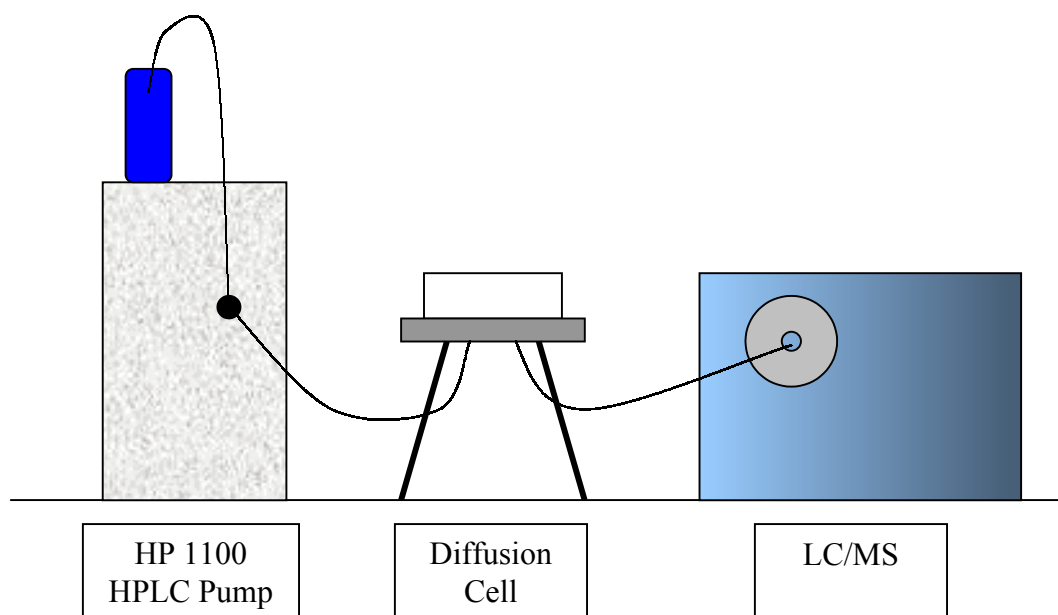


Figure 2-7: Second prototype schematic. The instrumentation schematic for the second prototype is displayed here. Figure is not to scale.

### Third Prototype

A third prototype was fabricated by ARS using one-half scale dimensions of the second prototype. The position of the inlet/outlet ports was also changed relative to the donor phase tank dimensions. All other aspects of the design remained unchanged from the second prototype. The revised cell is shown in figure 2-8. The order of instrumentation was also changed to draw receptor phase solvent through the cell, as shown in figure 2-9. This was the final design used in all subsequent testing described in specific aims two and three.

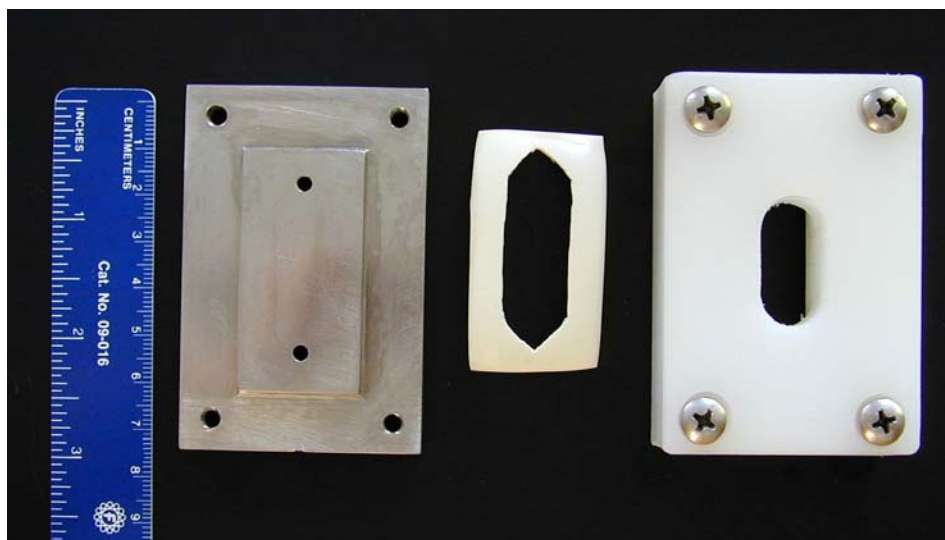


Figure 2-8: Third prototype photograph. Components of the third cell from left to right: receptor phase inlet plate, receptor phase channel, donor phase tank. The membrane is not shown. The receptor phase chamber is squared on the membrane contact side, but was left oval on the upper surface visible in the photograph.

### Specific Aim Two: Validation Testing

#### Membranes and Chemicals

Prolastic membranes were obtained (0.01" thickness) from Pillar Surgical Corporation (La Jolla, CA) with all of the membranes coming from a single production lot. Membranes were equilibrated overnight in 50% ethanol/water prior to use. Female hairless mouse skins (SKH-hr-1, Charles River) were a gift from Dr. Ken Sloan. Methyl 4-hydroxy benzoate was obtained from Fisher Scientific (Pittsburgh, PA). The Ethyl, propyl and n-butyl 4-hydroxy benzoate esters were obtained from Sigma/Aldrich (St. Louis, MO). The amyl and hexyl 4-hydroxy benzoate esters were obtained from TCI America (Portland, OR). The heptyl and octyl 4-hydroxy benzoate esters were obtained from Alfa Aesar (Ward Hill, MA). Ethanol was purchased from AAPER Chemical Company (Shelbyville, KY) and

distilled water was produced in house using a Megapure MP-1 still (Barnstead/Thermolyne Dubuque, IA). Saturated solutions of the permeants were prepared two days before use by adding an excess of chemical to 50% ethanol/water and leaving it to stir for at least 24 hours after saturation was reached. The solutions were filtered before use.

### Instrument Setup

Tuning. The LCQ was tuned for each of the probe chemicals by infusing a 100 µg/ml standard into a solvent stream entering the instrument. The solvent used was 50% ethanol/water introduced at a rate of 100 µl/min; this is the same rate used in the diffusion cell. The instrument's ion optic parameters were adjusted to maximize the signal for the probe compound. The APCI vaporizer temperature was set to 300 °C and the sheath flow was set to 30 units; auxiliary gas was not used. The capillary temperature was set to 150 °C. The corona discharge voltage was 4.5 kV. These settings were then saved as a tune file, to be used when evaluating samples and standards. This was done for each of the compounds.

Cell assembly. The cell was assembled as shown in figure 2-4 with the spacer sandwiched between the steel plate and the membrane. The instrumental configuration is shown in 2-9. Solvent was drawn from a reservoir by siphon into the diffusion cell and was transferred by the HPLC pump to the LCQ at a rate of 100 µl/min. The cell is situated 2-3 cm lower than the solvent reservoir to maintain a slight positive pressure head (figure 2-9). After filling the receptor phase chamber with solvent, the flow in the cell was allowed to equilibrate for 15 minutes with the pump running. A saturated solution of probe compound was then placed on the

membrane and the top of the tank was sealed with parafilm to prevent evaporation.

The LCQ was set to acquire data using the compound's tune file parameters.

Acquisition was performed in full scan mode and run times typically exceeded 5 hours. Each chemical was analyzed in triplicate.

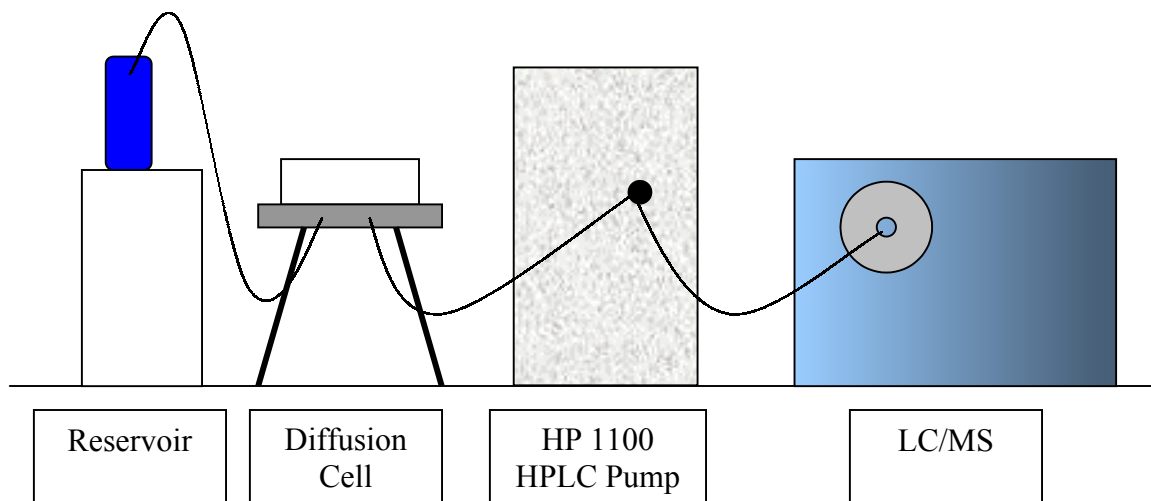


Figure 2-9: Third prototype schematic. The instrumentation schematic was changed for the third prototype. The cell now draws solvent from a reservoir via siphon action. The HPLC pump pulls the receptor phase through the cell and directs it to the LC/MS. Figure is not to scale.

Quantitation. Standard curves were prepared for quantitation. Standards were prepared as described above and 50  $\mu\text{l}$  aliquots were injected into the LCQ at a rate of 100  $\mu\text{l}/\text{min}$ . Data from the standards was acquired using the specific probe compound tune file. The relationship between response and concentration is assumed to be analogous to Beer's law for absorption. Specifically, a linear relationship exists between the magnitude of the instrument response and the concentration of the solution being infused. Relatively large volumes were injected to yield broad peaks and thereby simulate direct infusion. The intensity response was taken as an average

across the top of the standard peak, as shown by the region labeled "A" in figure 2-10, and was plotted versus concentration. The resulting plots were generally linear over a given concentration range, confirming the Beer's law assumptions (see figures A-1 and A-2 in appendix A). Linear response ranges generally do not span more than two orders of magnitude in ion trap mass spectrometers. Linear plots were fitted to data ranges surrounding the experimental value. The averaged response from the steady state region of the flux chromatogram was then regressed against the linear portion of the standard curve to calculate concentration. The LCQ reports data in scan intervals, so flux was calculated by the method below:

$$\begin{aligned} &(\text{Average minutes/scan})(\text{volume cleared/min})= \text{cm}^3/\text{scan} \\ \text{Flux} &= (\text{cm}^3/\text{scan})(\text{conc. mg/ml})/(\text{area})(\text{average min./scan})(60 \text{ min/h}) \\ &= \text{mg/cm}^2 \text{ h.} \end{aligned}$$

Solubility. Compound solubilities in water and ethanol/water were determined by preparing saturated solutions of each chemical as described above, then diluting as appropriate and measuring concentration by UV absorption using an HP 1100 single wavelength detector set to 254 nm, or by mass spectrometry using a Finnigan/MAT LCQ. Absorption or mass spec intensity values were regressed against a standard curve for each compound. Measurements were performed in triplicate.

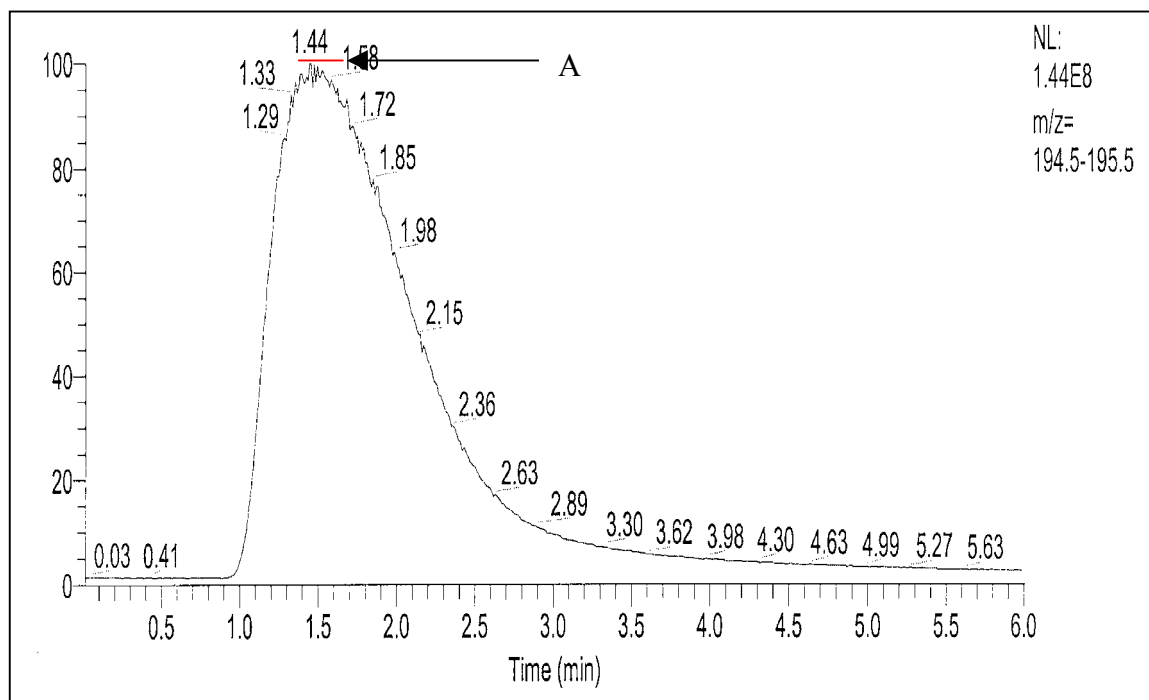


Figure 2-10: Quantitation.

### Effect of Ethanol on Permeability

Ethanol is known to enhance the penetration of chemicals through PDMS membranes.<sup>39,40,42,48</sup> In order to assess the nature of ethanol's effect with our compounds, a series of exposure experiments were performed. Caffeine was used as a reference compound because it should behave in a manner similar to theophylline, another commonly used probe compound. Theophylline has been shown to not damage skin.<sup>56,57</sup> It was felt that caffeine's lack of nitrogen bonded protons would make it less likely to chemically interact with the membrane. Membranes were washed in water and the flux of caffeine from a saturated solution in water was then

measured. The membranes were soaked over 12 hours in fresh water with two rinses to remove any caffeine remaining in the membrane. The flux measurements were then repeated.

To assess the effect of ethanol, a second set of flux measurements were taken using fresh membranes and solutions of caffeine in ethanol/water. The membranes were soaked overnight in 50% ethanol/water and then caffeine was applied in ethanol/water. After measuring the flux of caffeine, the membranes were washed over 24 hours in 50% ethanol/water with two solvent rinses. After equilibrating the membrane in water, the flux experiment was then repeated using caffeine in water.

#### LC/MS Diffusion Cell Validation

The flux of each member of the 4-hydroxybenzoate ester series from methyl to octyl (figure 2-11) was measured. Saturated solutions of each chemical in 50% ethanol/water were applied to PDMS membranes in the manner described above. Measurements were taken in triplicate. Data were acquired in full scan mode using each chemical's specific tune file parameters. Run times were typically 5 hours, but were extended to 8 for some of the larger compounds.

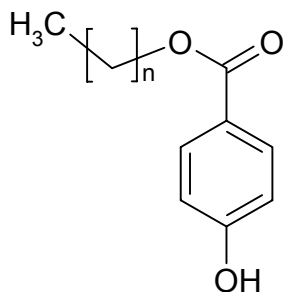


Figure 2-11: Ester series. The ester series of 4-hydroxybenzoic acid differ in the number of carbons on the carbonyl oxygen.



### Franz Cell

The fluxes of methyl, ethyl, propyl and n-butyl 4-hydroxybenzoate were also evaluated across PDMS sheeting using a Franz cell, under the guidance of Dr. Kenneth Sloan. The membranes were allowed to soak overnight in 50% ethanol/water to equilibrate. Squares measuring approximately 4x4 cm were cut from the sheets and mounted on the cells; the cells were maintained at 32 °C. Fresh receptor phase of 50% ethanol:water was placed in the lower chamber and saturated donor phase was placed in the upper chamber and covered with parafilm. The receptor phase was gently stirred during the experiment. The receptor phase was removed every 2 hours and stored in a tightly capped vial for analysis; the donor phase was replaced every 6 hours. Standards were prepared in 50% ethanol/water; standards and samples were analyzed using a Waters 996 photodiode array detector. Sample values were compared against a Beer's law standard curve with linear data fitting. The flux was calculated by plotting the cumulative amount penetrated vs. time and taking the slope of the line. This value was then normalized to the cell volume and membrane surface area.

### Hairless Mouse Skin, LC/MS Cell

Experiments using methyl, ethyl, and n-butyl 4-hydroxybenzoate were repeated with hairless mouse skin as a membrane in the LC/MS diffusion cell. Mice were sacrificed by cervical dislocation and the skin was harvested by blunt dissection. Skin was equilibrated overnight in 50% ethanol/water at 4°C before use. A section of the skin was cut to size and mounted in the cell. To determine how long a single section of skin would be useable, we performed a series of exposure/washout

experiments similar to those done with the PDMS membranes. Caffeine was applied as a saturated solution in 50% ethanol/water and the flux measured. The skin was then washed out overnight with fresh solvent (two rinses) and the caffeine was reapplied. This was performed a total of 3 times.

The fluxes of four 4-hydroxybenzoate esters, methyl through n-butyl, were determined by applying saturated solutions of each to skin. Data acquisition utilized the tune files generated for the PDMS experiments. Data was acquired in full scan with runs typically lasting eight hours.

### Specific Aim Three: Applications

#### Membranes and Chemicals

Mice were sacrificed by cervical dislocation and the skin was harvested by blunt dissection. Skin was equilibrated overnight in 50% ethanol/water at 4°C before use. Caffeine and theophylline were purchased from Sigma/Aldrich (St. Louis, MO). Testosterone was obtained from Sigma Chemical (St. Louis, MO). Ethanol was purchased from AAPER Chemical Company (Shelbyville, KY) and distilled water was produced in house using a Megapure MP-1 still (Barnstead/Thermolyne Dubuque, IA). Saturated solutions were prepared two days before use by adding an excess of chemical to 50% ethanol/water and stirring for at least 24 hours after saturation was reached. The solutions were filtered before use; only solutions (not suspensions) were applied.

### Mixture of Caffeine and Theophylline

A saturated solution was produced by first mixing the caffeine and theophylline in equal proportions, then adding excess of the mix to 50% ethanol/water. The solution was stirred for twenty-four hours past obvious saturation. The instrument was configured as described before and in figure 2-9. The solution was applied to the skin and receptor phase flow rate was set to 100  $\mu\text{l}/\text{min}$ . The APCI vaporizer temperature was 300  $^{\circ}\text{C}$ , the sheath flow was 30 units and the corona discharge was 4 kV. The LCQ was set to acquire data using the caffeine tune parameters. Previous experience had shown there to be only negligible differences between the caffeine and theophylline settings. Data was acquired in full scan mode.

Standard curves for both chemicals were prepared as previously described by dissolving them separately in 50% ethanol/water. Flux was calculated as described before.

### DEET and Permethrin

Commercial grade DEET was purchased at a local trail shop (Brasington's Adventure Outfitters, Gainesville, FL) as Ben's 100 Max (Tender Corp., Littleton, NH) and was reported to be 95% meta, 5% ortho and para isomers. Permethrin was purchased from ChemService Inc (West Chester, PA) as a crystalline standard.

To determine the nature of DEET's enhancement of dermal penetration, a repeat application study was performed. Hairless mouse skin (prepared as before) was mounted in the cell after equilibrating in 50% ethanol/water overnight. A saturated solution of caffeine was then applied and its flux through the skin measured. The skin was washed out overnight and a 20% solution (v/v) of DEET in 50%

ethanol/water was applied and its flux measured. After washing the DEET out overnight, caffeine was re-applied to determine if DEET permanently alters the skin's barrier properties.

A saturated solution of permethrin in 50% ethanol/water was prepared as described before. A 20% solution of permethrin in DEET (neat) was prepared by removing some of the un-dissolved permethrin from the ethanol solution, drying it and then dissolving it in DEET (neat). This was done as we had exhausted our supply of crystalline permethrin. This unconventional technique would prove to be informative later. Separate formulations of permethrin alone (alcohol vehicle), DEET alone and permethrin + DEET were applied to mouse skin and the flux of each measured. Chromatographic data were regressed against standard curves as described in specific aim two.

### Testosterone

A saturated solution of testosterone was prepared by dissolving an excess in 50% ethanol/water. The solution was stirred for twenty-four hours past obvious saturation. The LCQ was tuned by infusing a 100 µg/ml solution of testosterone in 50% ethanol/water into the APCI source. The source temperature was 300°C, the sheath flow was 30 units and the corona discharge voltage was 4 kV. A saturated solution of testosterone was applied to the skin and the donor phase chamber was sealed with Parafilm® to prevent evaporation. Data was acquired for 20 hours in full scan mode using the testosterone tune file parameters. A standard curve for testosterone was prepared and quantitation was performed as previously described. Experiments were performed in triplicate.

## CHAPTER 3 RESULTS

### Specific Aim 1

#### MIMS Probe

No useful data were generated from the MIMS probe experiments. The method for attaching a membrane to the unit consistently resulted in leaks, or a rupture.

#### First Prototype

The first prototype proved capable of producing useful flux data. The chromatograms produced using this cell are shown in figure 3-1. These show the lag time and steady-state flux for n-butyl 4-aminobenzoate, and theophylline. The lag time for n-butyl 4-aminobenzoate corresponded to those reported by Flynn *et. al* <sup>19,58</sup> for the same and similar compounds. The device proved not to be robust enough to withstand extensive testing, so further experiments were not conducted using the first prototype.

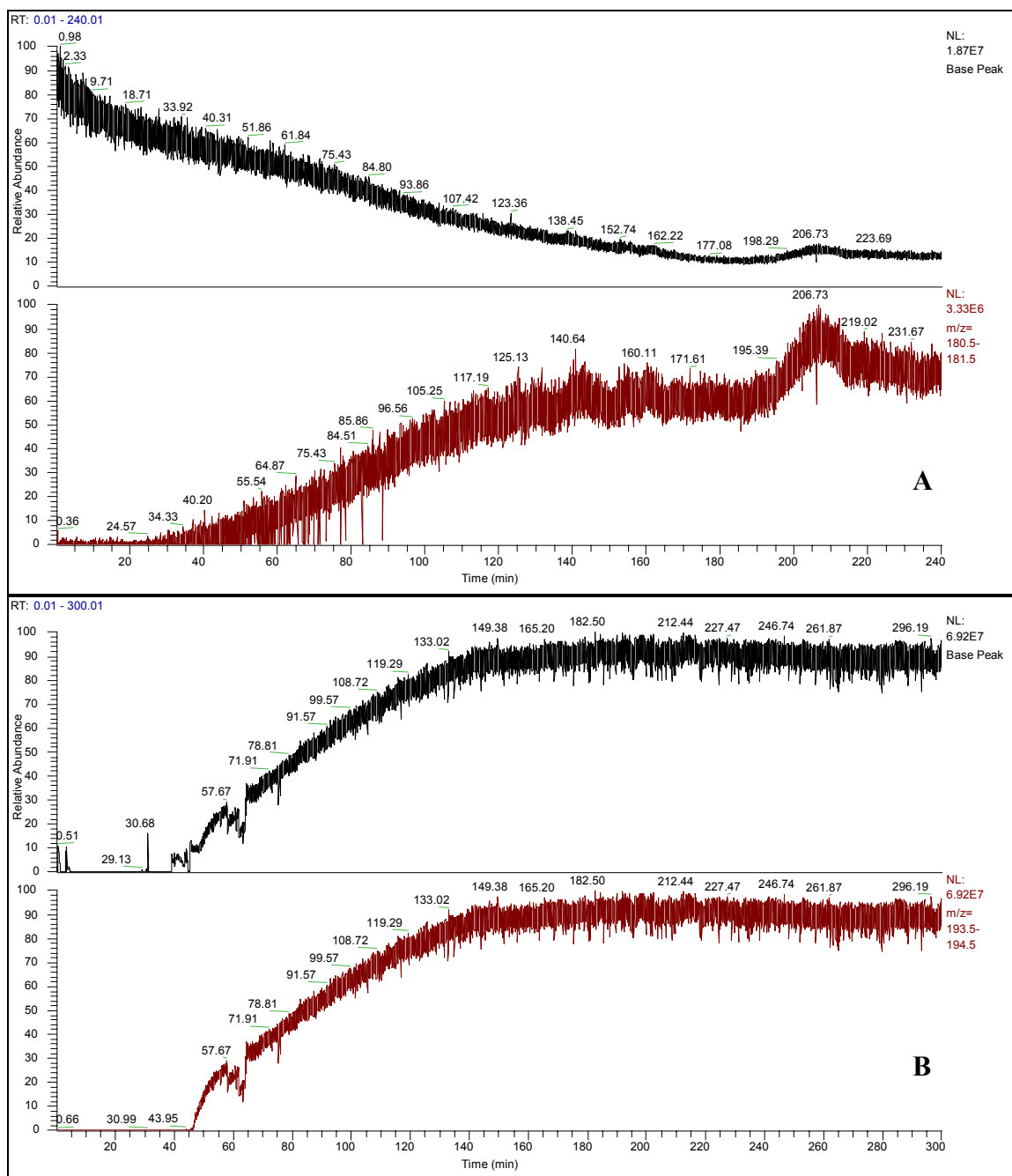


Figure 3-1: Representative flux chromatograms; first prototype. A: Theophylline. B: n-Butyl 4-Aminobenzoate. The upper panel in each chromatogram is the total ion current. The lower panel is the signal filtered for the molecular weight of the chemical.

## Second Prototype

PDMS membranes. The second prototype was able to provide reproducible data and withstand extensive handling (the first prototype was extremely delicate and survived only a handful of experiments). Typical spectra are shown in figure 3-2. Determining quantitative flux values using this device proved difficult for a number of reasons. First, the cell was driven in a positive pressure mode; the HPLC pump pushes solvent through the cell, into the LCQ. The resultant pressure tended to distend the membrane, often severely. Minor variations in the cell height relative to the LCQ inlet had noticeable effects on the degree of distension. The effective membrane surface area and the receptor phase volume, and subsequently the flux, was impossible to determine in a reproducible manner. A second problem was a design flaw in the dimensional relationship between the donor and receptor phase chambers. The shape of the donor phase membrane surface differed from that of the receptor phase; figure 3-3 illustrates the nature of the problem.

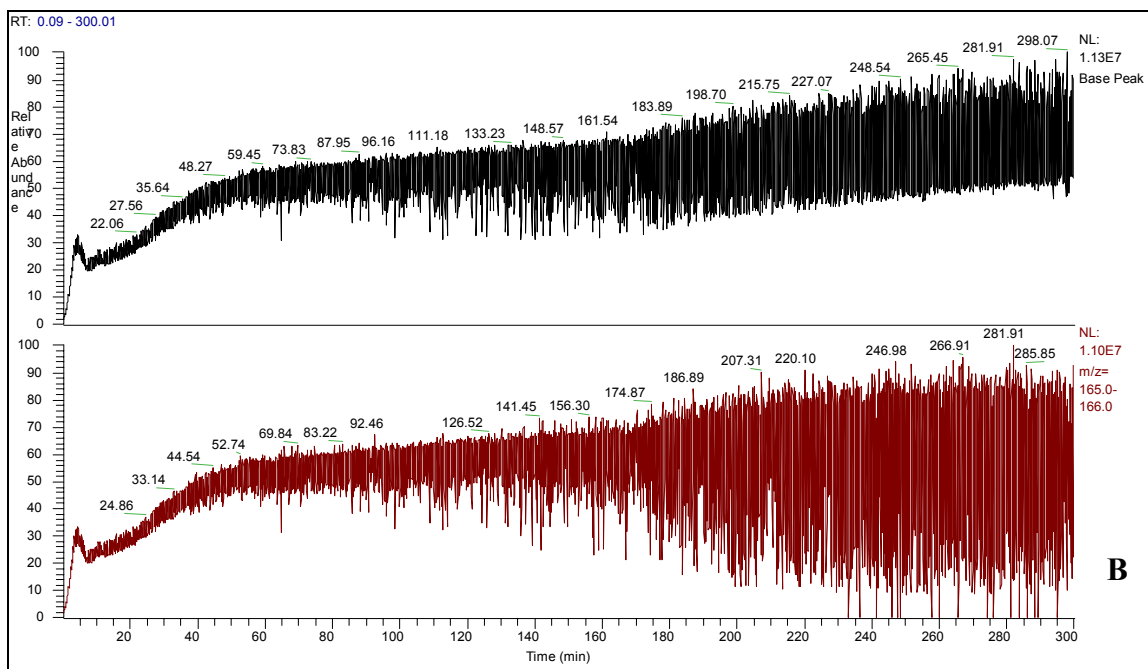
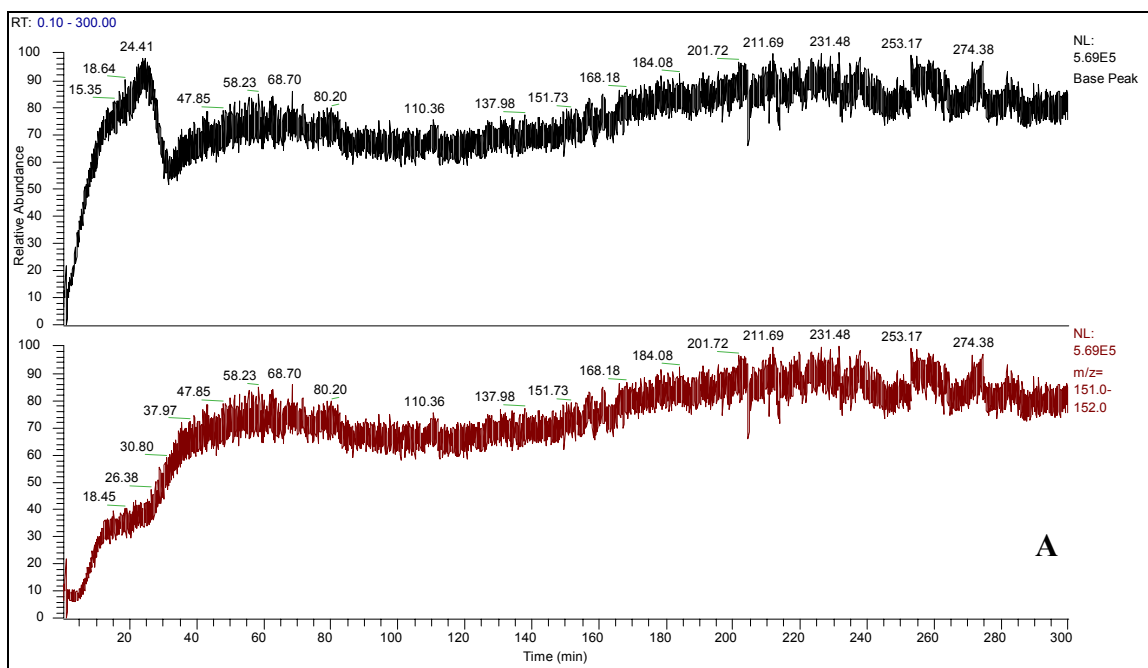


Figure 3-2: Flux chromatograms: second prototype. A: Methyl 4-Hydroxybenzoate; B: Ethyl 4-Hydroxybenzoate. The upper panel in each chromatogram is the total ion current. The lower panel is the signal filtered for the molecular weight of the chemical.



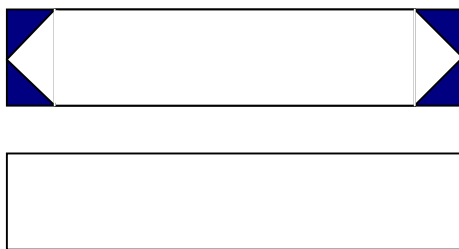


Figure 3-3: Chamber problem, second prototype. The input (upper figure) and receptor (lower figure) geometries are not equivalent.

Mouse skin. The results of an application of testosterone to hairless mouse skin are shown in figure 3-4. While testosterone normally requires the addition of a radio-label for detection in transdermal studies, its flux is clearly visible using the second prototype. Quantitative measurements were not done for the reasons stated above. The results of a nicotine patch application to hairless mouse skin are shown in figure 3-5. Again, quantitative measurements were not made for the reasons stated above.

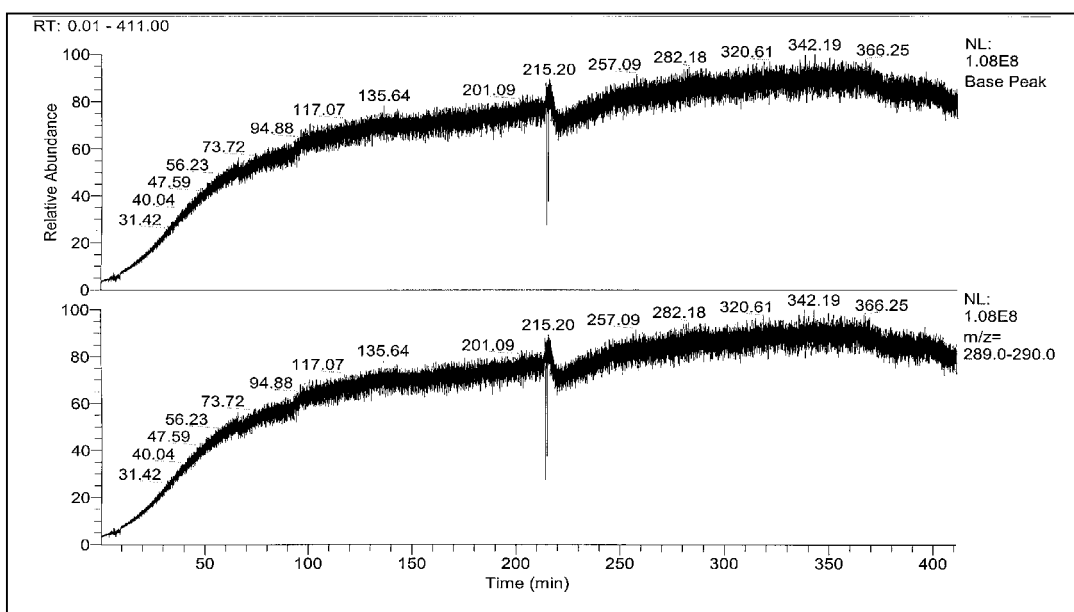


Figure 3-4: Testosterone flux chromatogram: second prototype. The flux of testosterone from an ethanol suspension through hairless mouse skin is shown. The upper panel is the total ion chromatogram and the lower is filtered for the molecular weight of testosterone.

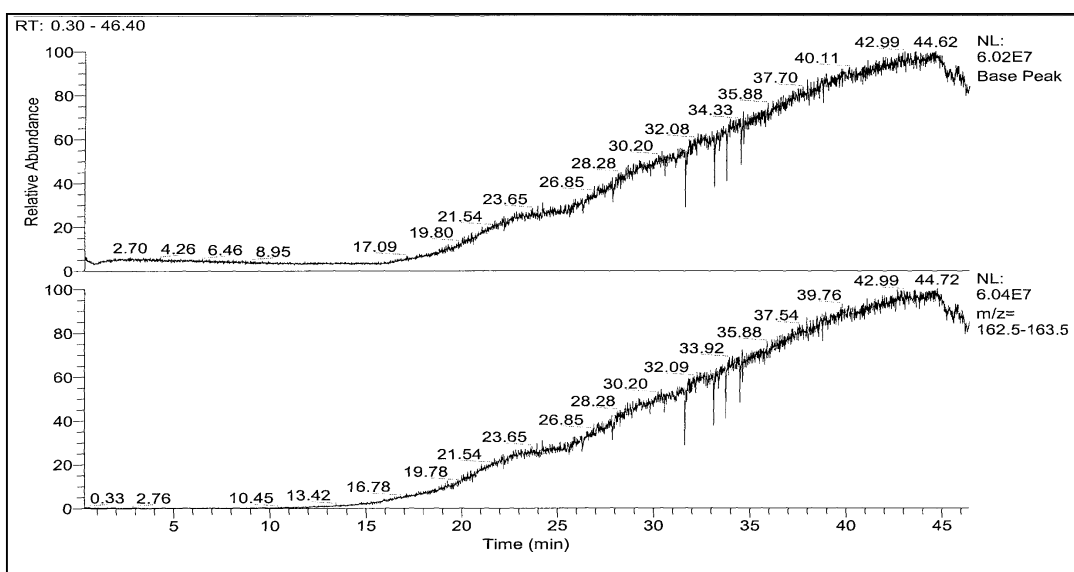


Figure 3-5: Nicotine flux chromatogram: second prototype. The flux of nicotine from a Nicoderm CQ® transdermal patch through hairless mouse skin is shown. The upper panels is the total ion chromatogram, while the lower is filtered for the molecular weight of nicotine.

## Specific Aim 2

### Solubility Values

The water and solvent (50% ethanol/water) solubility values for the 4-hydroxybenzoate series are listed in table 3-1. The water solubility data shows a regional peak at the amyl ester (figure 3-6). The solvent solubility data contain more variability than the water solubility values. The vehicle (50% ethanol/water) solubility values trend downward, with an exception again occurring at the amyl ester. The break between propyl and n-butyl corresponds to a change from crystalline to liquid excess solute formed at saturation. The vehicle solubility values are plotted in figure 3-7.

Table 3-1. Solubility vs. carbon number for esters of 4-hydroxybenzoic acid. All values are in mg/ml.

<b>Carbon number</b>	<b>Swater</b>	<b>+/- S. D.</b>	<b>Ssolvent</b>	<b>+/- S. D.</b>
1	2.199	0.026	100.706	0.686
2	1.084	0.026	87.528	6.047
3	0.557	0.017	87.773	2.876
4	0.084	0.030	53.692	15.041
5	0.137	0.017	71.080	19.397
6	0.028	0.019	23.951	5.273
7	0.005	0.001	17.461	4.150
8	0.005	0.001	12.129	4.543

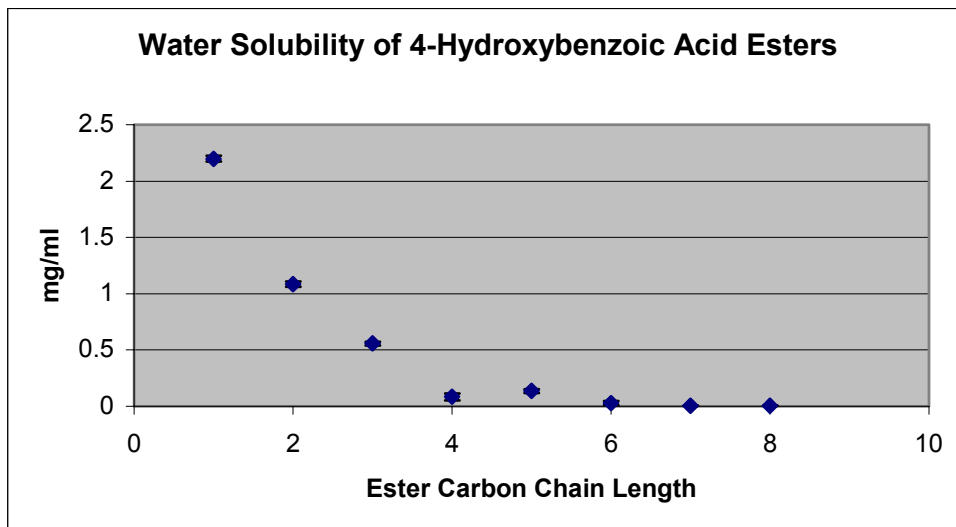


Figure 3-6: Water solubility of the 4-hydroxybenzoate ester series plotted vs. carbon number.

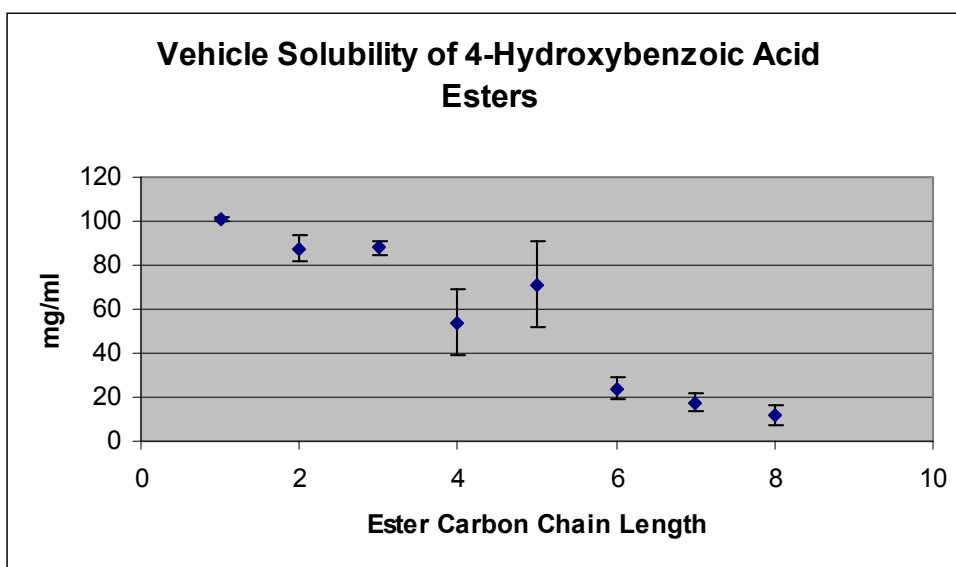


Figure 3-7: Vehicle (50% ethanol/water) solubility of the 4-hydroxybenzoate ester series plotted vs. carbon number.

#### Effect of Ethanol on Permeation

The flux values of caffeine from water and solvent for serial applications are shown in table 3-2. The first two columns show the difference in flux for serial

applications of saturated solutions of caffeine in water. The ethanol/water data show the flux of caffeine from water is reduced through PDMS membranes that have been pre-treated with a saturated solution of caffeine in 50% ethanol/water. The membranes were washed overnight in clean solvent (ethanol/water), equilibrated in water, and then a saturated solution of caffeine in water was applied. All flux units are in  $\text{mg}/\text{cm}^2 \text{ h}$ . Reapplication of caffeine in water does not change the membrane characteristics. Serial applications of caffeine in water do not seem to alter the membrane, as first and second application flux values are nearly identical. Serial applications of caffeine in solvent (50% ethanol/water) followed by caffeine in water, separated by an overnight wash-out interval in ethanol/water, show a decrease in caffeine flux from water compared to membranes pretreated with water only (figure 3-8); the difference is significant at a p value of 0.02 using the student's t-test.

Table 3-2: Comparison of caffeine flux through PDMS membranes from water and ethanol:water.

<b>Flux (<math>\text{mg}/\text{cm}^2 \text{ h}</math>)</b>					
<b>membrane</b>	<b>Water</b>		<b>membrane</b>	<b>Ethanol:Water</b>	
	<b>Run 1</b>	<b>Run 2</b>		<b>Run 1 E:W</b>	<b>Run 2 W</b>
<b>1</b>	<b>2.10E-02</b>	<b>2.58E-02</b>	<b>1</b>	<b>3.06E-02</b>	<b>9.60E-03</b>
<b>2</b>	<b>1.56E-02</b>	<b>1.80E-02</b>	<b>2</b>	<b>2.70E-02</b>	<b>1.50E-02</b>
<b>3</b>	<b>2.88E-02</b>	<b>1.98E-02</b>	<b>3</b>	<b>3.36E-02</b>	<b>1.74E-02</b>
<b>4</b>	<b>3.00E-02</b>	<b>2.94E-02</b>	<b>4</b>	<b>4.74E-02</b>	<b>1.38E-02</b>
<b>5</b>	<b>3.06E-02</b>	<b>2.52E-02</b>	<b>5</b>	<b>5.70E-02</b>	<b>1.68E-02</b>
<b>6</b>	<b>1.68E-02</b>	<b>2.64E-02</b>	<b>6</b>	<b>5.82E-02</b>	<b>1.26E-02</b>
Average	2.38E-02	2.41E-02		4.23E-02	1.42E-02
SD	6.84E-03	4.32E-03		1.37E-02	2.88E-03

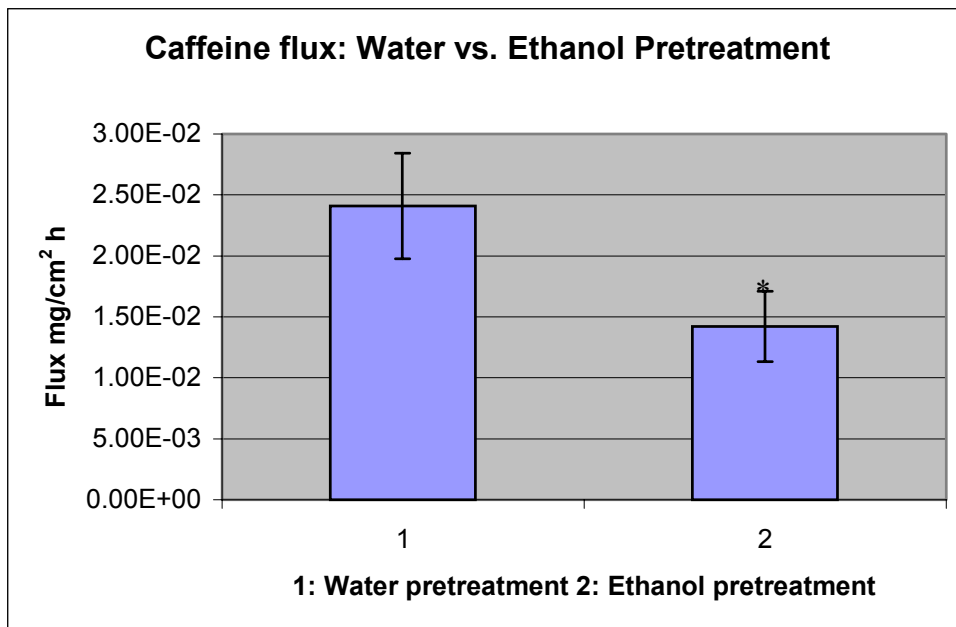


Figure 3-8: Effect of water vs. ethanol/water pretreatment on caffeine flux through PDMS. Student's t-test \*  $p = 0.02$ .

#### Validation Test: LC/MS Cell

The flux values of methyl to octyl 4-hydroxybenzoate are listed in table 3-3 and are plotted vs. carbon number in figure 3-9. The value for heptyl 4-hydroxybenzoate was omitted, as it was clearly an outlier; the heptyl value was over an order of magnitude lower than any of the other series members. Examination of the chromatograms and data-files generated for the heptyl run indicate that the LCQ was not functioning properly.

Table 3-3: Flux values for members of the 4-hydroxybenzoate series.

<b>Ester</b>	<b>flux (mg/cm<sup>2</sup> h)</b>	<b>+/- S. D.</b>
methyl	0.40	0.10
ethyl	0.43	0.01
propyl	0.49	0.04
butyl	0.91	0.15
amyl	1.21	0.19
hexyl	1.06	0.15
octyl	0.82	0.04

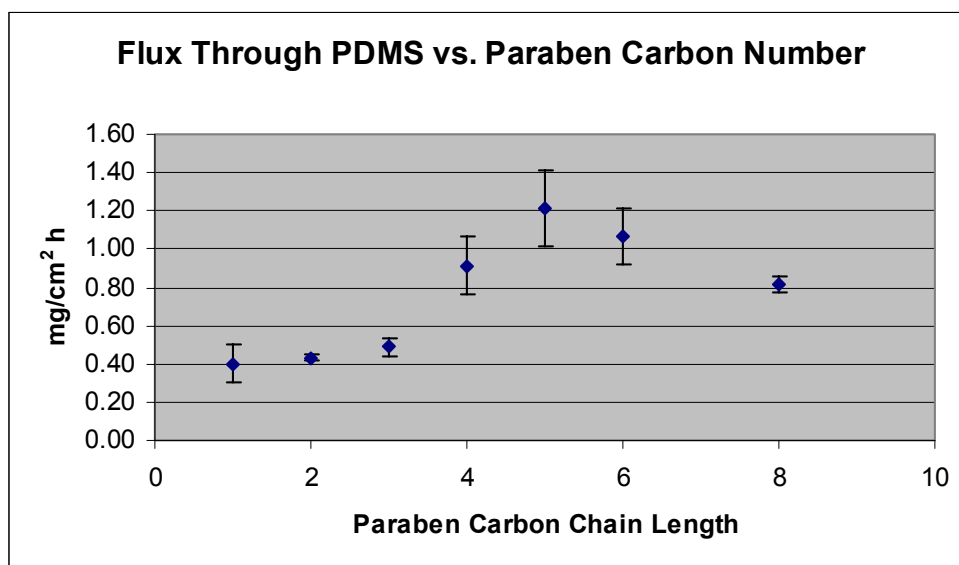


Figure 3-9: Flux of the 4-hydroxybenzoate ester series through PDMS membranes from saturated ethanol/water solutions. The flux values are plotted vs. carbon number of the alkyl chain on the ester.

#### Validation Test: Franz Cell

The flux values of four esters of 4-hydroxybenzoic acid are shown in table 3-

4. The data are graphically presented in figure 3-10. A comparison between the

LC/MS and Franz cell values is made in figure 3-11. The values from the LC/MS cell, while being consistently larger, follow the same general rank order and display the same trend as those measured using the Franz cell.

Table 3-4: Flux values: Franz vs. LC/MS.

Static vs. LC/MS Cell				
Carbon	Franz		LC/MS	
number	mg/cm <sup>2</sup> h	s.d.	mg/cm <sup>2</sup> h	s.d.
1	0.28	4.00E-03	0.40	1.00E-01
2	0.29	4.00E-03	0.43	1.00E-02
3	0.31	2.50E-02	0.49	4.24E-02
4	0.39	5.00E-03	0.91	1.50E-01

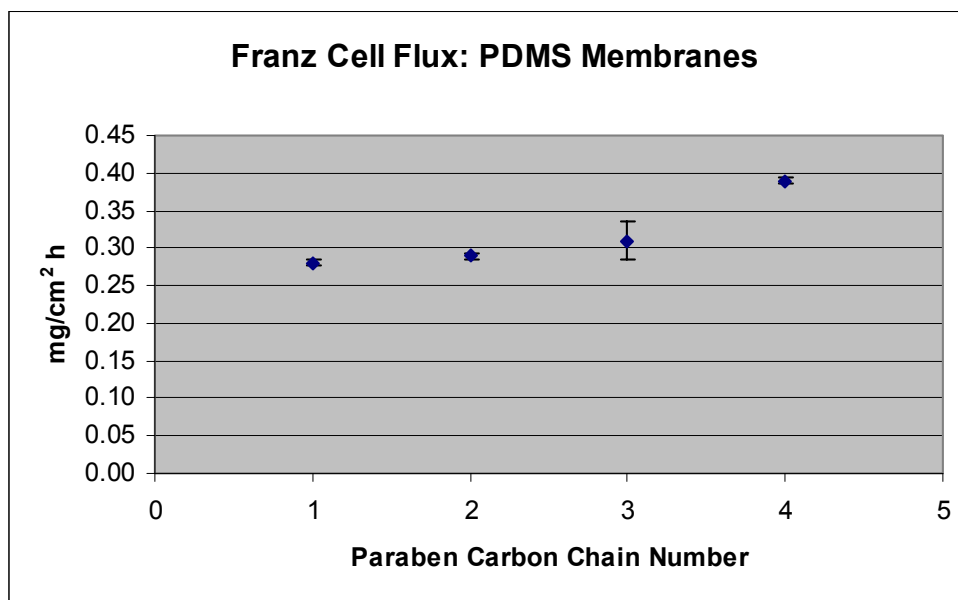


Figure 3-10: Plot of paraben series fluxes. Saturated solutions of each paraben in 50% ethanol/water were applied to PDMS membranes held in a Franz diffusion cell.



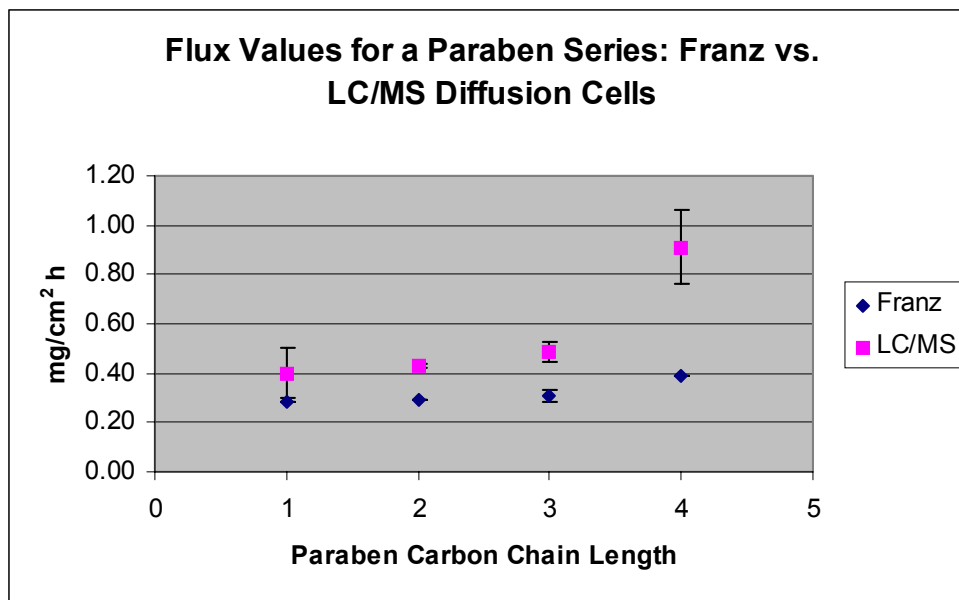


Figure 3-11: Comparison of flux values from Franz (static) and LC/MS diffusion cells. Saturated solutions of each paraben in 50% ethanol/water were applied to PDMS membranes.

#### LC/MS Validation: Mouse Skin.

The results of multiple caffeine applications to mouse skin are shown in figure 3-12. The caffeine flux values are steady over the first two applications before increasing at the third. While the flux values increase from the second to the third application, the standard deviations overlap, so there is no statistical difference. A full twenty-four hours (application plus wash-out) separated each application.

The flux values for methyl, ethyl and propyl 4-hydroxybenzoate across mouse skin are plotted in comparison to the corresponding PDMS values in figure 3-13.

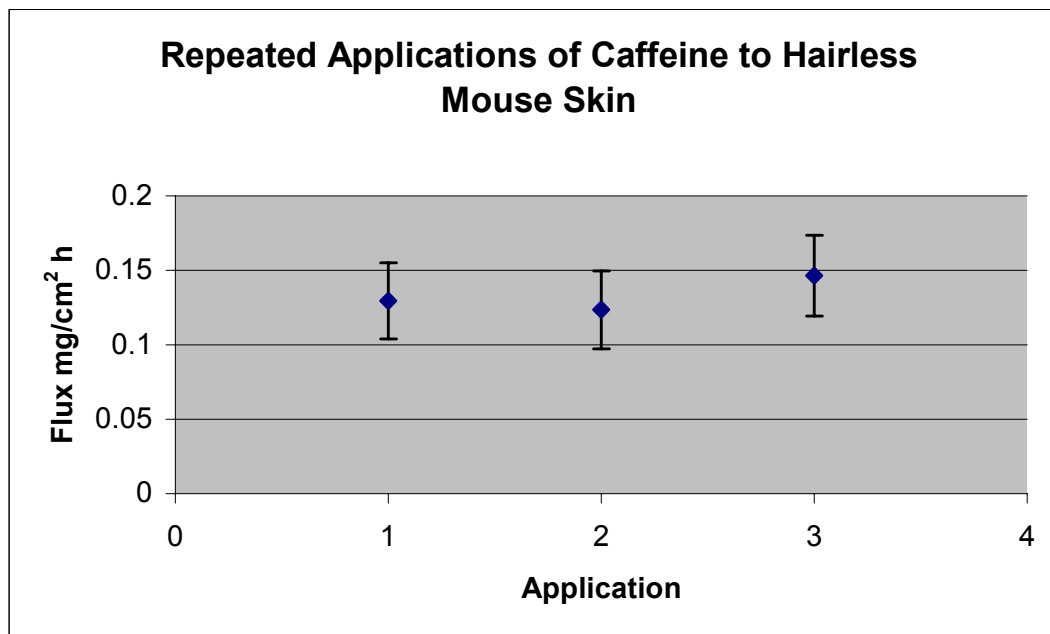


Figure 3-12: Repeated applications of caffeine to hairless mouse skin.

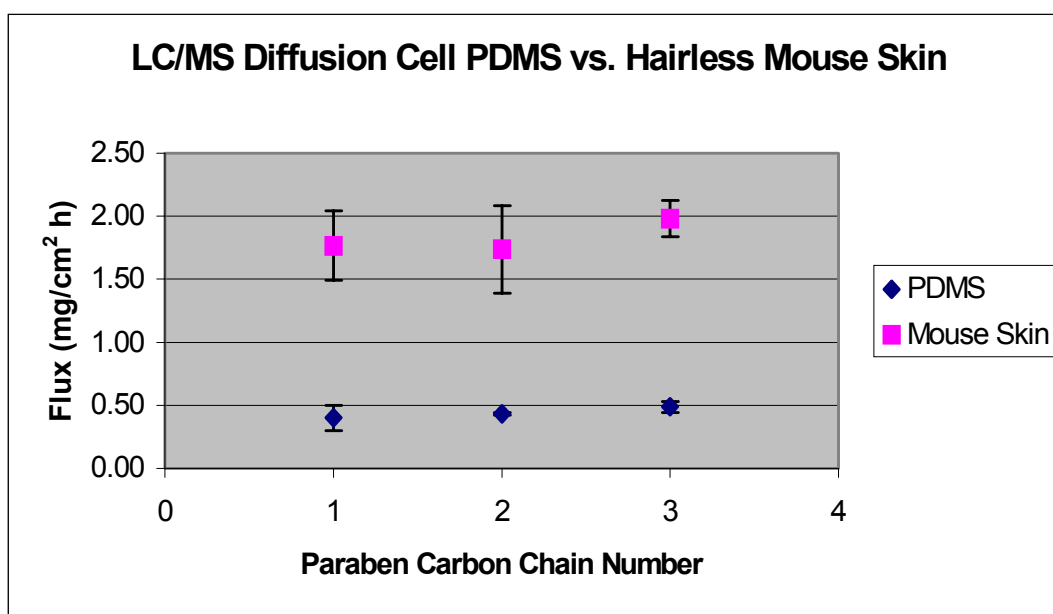


Figure 3-13: LC/MS diffusion cell, PDMS vs. hairless mouse skin.

Specific Aim 3Chemical Mixture: Caffeine and Theophylline

The chromatogram in figure 3-14 shows the ability of the LC/MS cell to resolve a mixture of caffeine and theophylline as it passes through hairless mouse skin. The upper panel is the total ion chromatogram generated by scanning from 100-500 m/z. The middle panel shows the signal filtered for the molecular weight of theophylline (M+1 181 amu) and the third panel is the signal filtered for caffeine (M+1 195). Table 3-5 shows the flux values for caffeine and theophylline through hairless mouse skin measured using the LC/MS cell.

Table 3-5: Hairless mouse skin flux values.

<b>Flux mg/cm<sup>2</sup> h</b>			
<b>Replicate</b>	<b>Caffeine</b>	<b>Theophylline</b>	<b>Testosterone</b>
1	0.04	0.06	0.19
2	0.10	0.08	0.19
3	0.05	0.05	0.10
4	0.07	0.03	
5	0.08	0.04	
<b>Average</b>	0.07	0.05	0.16
<b>+/- s.d.</b>	0.02	0.02	0.05

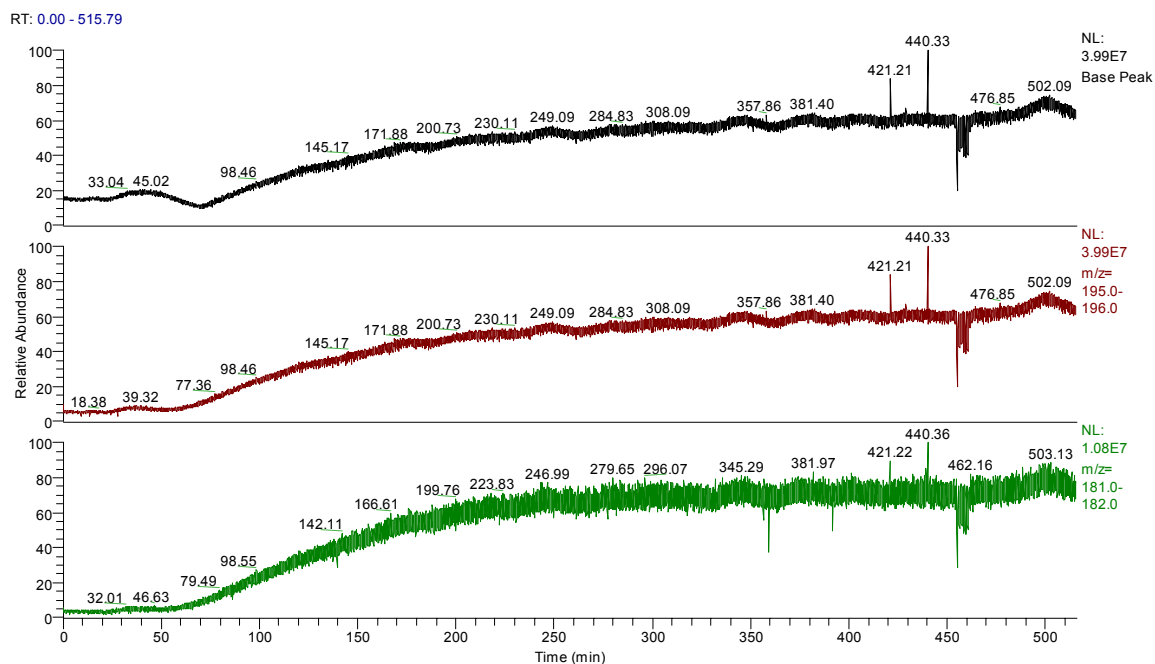


Figure 3-14: Flux of a caffeine/theophylline mixture. The upper panel is the total ion chromatogram. The second and third panels are the signal filtered for the molecular weights of caffeine and theophylline, respectively.

### Testosterone

Figure 3-15 shows the flux of testosterone across hairless mouse skin from a saturated solution in 50% ethanol/water. The chromatogram is filtered for the molecular weight of testosterone (M+1 289). The flux value of testosterone using the LC/MS cell is listed in table 3-5.

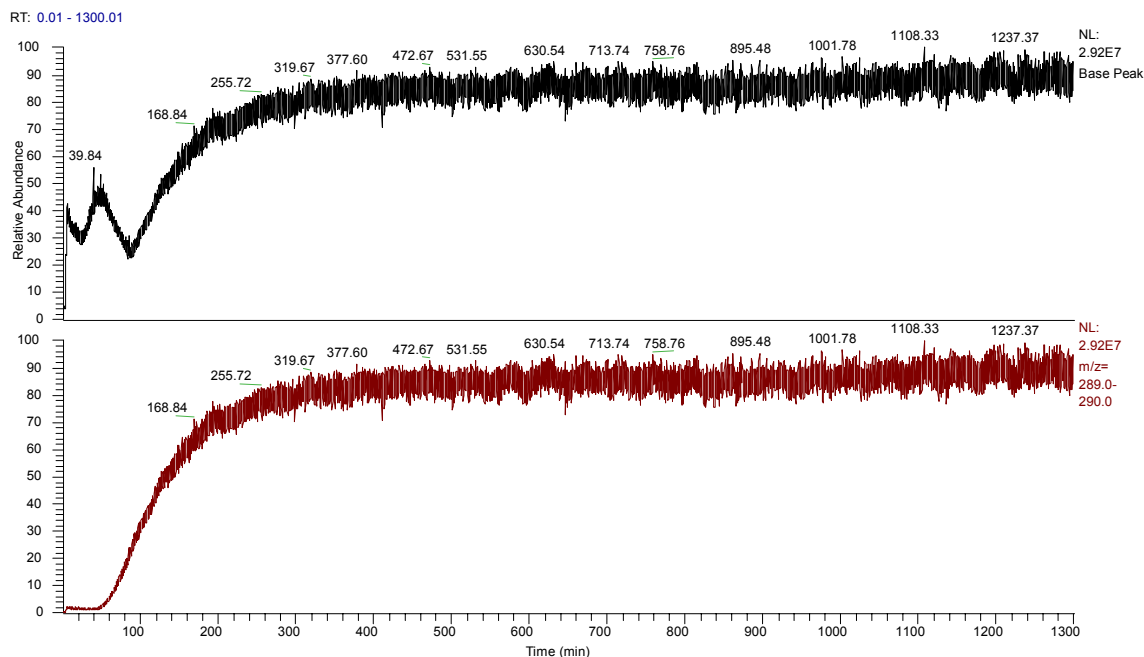


Figure 3-15: Testosterone flux through hairless mouse skin. The upper panel is the total ion chromatogram. The lower panel shows the signal filtered for the molecular weight of testosterone.

#### Chemical Mixture: DEET and Permethrin

The flux of DEET through hairless mouse skin is shown in the uppermost panel of figure 3-16. The flux of permethrin was surprisingly not observed. However, a chemical of molecular weight  $M+1=383$  was observed to be penetrating the skin, shown in the middle panel of figure 3-16. Direct injection of the ethanol/permethrin saturated solution into the LC/MS showed the presence of the  $m/z$  383 molecule and the absence of permethrin. A molecular weight of 383 is consistent with permethrin after undergoing a solvolysis reaction as shown in figure 3-17. The lack of the  $Cl^{35}:Cl^{37}$  isotope ratio signature in the mass spectrum of figure 3-16 is also consistent with the proposed mechanism. Were the molecule di-chlorinated (as

permethrin is) a ratio of 100:65:10 would have been seen for the X, X+1 and X+2 ions respectively; a singly chlorinated molecule would have had a ratio of 100:32.5, for the X: X+1 ions.

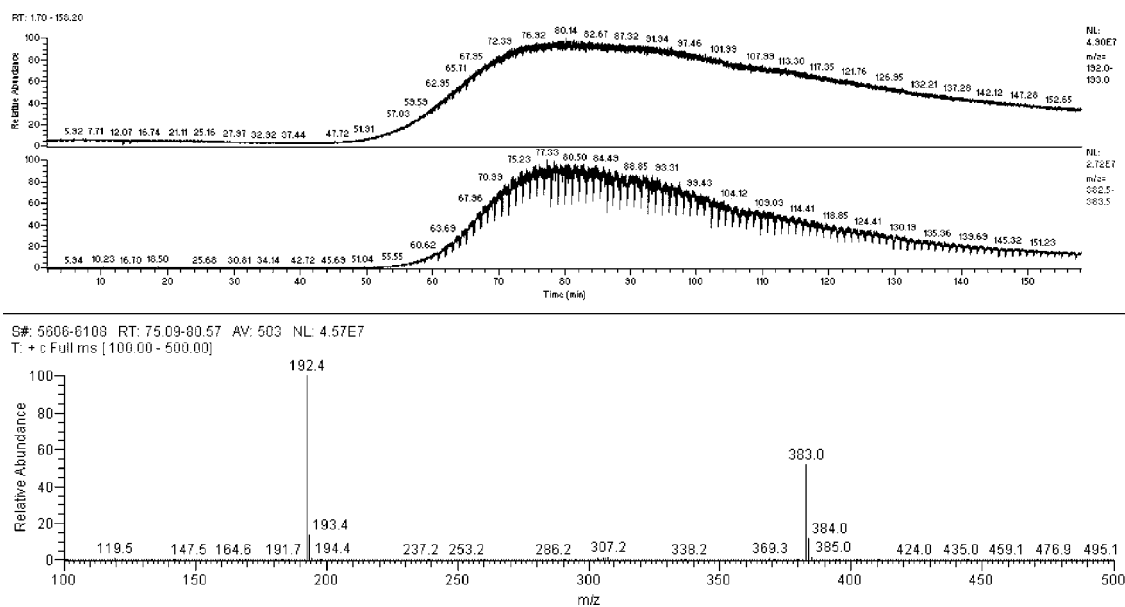


Figure 3-16: Flux of DEET + m/z 383 molecule.

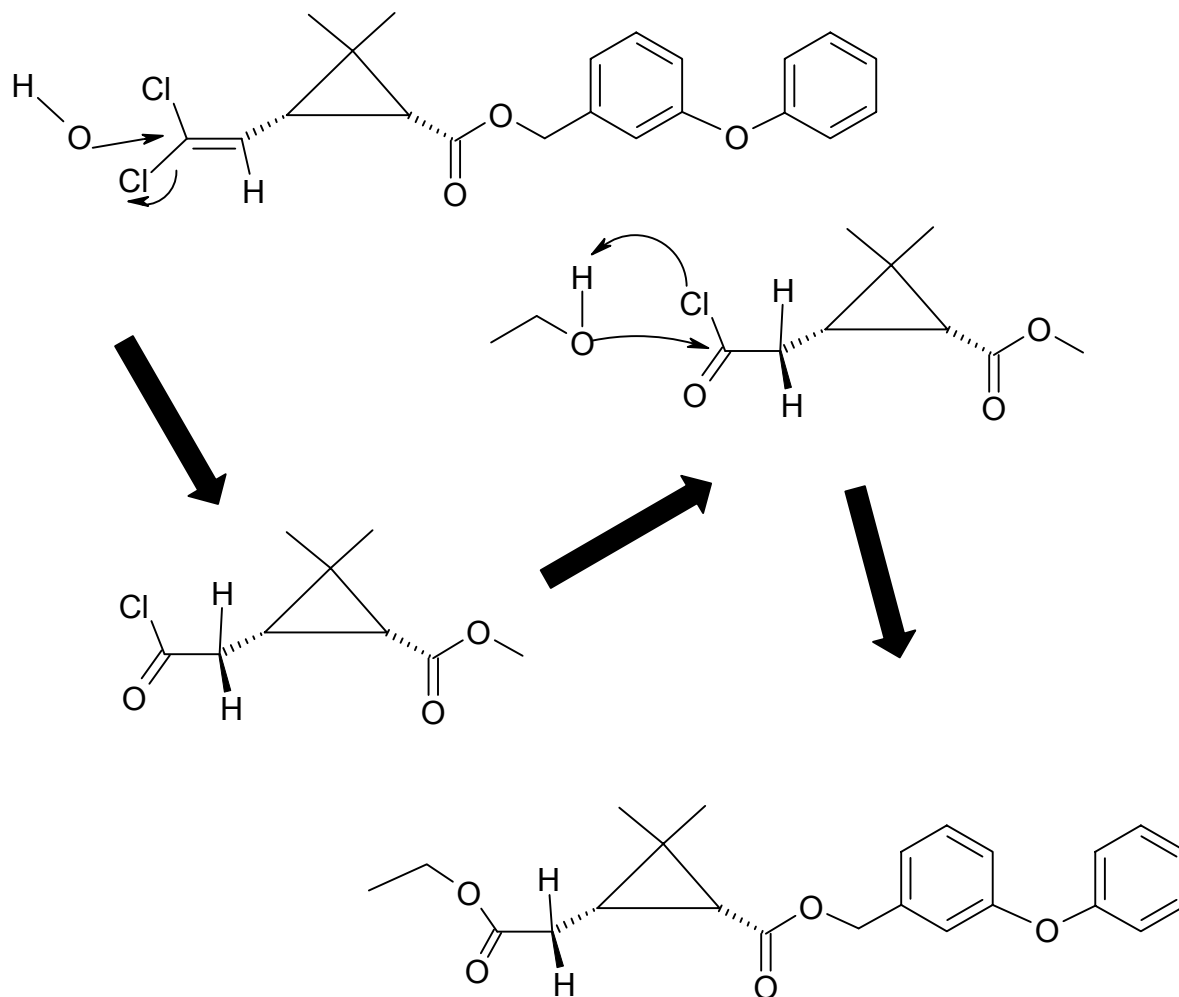


Figure 3-17: Possible permethrin solvolysis mechanism. Mechanism suggested by Ken Sloan.

## CHAPTER 4 DISCUSSION

### Specific Aim One: Cell Construction

The goal of this work was to construct a diffusion cell that could be coupled to an LC/MS detector while operating in a continuous flow mode. The device would need to function without frequent monitoring by laboratory personnel. The cell would have to be comparable in operation and performance to the widely used Franz cell.

### Membranes and Probe Chemicals

During the development of the transdermal diffusion cell, PDMS membranes were chosen for the performance evaluation phase because a large body of data exists regarding the flux values of various chemicals through them. At one time PDMS membranes were considered as a surrogate for skin in transdermal experiments. In particular, several researchers [39,40,42,48,49](#) have collected data regarding the flux of the p-amino and p-hydroxyl benzoate ester series, as well as a variety of other chemicals, [35,36,50-54,59](#) through PDMS membranes. They found that a direct correlation between rates of diffusion through PDMS membranes and skin could not be established for a wide range of chemicals. However, in the course of these investigations, a large number of flux values were reported in the literature. Since the goal was to produce a device that mimicked the kinetics of classic Franz diffusion cells, this data set provided us with a base from which to work.



A second reason for using a PDMS membrane in the design phase was associated with its physical properties. The membranes are physically rugged, chemically uniform and not subject to spoilage, all traits not shared by the more commonly used membrane, hairless mouse skin. Additionally, PDMS requires little prep-time and can be stored ready for use. This makes it ideal for prototype work where modifications are numerous and would have required a large supply of animals to be kept on hand. Using the PDMS membranes also eliminated the regulatory complications associated with animal experimentation.

The PDMS membranes used by previous authors were produced by Dow-Corning under the trade name of Prolastic®. In the interval since those works were published, Dow-Corning has ceased production of Prolastic® membranes. The formulation and production rights were transferred to Pillar Surgical (La Jolla, CA), which now produces the Prolastic® line of products; Prolastic® sheeting was procured in 0.01" thickness, the same as used in the references.

The choice of chemicals used for the initial trials were based on previous studies by two groups: Twist and Zatz <sup>39,48,60</sup> and Flynn *et al.* <sup>19,29</sup> They had studied the p-hydroxyl- and p-aminobenzoate ester series, respectively, from methyl to butyl with an eye toward describing the physical and chemical processes at work in diffusion through PDMS membranes. These compounds provided the graded range of polarity and water solubility required for describing the diffusion phenomenon as well as for constructing predictive models of dermal penetration. In addition, the methyl and ethyl esters of both series have been used in pharmaceutical and cosmetic preparations as preservatives and stabilizers. A mixture of 50% ethanol/water was

used as the donor and receptor solvents based on previous work.<sup>18,39,48,49</sup> The ethanol/water mix allows for the dissolution of hydrophobic compounds as well as retarding microbial growth in the diffusion cell when utilizing animal skin.

All diffusion experiments were performed using a balanced cell apparatus, meaning that the donor and receptor phase solvents were identical. This was done to eliminate issues of solvent counter current diffusion that can occur in an unbalanced system. This is when solvent from the receptor phase enters the donor chamber by osmotic diffusion and as a result, the donor phase composition changes over the course of an experiment. For testing purposes, a simple system free of extraneous issues was desired. Buffer systems were avoided as non-volatile salts will block the LC/MS inlet.

### Prototype Construction

#### MIMS probe

The first attempts at construction of a suitable flow through diffusion cell centered on converting an existing Membrane Inlet Mass Spectrometer (MIMS) probe (MIMS Technology Inc., Palm Bay, FL) (figure 2-1). The MIMS probe was originally designed to act as a direct injection probe for the introduction of volatile chemicals into the vacuum chamber of a mass spectrometer.<sup>55,61</sup> A liquid sample was passed through a chamber on the end of the probe, which was inserted into the mass spectrometer's direct injection port. A membrane separated the liquid sample from the high vacuum chamber. Volatile molecules could pass through the membrane into the mass spectrometer, leaving salts and other non-volatile materials behind. In a sense, the membrane functioned as a filter.

It was reasoned that the probe could be used as a diffusion cell merely by reversing the direction of diffusional flow. The probe was configured as shown in figure 2-3. However a number of problems with this approach became evident. Flux through a membrane is measured in terms of amount per unit time and area; it is typically expressed as  $\text{mg}/\text{cm}^2 \text{ h}$ . In absolute terms, the limit of detection for a diffusion cell is directly related to the surface area of the membrane available to the donor and receptor phases. The MIMS probe has a very small ( $> 0.2 \text{ cm}^2$ ) area available for diffusional exchange. Based on the volume of receptor phase cleared per hour and per square cm of membrane in the classic cell, it was determined that a flow rate of  $10 \mu\text{l}/\text{min}$  would be required using the MIMS probe to maintain sink conditions. This flow rate was achieved using a syringe pump. Even at this low rate of flow, problems maintaining a leak proof seal between the membrane and the probe body were encountered. High pressures would cause the membrane and o-ring assembly to extrude from the retaining ring, resulting in a leak. Increasing the tightness of the retaining ring often caused the inlet or outlet channels to be blocked by the o-ring, resulting in either no flow, or a ruptured membrane. The system for attaching a membrane to the probe required six screws to pass through the membrane (figure 2-1). This resulted in a decrease in the useable area on the membrane and decreased its strength, contributing to the leakage problems.

The low flow rate necessitated the use of an ESI source to introduce the receptor phase into the mass spectrometer. In this source, liquid effluent is passed through a charged needle along with a coaxial flow of nitrogen; the result is the production of gas phase ions. The ESI source is a soft ionization mode and is often

unable to ionize weak acids or bases without the help of solution chemistry such as a pH change. Since we were attempting to duplicate the conditions of a static cell apparatus, using ethanol/water as the donor and receptor phases, changing the pH in the cell was not an option. When the ESI source proved unable to ionize the test chemicals in the ethanol/water solution, solvent of a lower pH was added downstream of the diffusion cell before the effluent entered the mass spectrometer. This was attempted in two ways; by teeing in a flow of ethanol/water pH 4.0 before the source and by introducing the same solvent into the ESI source via the sheath liquid port. Both of these methods often raised the backpressure on the diffusion cell, causing the membrane to leak or rupture.

The APCI source is a more efficient method of producing ions in an LC/MS. In an APCI source a liquid stream is flash vaporized at temperatures  $> 300^{\circ}\text{C}$ , mixed with nitrogen gas and then passed through a corona discharge field. The corona discharge induces the formation of a plasma from the nitrogen gas. It is within this plasma that chemicals of interest are ionized. While it is a soft ionization method, typically producing  $M+1$  molecular ions, it requires liquid flows greater than  $100\ \mu\text{l}/\text{min}$ . Flow rates of this magnitude routinely burst the membrane on the MIMS probe. In summary, the conversion of the MIMS probe for use as a diffusion cell proved to be technical unfeasible.

#### First prototype

After it became apparent that the shortcomings of the MIMS probe could not be overcome, design was started on a new diffusion cell. The new design had to satisfy several criteria. It would have to use a membrane surface area comparable to that of the Franz cell, so as to maximize the amount of analyte passing through the

membrane. It would also have to accommodate higher flow rates in the receptor phase so as to take advantage of the more efficient ionization sources available on the mass spectrometer such as APCI. The receptor phase would have to move at a rate that allowed analyte concentration to reach detectable levels and not generate excessive backpressure. On the other hand, the receptor phase would also have to move through the cell rapidly enough to maintain sink conditions on the receptor side of the membrane.

Modifying a standard Franz cell was considered and rejected due to its large receptor volume to membrane surface area ratio. The relatively large receptor volume of a Franz cell requires the compartment to be stirred in order to prevent the formation of concentration gradients; without vigorous stirring, the measured concentration would vary relative to the placement of the sampling port. Flow rates would have to vary, based on what portion of the diffusion event was being observed. Early events, such as determining lag phase, would require a slower flow rate so that the analyte was not overly diluted, while steady state measurements would require faster flows so that the osmotic gradient was not impeded by rising concentration in the receptor fluid. A cell with a high surface area to receptor phase volume ratio was needed.

Flow through devices such as the Bronaugh<sup>20</sup> and Squier<sup>21</sup> designs are in wide use, but have some potential flaws. Both designs utilize circular receptor phase chambers with sampling ports meeting the chamber perpendicular to the tangent line. This can lead to the uneven expansion of flow as fluid enters and leaves the chamber, giving rise to eddy currents. Thus, the concentration gradient is not equal across the

entire membrane. A second shortcoming stems from the small surface areas employed, typically on the order of 1-4 cm<sup>2</sup>. Chemicals with low flux values are difficult to measure without larger surface areas. Finally, some of these devices operate at extremely low flow rates to reduce operating pressures. Flow rates below 100 µl/min preclude the use of efficient APCI methods available with LC/MS instruments.

These considerations lead to the design of the first prototype cell depicted in figure 2-4. This prototype cell was constructed from microscope slide glass held together by marine silicone and was originally intended to act only as a non-functioning model. It consisted of a donor phase reservoir that sat on top of the receptor phase channel; the two phases were separated by the membrane. The donor phase chamber measured approximately 0.5" h x 2" l x 1" w; due to the construction method, the chamber was not square. A spacer, originally constructed from overhead acetate sheeting, created a thin channel for the receptor phase to flow through; the channel was approximately 0.01" thick. The shape of the receptor channel was inspired by work done on field flow fractionation cells and was designed to minimize turbulence in the moving receptor phase;<sup>62</sup> turbulence could produce pockets of immobile receptor phase or eddies in the receptor phase stream. The triangular points at each end of the cell ease the transition from a point flow to a wide column. It was decided to use the thin channel to avoid the creation of layers in the receptor phase. The thin receptor channel allows the movement of small volumes of solvent past a large area of membrane, with adequate flow rates to maintain sink conditions. When a large receptor phase volume is used, it must be stirred to prevent the formation of

static layers that differ in chemical concentration. Stirring in a flow through cell can affect the actual solvent velocity in the cell as the stir-bar may act as an impeller. Using a larger receptor phase volume increases the time required for mixing and equilibration. The required flow rate for the cell was 100  $\mu\text{l}/\text{min}$  (based on extrapolations from static cell experiments), a rate easily accommodated by this design.

The higher flow rate allowed the use of the more efficient atmospheric pressure ionization (APCI) source, rather than the ESI source. Effluent from the cell enters a heater in the source where it mixes with nitrogen and is flash-vaporized at 300 °C. Ionization is achieved in the APCI source by passing the nebulized solvent through a corona discharge plasma; a needle in the source is held at high voltage, typically 4-5 kV, to produce the discharge plasma. This plasma ionizes molecules regardless of solution chemistry while avoiding fragmentation, typically resulting in the production of an M+1 ion. Using the APCI source thereby eliminated the need to adjust the solvent pH downstream of the diffusion cell.

The initial prototype, while crude, provided flux data (figure 3-1) that showed the concept to be workable. We were able to observe the fluxes of methyl and ethyl 4-hydroxybenzoate, n-butyl p-aminobenzoate and theophylline through a sheet of PDMS. However, the prototype was not durable enough to withstand repeated handling during experiments. The data generated were sufficient to justify the construction of a more refined prototype.

### Second prototype

The second prototype was able to reproduce data generated from the first prototype and it eliminated the problems of fragility inherent in its predecessor. The

chromatograms in figures 3-2, 3-4 and 3-5 show the ability of the second prototype to measure the transmembrane flux of a number of chemicals. Distinct lag and steady state regions can be seen in the chromatograms. Figures 3-4 and 3-5 are especially interesting. Figure 3-4 shows the flux of testosterone across hairless mouse skin from an ethanol suspension. Testosterone is notoriously difficult to measure without resorting to the use of radio-labels. However, its flux is readily evident using the LC/MS diffusion device. Figure 3-5 shows the flux of nicotine from a commercial nicotine patch applied to hairless mouse skin. This demonstrates the ability of the device to evaluate flux from vehicles other than bulk solutions.

The second prototype (figures 2-5 and 2-6) yielded useful data, but suffered from a number of flaws that prevented its extensive use. The first was in the design of the donor phase tank in relation to the receptor phase ports shown in figures 2-5 and 2-6. When the cell was assembled, the donor phase side of the membrane was rectangular in shape, but the receptor phase side was restricted to the polygon described by the receptor phase channel (figure 3-3). This meant that the input and output surface areas were not equivalent. The membrane size dictated by the cell design was also a problem. While the two square inches ( $12.9 \text{ cm}^2$ ) of membrane provided a great deal of sensitivity for low flux compounds, experiments consumed PDMS membranes at a rapid rate. Initial experiments using hairless mouse skin further highlighted this shortcoming; it had been difficult to obtain a large enough sample of skin from a mouse using this design. The original instrument configuration (figure 2-7) had the cell located between the pump and the mass spectrometer; the pump pushed solvent through the cell into the mass spectrometer. This resulted in the



buildup of pressure within the cell, causing the membrane to bulge, and making the determination of the actual receptor phase volume difficult. This distortion of the membrane was incremental during an experiment, so that the membrane surface area and receptor phase volume changed over time. Consequently, the flux could not be accurately calculated. Concerns were raised as to the effect of the higher pressure on membrane integrity, especially with regard to skin.

In order to address these problems, a redesigned third cell was fabricated by ARS (figure 2-8). The construction materials are the same as those used in the second prototype. In this design, the relation of the donor phase and receptor phase chambers was altered to place the inlets beyond the margin of the membrane rectangle. The cell dimensions were reduced to accommodate the use of mouse skin as a membrane in Specific Aim Three. The order of instrumentation was also changed (figure 2-9) to eliminate issues with pressure within the cell. The cell now drew receptor solvent from a reservoir by a siphon action and the LC pump draws solvent from the cell.

### Specific Aim Two: Validation Testing

New scientific devices must be tested against a known standard to ensure that the data produced is comparable to that obtained using accepted procedures, and not an artifact of the design. In this work the flux values of a number of compounds across a synthetic membrane as measured by a static cell and the LC/MS device were compared. Ester series are often used in diffusion work as they possess a range of solubility and polarity values with little structural variation. The ester series of 4-

hydroxybenzoic acid was utilized here to that end. Members of this series have been investigated by previous workers<sup>39,48</sup> and are commercially available. The first three members of the 4-amino benzoic acid ester series were used in evaluating the second prototype; however, subsequent members of the series were not readily available.

PDMS membranes were used for the reasons elaborated on earlier. It was decided to include limited testing of the ester series using mouse skin.

### PDMS

Effect of ethanol on PDMS. Membranes that have been equilibrated in water show a higher flux of caffeine from a water solution than membranes that have been soaked in ethanol, then equilibrated in water. Ethanol has the apparent effect of lowering the flux of chemicals applied to PDMS membranes as water solutions. It is possible that the ethanol is removing some species from the membrane. If this process is ongoing, it could affect the measurement of flux. However, this phenomenon may be of little concern to this work for a number of reasons. Were the process an ongoing one, it would be expected that steady state would never be truly reached; alternatively it might be reached at different time points depending on when an experiment was started in relation to the leaching process. The flux would plateau and then slowly decline, or the lag times would vary greatly. This has not been observed in either the Franz or the LC/MS cell experiments. Steady state flux is attained and maintained for time periods exceeding eight hours in both devices. Furthermore, other authors have reported that the extraction of material by alcohol solvents had no effect on subsequent flux measurements.<sup>48</sup> In those experiments, membranes were soaked in methanol and then air dried before use. It is more likely that damage occurs when PDMS is moved from an ethanol equilibration to water. In

either case, the damage is peripheral to the validation experiments. All of the Franz and LC/MS validation experiments were done using membranes equilibrated in ethanol solutions; donor and receptor phases were also ethanol solutions. Any damage done before the measurements is apparently equivalent, since repeated measures on separate membranes using the LC/MS show similar results. The potential for damage done by removing the ethanol and replacing it with water is not applicable, as this was not done during the validations.

PDMS validation. The flux data for the 4-hydroxybenzoate series show an apex at the amyl ester. This behavior is consistent with the work of Flynn and Yalkowsky<sup>19</sup> who, using an analogous series of 4-aminobenzoates dissolved in isopropanol, reported a break in flux data at the butyl member. A similar phenomenon has been reported regarding the flux of a series of alkanols across skin when applied as aqueous solutions.<sup>3,4</sup> Direct comparisons with similar experimental work must be done with caution however. Trans-membrane diffusion is affected greatly by the nature of the solvent vehicle (reviewed in Twist and Zatz<sup>60</sup>). While flux values from non-interactive solvents, such as polyethylene glycol or propylene glycol, are similar they can vary greatly from interactive solvents such as alcohols. The alcohol carbon chain length, as well as its mole fraction in water, affect the flux of a molecule to a great degree through both skin and PDMS.<sup>39,40,42,48</sup>

The degree of variation for some of the flux values measured for the paraben series was larger than expected, based on those observed in the literature. While the variation seen with the PDMS membranes is comparable to that seen using animal skin, it was expected to be lower as PDMS is more consistent in nature. The likely

source of the variation was due to the manual nature of the quantitation process. Averaging the ion current intensity across the response peak manually probably introduced some degree of error to the measurement of the receptor phase concentration. The range of linearity obtainable with the LCQ was also an issue. Ion trap mass spectrometers generally have short linear response ranges.<sup>43</sup> This is caused by the occurrence of space charging in the ion trap as concentrations of a molecule increase. Calibration curves must be maintained on a regular basis to compensate for this fact. It is possible that some of the concentration values used in the flux measurements were determined using inaccurate calibration values. It is also possible that the nature of the receptor phase differed enough between the calibration and experimental systems to cause inaccurate concentration measurements.

Franz cell comparison. The flux values for methyl, ethyl, propyl and n-butyl 4-hydroxybenzoate are slightly higher when measured using the LC/MS device than using the Franz cell (figure 3-11, table 3-4). The data do show the same general rank order and relationships as those from the Franz cell. This is a common feature of flow-through cells<sup>20,21</sup> and may be due to their higher clearance rate. A higher rate of clearance in the receptor phase likely maintains sink conditions better than a static cell; therefore diffusion in the flow-through cell is not impeded by the build up of solute. This again has been observed by other researchers.<sup>20,21</sup> It should be noted that the butyl ester differs from its series antecedents in that it forms a liquid phase at "saturation". Whether the ethanol solution is truly saturated in the thermodynamic sense is debatable; however, the same solution was used to test both the Franz and the LC/MS cell. It is the comparison between these two measures that is of interest here.

Solubility data. The water solubility values for the 4-hydroxybenzoate series show a regional vertex at the amyl ester. This behavior is consistent with the flux data gathered for the PDMS membranes. Synthetic PDMS membranes are largely lipophilic in nature.<sup>38</sup> For a purely lipid-like membrane, as water solubility decreases and lipid solubility increases, transmembrane flux should increase. The solvent solubility data shows a similar downward trend through the series, with an apparent localized rise at the amyl ester. However this can not be stated for certain, due to the variation in the butyl and amyl solubility values. This combination of increased water and ethanol:water solubility is what likely makes the amyl ester the highest performer among the series flux values.

Case of the amyl ester. The amyl ester of 4-hydroxybenzoic acid has proved to behave in an anomalous manner compared to other members of the ester series. It has the highest flux value for the entire series (figure 3-9), as well as having water and solvent (ethanol:water) solubilities that exceed the trend defined by the other series members (figures 3-6 and 3-7). It should therefore not be surprising that the amyl ester also possesses the highest melting point of the series, as shown in figure 4-1, and exists as an amorphous semi-solid at room temperature. Melting point is an indication of crystalline lattice strength, which in turn affects solubility. The amorphous nature of the amyl ester indicates the crystal lattice energy is very low, compared to other members of the series, hence its higher than expected solubility and its high transmembrane flux.

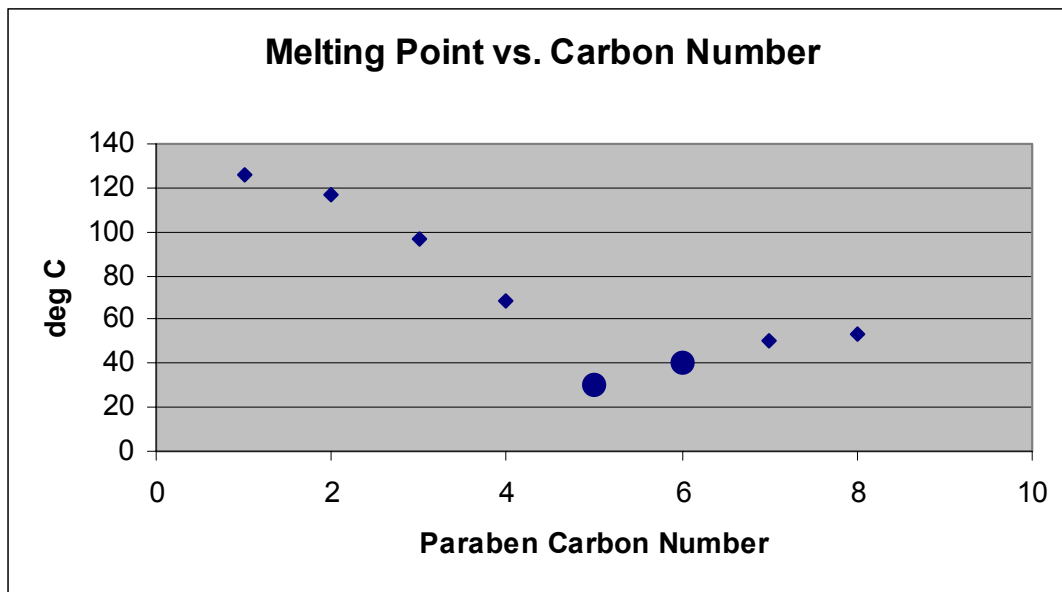


Figure 4-1: Melting points for 4-hydroxybenzoic acid esters. Values from manufacturer data.

#### Hairless Mouse Skin

Repeated applications of caffeine to hairless mouse skin were used to gauge how long a section of tissue was useable in the diffusion cell. Degradation of skin in diffusion cells can be due to microbial breakdown or solvent interactions. An application-wash out series showed skin to be stable in the LC/MS diffusion cell for seventy-two hours (figure 3-12); further experiments demonstrated enough variability to warrant not using skin beyond this point. These findings indicated that hairless mouse skin should be stable over the course of the subsequent experiments.

A subset of the paraben series was applied to hairless mouse skin (figure 3-13). The data follow the same general order of flux, with a slight increase through the series from methyl to n-butyl, as in the PDMS data (figure 3-11). This is consistent with earlier observations that skin has similar, but generally higher flux values for a

compound set, compared to PDMS membranes.<sup>39</sup> However, more variation was expected for the series values for their flux through skin and PDMS. Other workers have reported a larger variation of flux values for these and similar compound but using different solvent systems.<sup>39,47</sup>

### Specific Aim Three: Applications

The transdermal diffusion of numerous chemicals and drugs have been difficult to assess by conventional techniques. This may be due to their structure, such as testosterone, or their presence in a mixture of related compounds, such as polychlorobiphenols (PCB's). In these instances the approach has typically been to radiolabel the structure of interest; however, this does not guarantee the identity of what crosses the skin. A case in point would be studies of prodrugs, molecules designed to deliver an active compound by cleavage of a chemical modifier from the parent compound. Monitoring flux by tracking a radio labeled prodrug may, in reality, only measure the flux of a cleavage product and not the original parent molecule. Some sort of structure determination, typically done by NMR or MS, must be performed to verify the identity of the diffusant. Mixtures pose a similar problem. Some chemical toxicants typically co-exist in complex mixtures of related compounds. It would be desirable to measure the flux from the mixture, as other components may affect the penetration of the ultimate toxicant. Radio-labeling may be difficult in these instances, especially if the compound is a minor fraction of the mixture. Separation or synthesis of the toxicant would be required, followed by labeling and spiking of the original mixture. In this section, the ability of this device

to monitor the flux of these types of chemicals and mixtures without resorting to radio-labels is demonstrated.

### Mixture of Caffeine and Theophylline

Chemical mixtures can be difficult to measure in a single diffusion experiment using conventional techniques. This is especially true for chemicals that share structural features, and therefore have similar or identical absorption spectra. Traditionally some type of separation step, such as chromatography, has been employed in these situations. A second alternative would be to radio-label the compounds with different isotope tags. Mass spectrometry can differentiate between structurally related chemicals based on molecular weight and fragmentation patterns.

Caffeine and theophylline are two closely related compounds (differing only fourteen AMU) that will penetrate skin. Their absorption spectra are essentially identical. Presently available diffusion cells are unable to discriminate between the two when applied as a mixture, without resorting to separation techniques. Using the LC/MS cell, the fluxes of two chemicals are easily monitored as shown in figure 3-14. The signals from each chemical are separated by filtering the total ion chromatogram; the response from the ion of interest is then displayed. Any number of compounds in a mixture can be monitored in this manner. The advantage of simultaneous monitoring is that not only can the number of experiments be reduced, but the effects of added components on the flux of a compounds from a mixture can be shown in a concise manner.



### DEET and Permethrin

The insect repellent N, N-diethyl toluamide (DEET) is known to enhance the penetration of a wide range of chemicals.<sup>46</sup> Concerns have been raised over the ability of DEET to enhance the dermal transport of toxic substances such as pesticides. One case in particular involves the co-application of permethrin, a pyrethroid insecticide often applied to clothing.<sup>63-66</sup> The factors affecting the dermal absorption of permethrin are not entirely clear. A wide range of observations regarding the penetration of permethrin have been reported, ranging from limited absorption depending on the vehicle and administration site,<sup>67,68</sup> to no penetration in perfused *in-vitro* assays.<sup>69,70</sup> Conflicting results have been reported regarding the effect exerted by DEET on the permeation of permethrin;<sup>71,72</sup> the differences appear to be related to the solvent system used. Significantly, Baynes *et al.*<sup>71,72</sup> reported enhancement of permethrin's flux by DEET to occur only when the former was dissolved in ethanol, and not other organic solvents such as acetone or DMSO.

The effect of permethrin flux *in vivo* is typically studied by using radio labeling structures. Permethrin is applied to the skin of an experimental animal as a solution, usually in ethanol, with the possible co-administration of DEET. The disposition of permethrin and its metabolites is determined by the appearance of the radiolabel. Significant toxicological effects, mostly sensorimotor, neural and behavioral damage, have been reported in experimental animals using this technique.<sup>63-66,73,74</sup> These experiments demonstrated a method of simultaneously evaluating the flux of DEET and permethrin without the use of radio-isotopes, or extensive chromatographic separations.

The experiments using a mixture of DEET and permethrin applied to mouse skin served to highlight a unique strong point of the LC/MS diffusion cell. Labeled permethrin is typically applied in an alcohol vehicle for dermal penetration studies. However, the mass spectrometry results indicate that permethrin undergoes a solvolysis reaction in ethanol solution; a proposed pathway is shown in figure 3-17. The product of this reaction also penetrates skin (figure 3-16). The presence of the solvolysis reaction would have gone undetected, had traditional radio-labeling techniques been used. This solvolysis product may be responsible for the discrepancies observed between *in vitro* absorption experiments<sup>69-72</sup> and the *in vivo* toxicologic response seen when permethrin is applied in conjunction with DEET and pyridostigmine bromide.<sup>63-66,73,74</sup> A distinct possibility exists that the agent responsible for the effects seen in the above mentioned *in vivo* studies is not permethrin, but in reality a solvolysis product.

### Testosterone

Testosterone supplementation is clinically used to counteract the effects of declining hormone levels associated with aging in men. Administration is typically via intramuscular injection on a daily basis. In addition to being painful and inconvenient, delivery by injection can result in sudden increases in hormone levels post administration. A desirable alternative would be transdermal delivery. Testosterone could be administered over a longer period of time, avoiding the side effects associated with rapid changes in blood hormone levels. Delivery would be more convenient for the patient and eliminate the need for injections. Presently a dermal delivery device exists for testosterone in the form of a gel. However the gel

must be applied to the scrotum to maximize delivery, decreasing its desirability to many patients.

The transdermal flux of testosterone is difficult to measure, as it does not absorb strongly in the UV region of the spectrum, nor does it possess a useful fluorescence spectrum. Typically the flux of a radio-labeled drug is evaluated. This introduces problems in that the identity of the labeled structure cannot be known for certain without evaluation by a technique such as NMR or MS. The LC/MS diffusion cell is easily able to confirm the identity of the dermally penetrating steroid molecule without the use of radioactivity as shown in figure 3-15. The steady state flux, as well as the lag time, is easily evaluated in the testosterone chromatograms.

The data in table 3-5 indicate that testosterone outperforms the xanthine molecules by a factor of about 2.7. This would at first appear surprising, given that steroid molecules are notoriously difficult to deliver across skin. Other researchers, notably Kim *et al.* have reported lower levels for testosterone flux from ethanol/water solutions.<sup>75</sup> However the molar solubility of testosterone in the ethanol:water vehicle is roughly three times that of the xanthines. As ethanol penetrates skin and modifies its permeability, this would account for testosterone's increased flux. Significant differences exist between the LC/MS solvent system and that used by Kim *et al.* The LC/MS system uses a balanced cell with 50% ethanol:water in both the donor and receptor chambers. Kim *et al.* used 50% ethanol:water only in the donor phase; the receptor phase was composed of normal saline containing 40% propylene glycol (v/v). Thus, the solubility of testosterone in the receptor phase would have been lower than in the LC/MS system. Kim *et al.* also used a static cell system sampled at

approximately 2 hour intervals between 0 and 10 hours; no samples were taken between 10 and 20 hours. The use of static sampling raises the possibility of stasis, a buildup of testosterone to levels that eliminate sink conditions, lowering the observed flux values. The largest difference between this work and that of Kim *et al.* is in the pre-experimental treatment of the skin. In this work, skin was equilibrated overnight in 50% ethanol:water, while it was used fresh in the work of Kim *et al.* Ethanol has been shown to penetrate<sup>24</sup> and alter human skin in an irreversible manner when applied as a pure liquid.<sup>3,76</sup> This is apparently due to the removal of skin lipids, thereby breaking down the skin's barrier properties.<sup>76</sup> In doing so, it alters the solubility of skin to testosterone. There may not have been sufficient time in Kim *et al.*'s work for ethanol to fully penetrate the skin and enhance the transport of testosterone, as penetration enhancement by ethanol has been shown to be time dependent.<sup>76</sup> Alternatively, with regard to the pharmaceutical application of testosterone delivery, the overnight equilibration used here may have altered the skin to an unrealistic degree.

### Shortcomings

No device or technique is ever perfect, and so it is natural to identify areas where something might be improved. The LC/MS diffusion cell is no exception. In the course of validating and testing this device several areas of potential improvement have emerged. The first is how quantitation is performed. The mechanics of ion trap mass spectrometry dictates that their spectra are of a pulsative nature. This can result in chromatograms that are choppy and difficult to quantitate. A quadrupole

instrument might have been a more appropriate tool for measuring flux. Quadrupoles tend to give smoother spectra due to their higher scan rates and to the fact that the mass filter does not constrain ions in temporal space. The measurement of ion levels from standards and the chromatograms is presently subject to variations in operator technique. This may not be a problem, so long as the measurements are performed in a consistent manner over the course of an experiment.

The HPLC pump in present use with the system is a second limiting factor. Recent improvements in the design and availability of micro-flow HPLC pumps have made the delivery of micro-liter flow rates feasible. The flow rate utilized in this work (100  $\mu\text{l}/\text{min}$ ) is in the lowest region of reliable operation for the unit employed. It is also somewhat high for a cell of this size. A flow rate of 60  $\mu\text{l}/\text{min}$  might provide more useful information for slowly diffusing compounds, as well as avoid overloading of the ion trap.

Ethanol/water solutions were used for both donor and receptor phases both for their bacteriostatic properties and because they are amenable to the LC/MS. As was noted earlier, buffer solutions were not used as salts will block the LC/MS inlet. This instrumental shortcoming has since been eliminated from available LC/MS instruments by the implementation of orthogonal geometry sources. Orthogonal inlets bend ions through one and sometimes two 90° turns using oppositely charged cones. Future work could therefore utilize a wider array of receptor phase solvent systems.

The method for attaching the donor phase tank to the receptor phase plate could be greatly improved in later iterations of the design. Presently, screws are used

to mate the two pieces together. Ideally the pressure applied in the clamping process is even, in order to reduce distortion of the membrane and/or the receptor phase spacer. A latch down system would make this process easier.

### Application Issues

A number of individuals, upon viewing presentations regarding the LC/MS cell, have misconstrued its intended role. Criticisms have generally centered around the inability to run multiple cells in parallel without an accompanying bank of mass spectrometers. It must be emphatically stated that the LC/MS diffusion cell is not intended to supplant or replace traditional static diffusion cells. Rather, it is meant to be a tool to be used where static cells are inappropriate, such as the measurement of flux from mixtures, the observation of early flux events, or the monitoring of compounds not amenable to traditional detection techniques. For example, a new testosterone prodrug intended for transdermal delivery could be evaluated using the LC/MS cell to ensure that it crosses skin intact without the loss of the pro-moiety. Once the drug's transport has been confirmed, larger scale tests could be performed using static cells.

An area that the LC/MS diffusion cell could provide useful information is in the field of assessing the toxicological risk from dermal penetration of compounds. Presently dermal risk is estimated using predictive models, such as the Potts-Guy equation.<sup>6,9,29</sup> This has a number of disadvantages. Predictive models estimate dermal adsorption based on several factors, usually including the compound's molecular weight and a surrogate measurement of its solubility in skin, such as an

octanol/water partition coefficient. This assumes that the solvent carrying the toxicant does not change the permeability of the skin to the toxicant. This is clearly not the case for a number of solvents, as has already been mentioned. It is particularly a problem when a toxicant is present in a complex matrix, in which several components may function both solvents and as toxicants. In these cases, predictive models may underestimate the dermal absorption of a toxicant. Even when corrections can be made for a given solvent mixture, many exposure sites have unique matrix compositions, requiring multiple estimations. Matrix composition can vary within an exposure site in some instances. A second problem is of a more practical nature. People living in an area where a potential dermal toxicant is present are unlikely to accept a proclamation of safety based on "theoretical" calculations. It is here that the LC/MS diffusion cell could make a contribution. The dermal penetration of any number of chemicals can be measured using this device, regardless of matrix components or the structure of the potential toxicant.

### Summary

The hypothesis of this work was that a flow through diffusion cell could be designed that would take advantage of mass spectrometry as a detection method. It was further hypothesized that such a device would be able to evaluate compounds and circumstances that had been outside the realm of routine analysis using conventional techniques. To these ends, three specific aims were outlined. The first was that a device be developed that would be compatible with a commercially available LC/MS instrument. The second aim was to validate the cell by testing its response to an array

of chemicals and comparing the results to those generated using a static device. The third goal was to demonstrate the ability of the device to perform in applications that have traditionally been difficult using static devices.

Data supporting the achievement of each of these aims have been presented here. The third prototype LC/MS diffusion cell has been shown to be capable of operating in conjunction with a Finnigan/MAT LCQ LC/MS instrument. It has been shown to generate data comparable to those obtained using static diffusion cells. Finally, the measurement of flux from mixtures of similar chemicals, and of compounds not generally amenable to detection without the use of radio-labels, has been demonstrated.



APPENDIX A: STANDARD CURVES

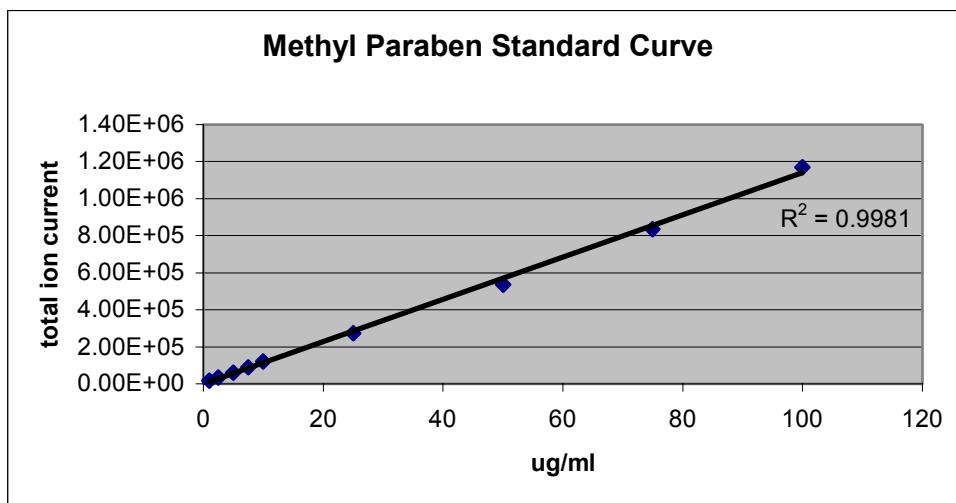


Figure A-1: Methyl paraben standard curve generated on the LCQ.

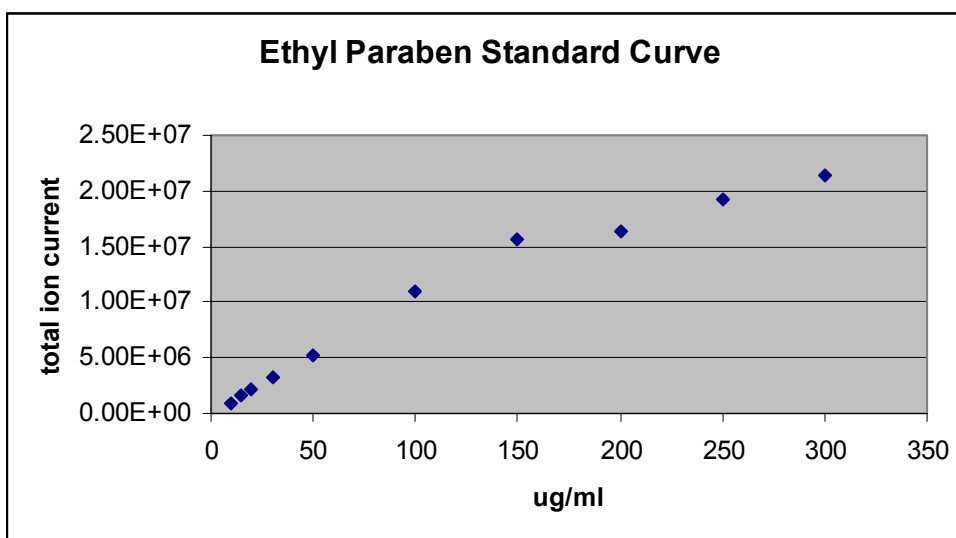


Figure A-2: Ethyl paraben standard curve generated on the LCQ showing typically non-linear distribution. Quantitation was done using linear fit lines to sections of the data.

## APPENDIX B: ENLARGEMENT OF FIGURES

A number of the flux chromatograms from chapter 3 are reproduced here in an enlarged format.

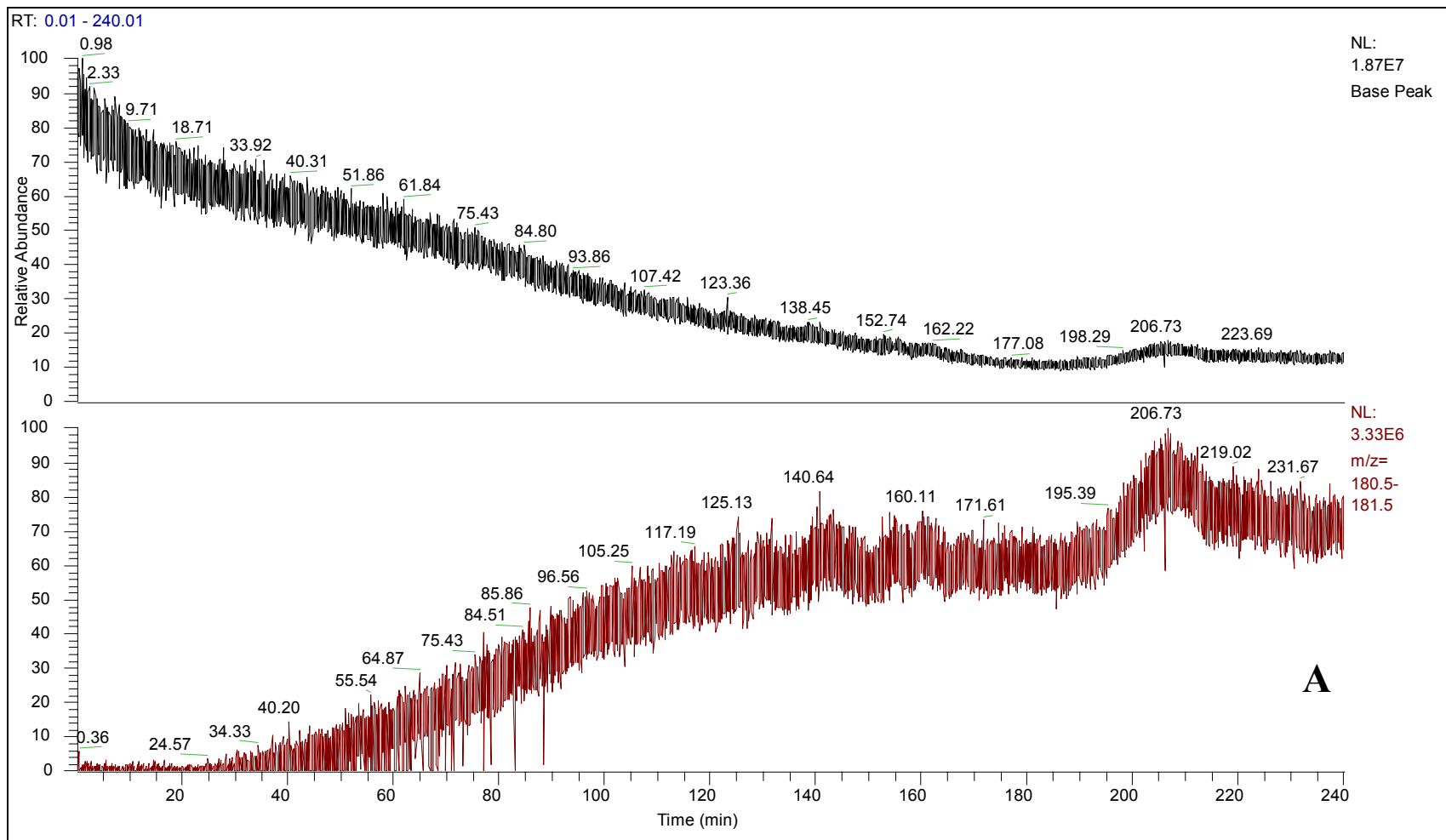


Figure B-1: Enlargement of figure 3-1 A.

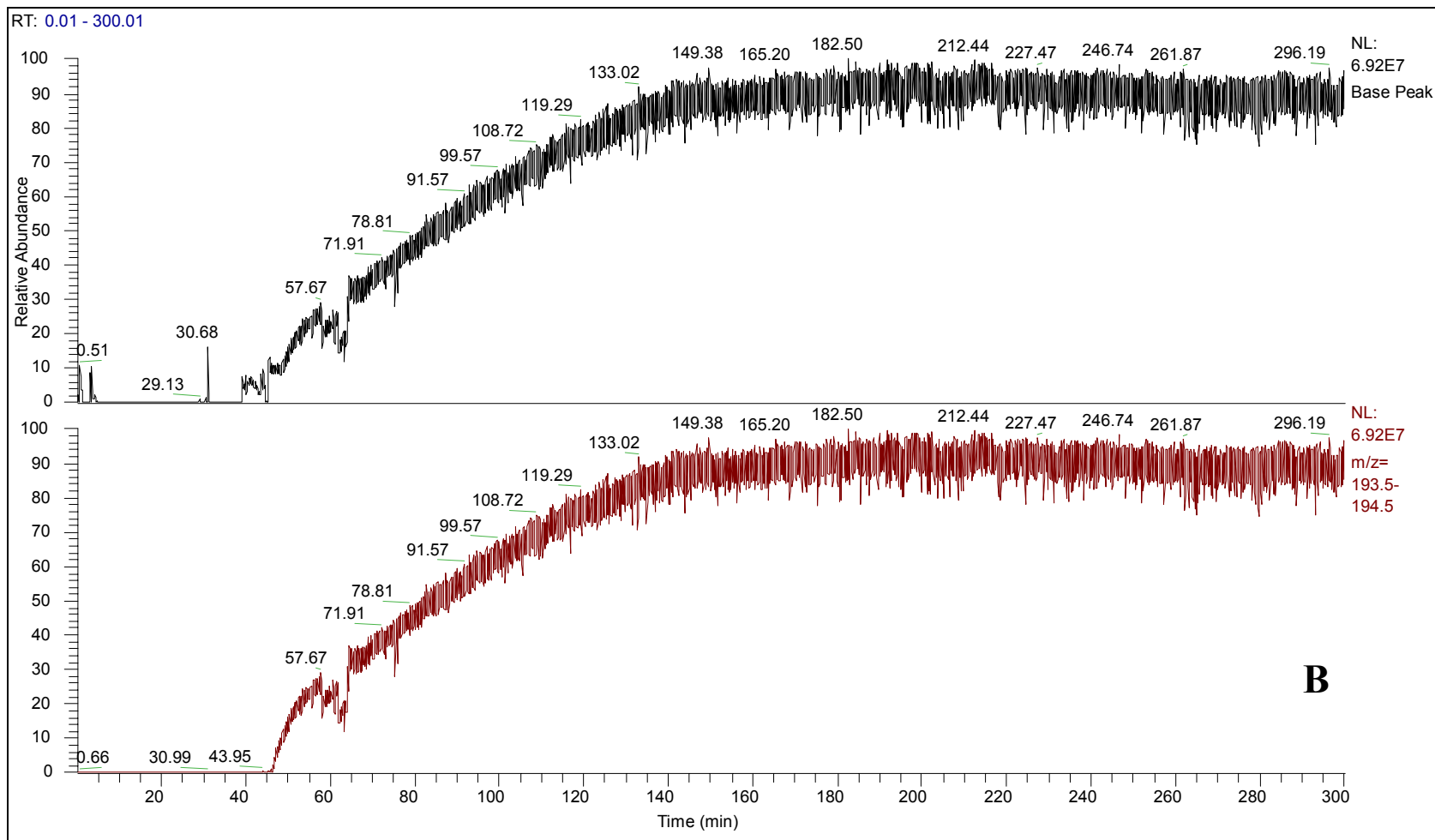


Figure B-2: Enlargement of figure 3-1 B.

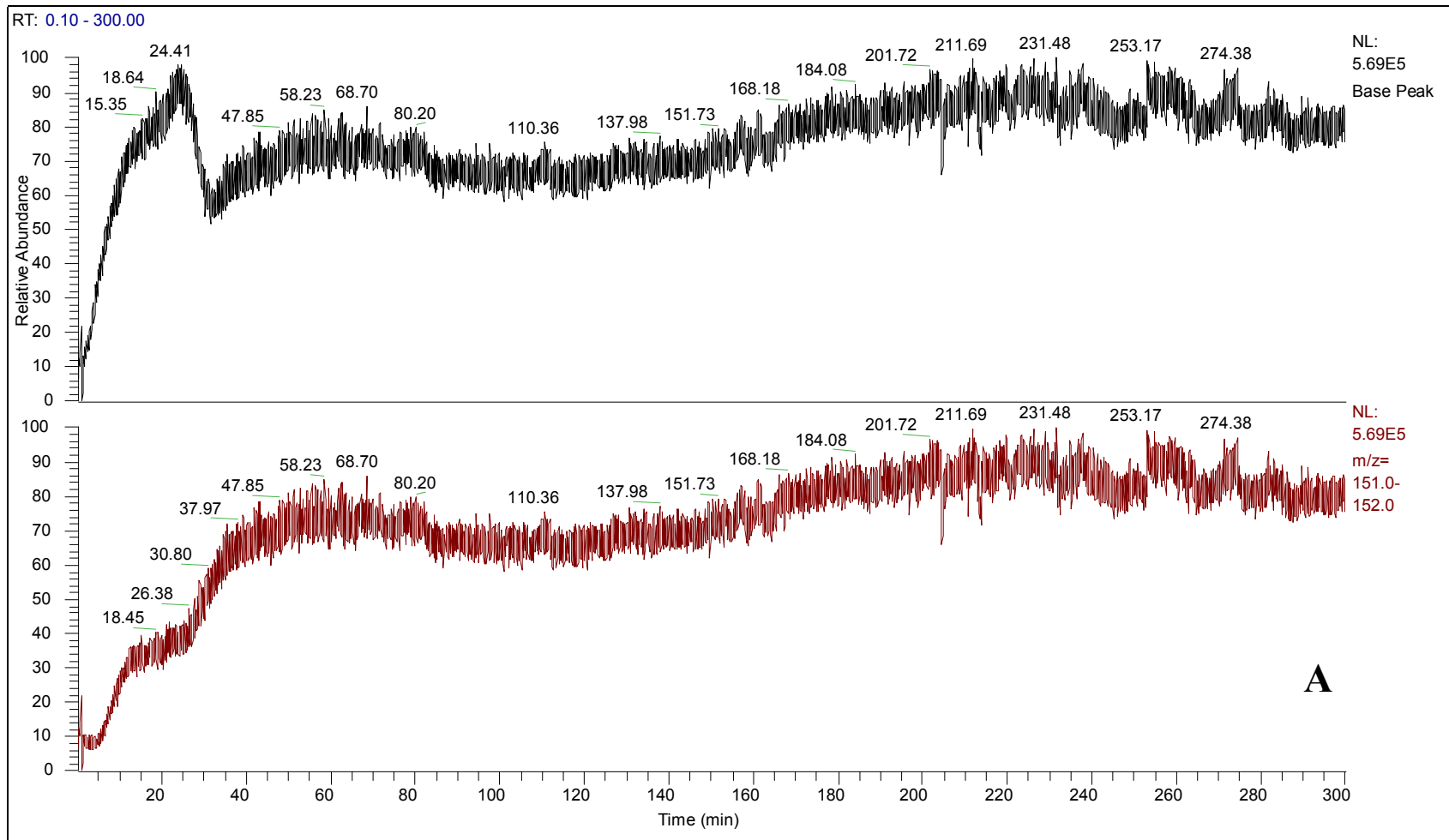


Figure B-3: Enlargement of figure 3-2 A. Methyl 4-hydroxybenzoate.

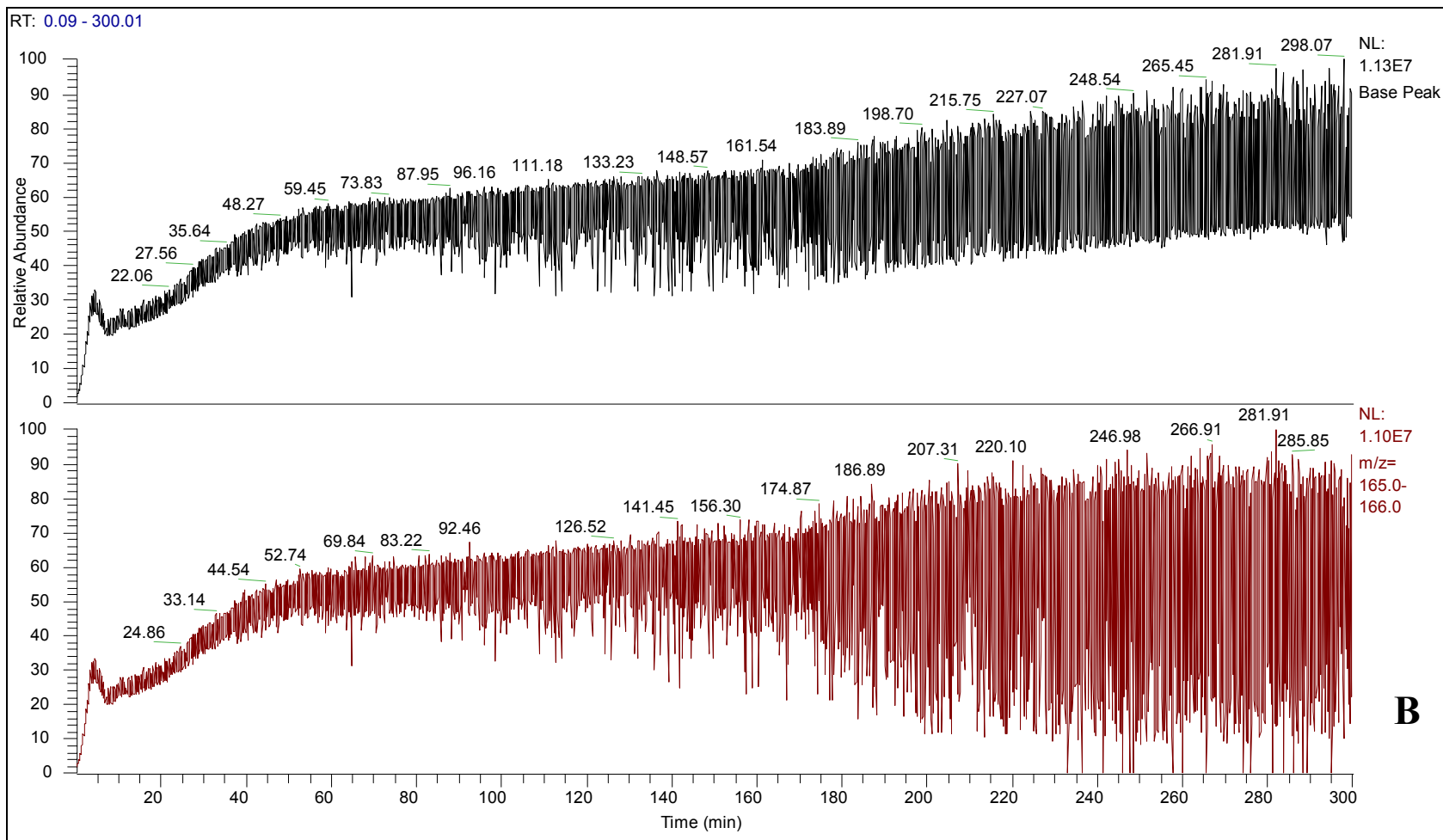


Figure B-4: Enlargement of figure 3-2 B. Ethyl 4-hydroxybenzoate.

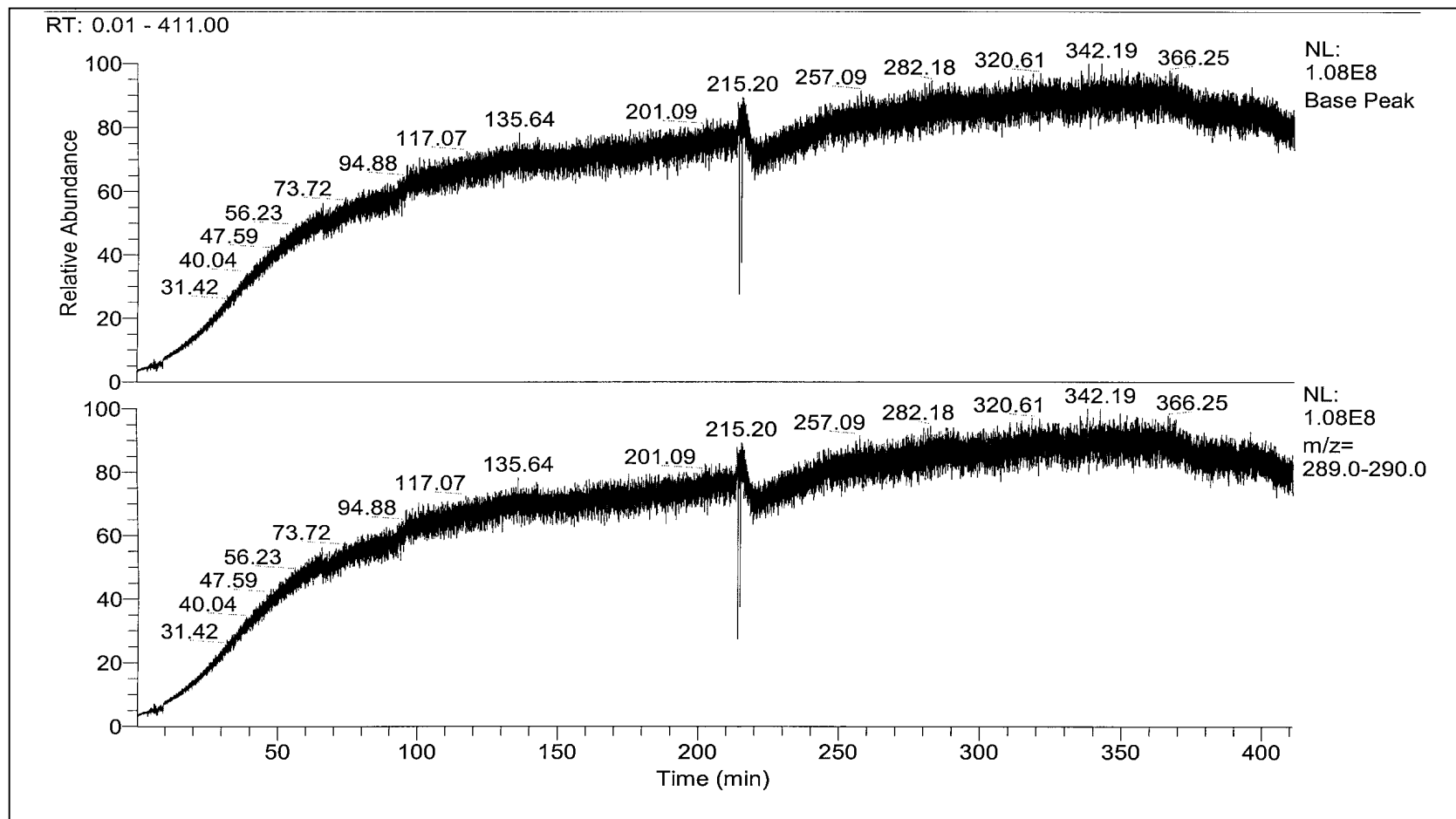


Figure B-5: Enlargement of figure 3-4. Testosterone.

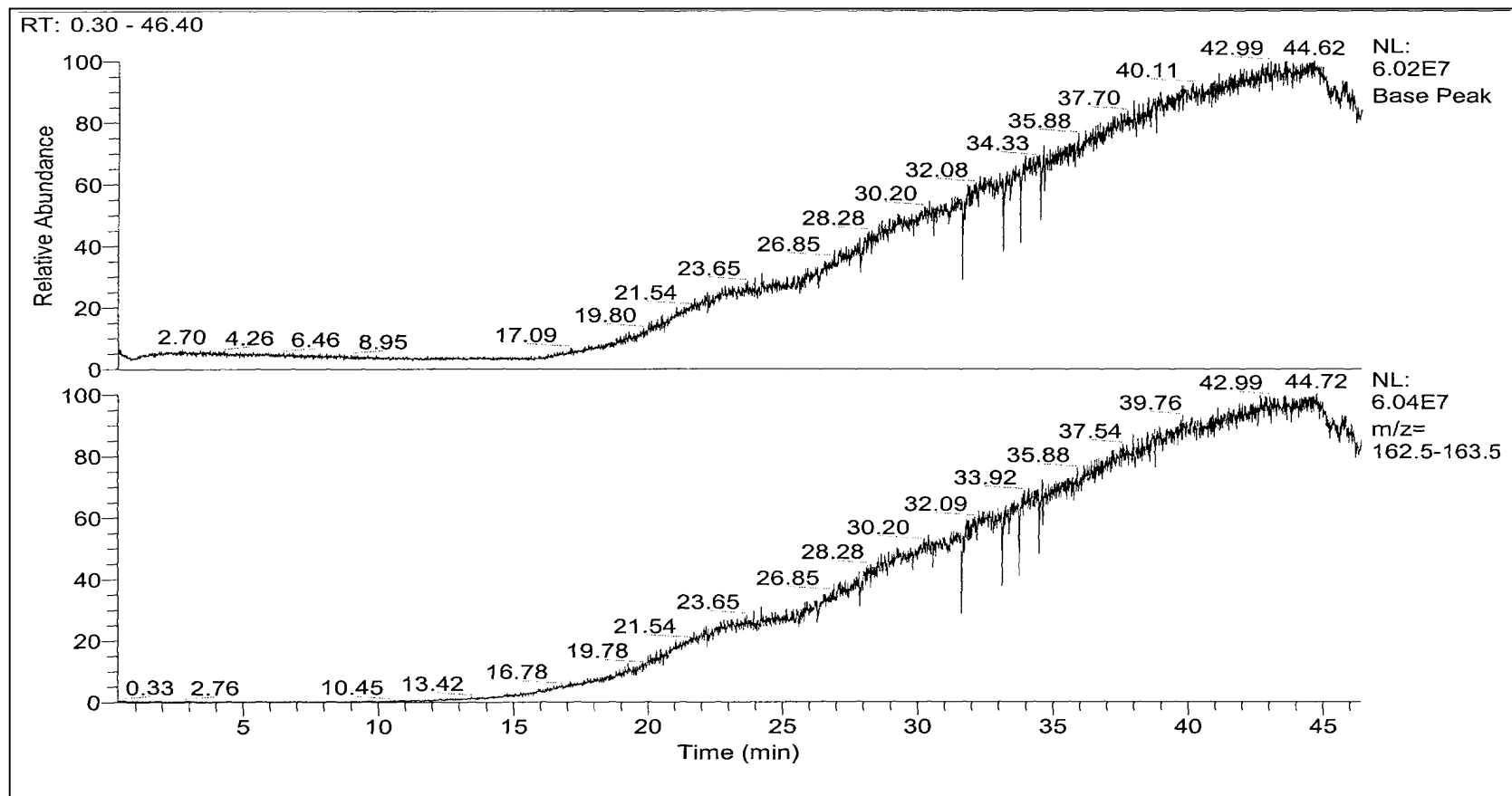


Figure B-6: Enlargement of figure 3-4. Nicotine.



RT: 0.00 - 515.79

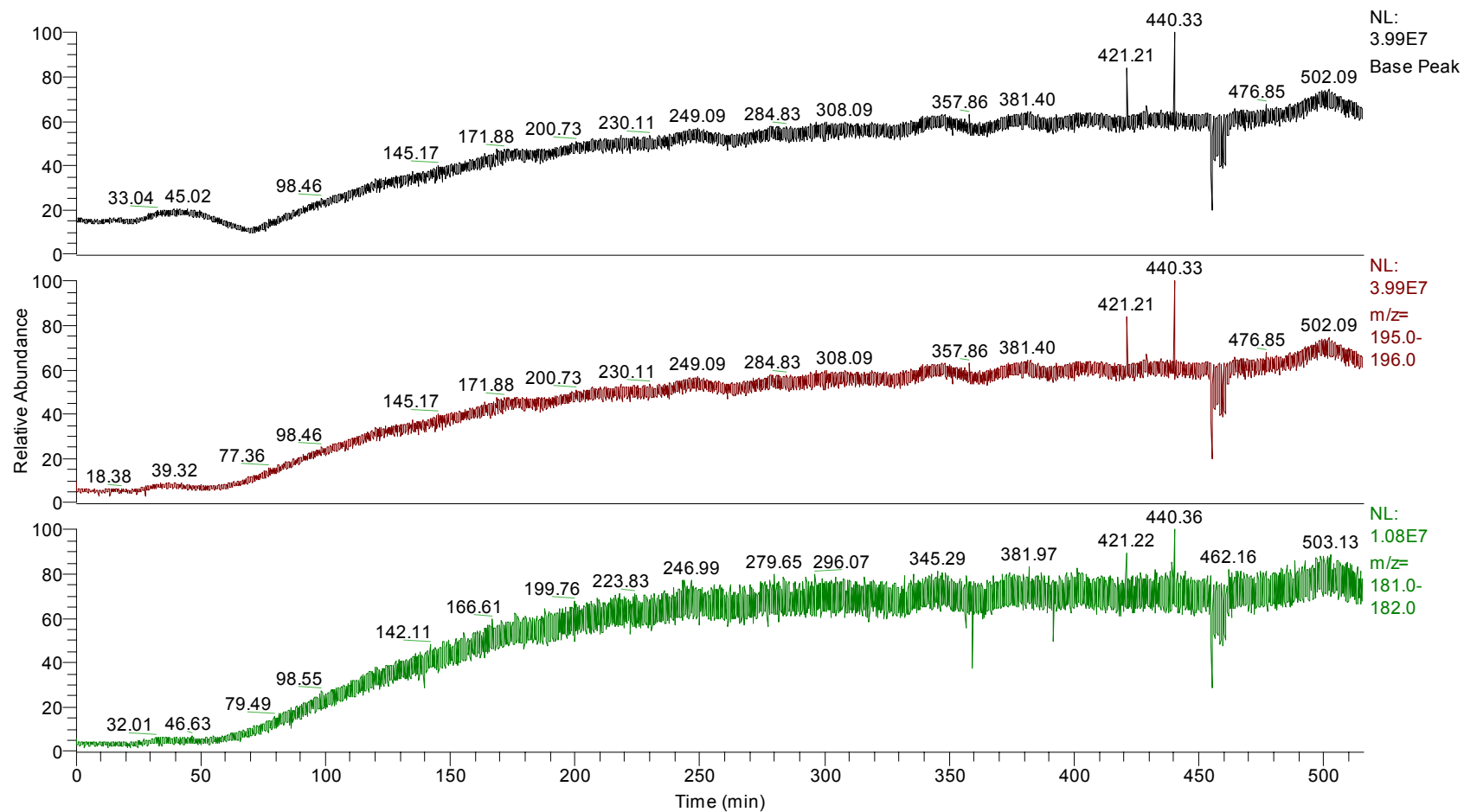


Figure B-7: Enlargement of figure 3-14. Caffeine and theophylline.

RT: 0.01 - 1300.01

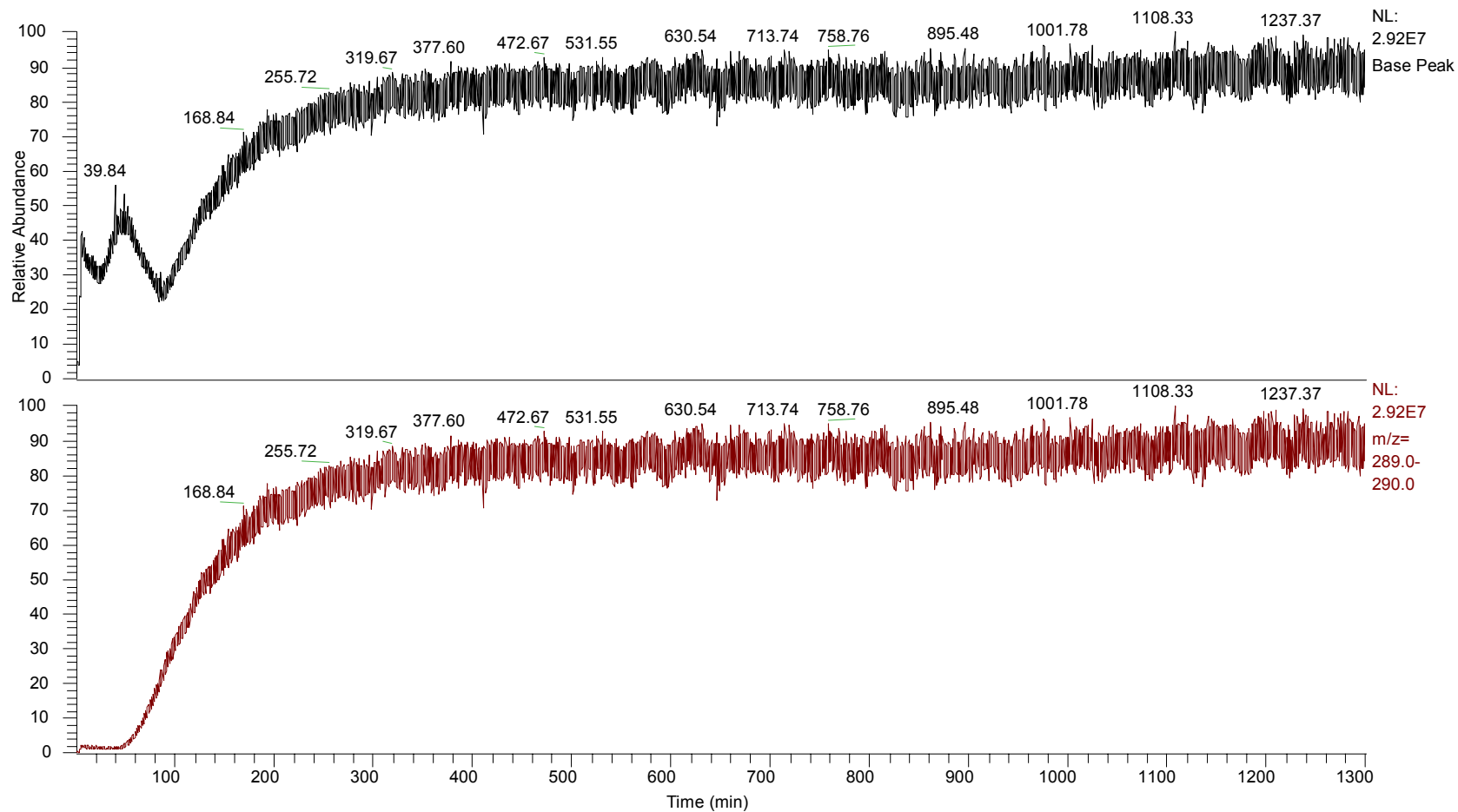


Figure B-8: Enlargement of figure 3-15. Testosterone.

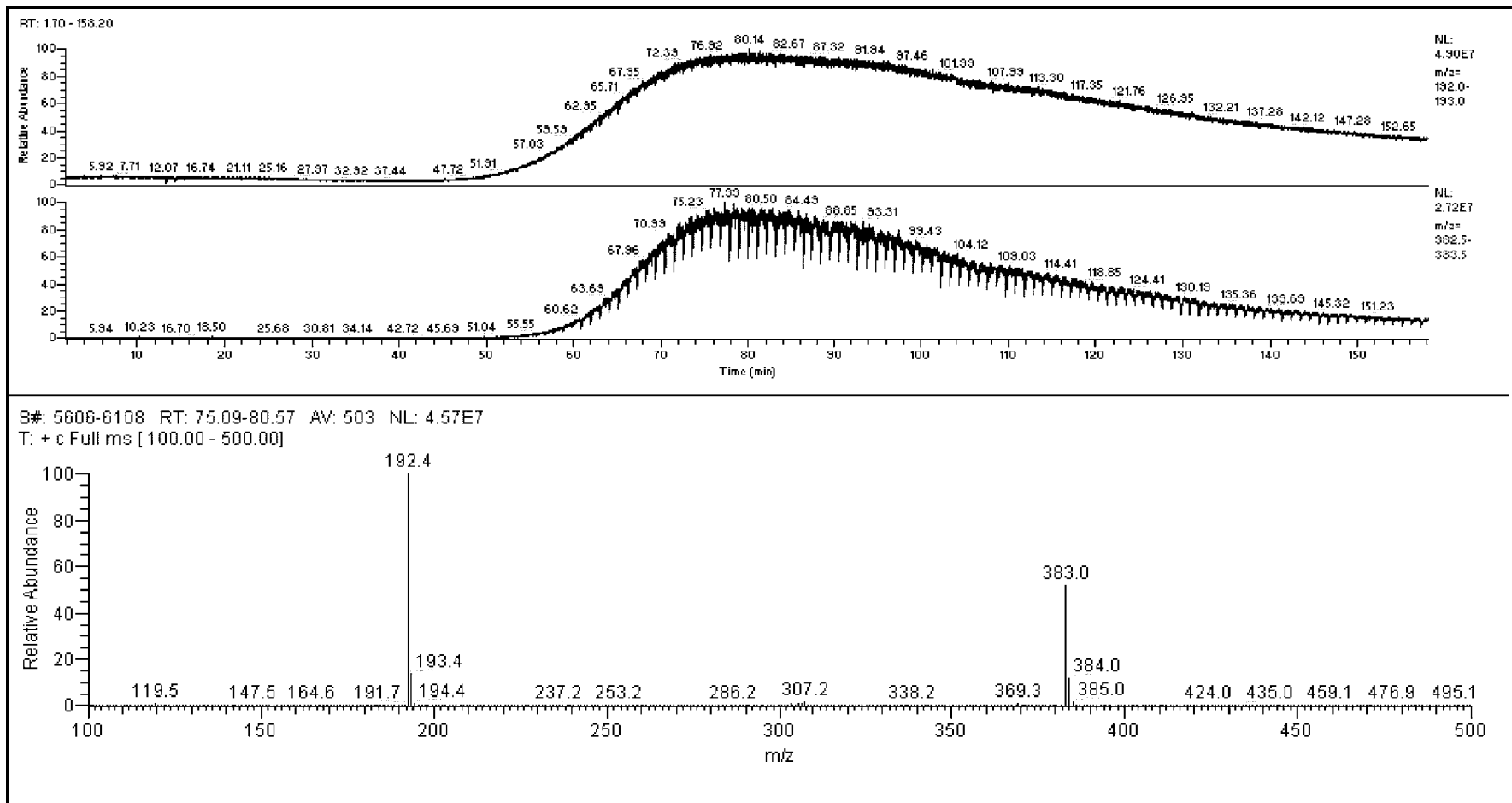


Figure B-9: Enlargement of figure 3-16. DEET and permethrin.

## LIST OF REFERENCES

- 1) Henry, C. M. Special Delivery: Alternative Methods for Delivering Drugs Improve Performance, Convenience, and Patient Compliance. *Chemical and Engineering News* **2000**, 49-65.
- 2) Finnin, B. C.; Morgan, T. M. Transdermal Penetration Enhancers: Applications, Limitations, and Potential. *Journal of Pharmaceutical Sciences* **1999**, 88, 955-958.
- 3) Scheuplein, R. J.; Blank, I. H. Mechanism of Percutaneous Absorption. IV. Penetration of Nonelectrolytes (Alcohols) from Aqueous Solutions and from Pure Liquids. *The Journal of Investigative Dermatology* **1973**, 60, 286-296.
- 4) Scheuplein, R. J.; Blank, I. H. Permeability of the Skin. *Physiological Reviews* **1971**, 51, 702-746.
- 5) Bunge, A. L.; Cleek, R. L. A New Method for Estimating Dermal Absorption from Chemical Exposure: 2. Effect of Molecular Weight and Octanol-Water Partitioning. *Pharmaceutical Research* **1995**, 12, 88-95.
- 6) Guy, R. H.; Potts, R. O. Penetration of Industrial Chemicals Across the Skin: A Predictive Model. *American Journal of Industrial Medicine* **1993**, 23, 711-719.
- 7) Abraham, M. H.; Chadha, H. S.; Mitchell, R. C. The Factors that Influence Skin Penetration of Solutes. *Journal of Pharmaceutics and Pharmacology* **1995**, 47, 8-16.
- 8) Potts, R. O.; Guy, R. H. A Predictive Algorithm for Skin Permeability: The Effects of Molecular Size and Hydrogen Bond Activity. *Pharmaceutical Research* **1995**, 12, 1628-1633.
- 9) Potts, R. O.; Guy, R. H. Predicting Skin Permeability. *Pharmaceutical Research* **1992**, 9, 663-669.
- 10) Roberts, W. J.; Sloan, K. B. Correlation of Aqueous and Lipid Solubilities with Flux for Prodrugs of 5-Fluoruracil, Theophylline, and 6-Mercaptopurine: A Potts-Guy Approach. *Journal of Pharmaceutical Sciences* **1999**, 88, 515-522.
- 11) Wilschut, A.; Berge, W. F. t.; Robinson, P. J.; McKone, T. E. Estimating Skin Permeation. The Validation of Five Mathematical Skin Permeation Models. *Chemosphere* **1995**, 30, 1275-1296.

- 12) Ussing, H. H. The Active Ion Transport through the Isolated Frog Skin in the Light of Tracer Studies. *Acta. Physiol. Scand.* **1948**, *17*, 1-37.
- 13) Flynn, G. L.; Smith, E. W. Membrane Diffusion I: Design and Testing of a New Multifeatured Diffusion Cell. *Journal of Pharmaceutical Sciences* **1971**, *60*, 1713-1717.
- 14) Chien, Y. W.; Valia, K. H. Development of a Dynamic Skin Permeation System for Long-Term Permeation Studies. *Drug Development and Industrial Pharmacy* **1984**, *10*, 575-599.
- 15) Franz, T. J. Percutaneous Absorption. On the Relevance of In Vitro Data. *The Journal of Investigative Dermatology* **1975**, *64*, 190-195.
- 16) Feldmann, R.; Maibach, H. Absorption of Some Organic Compounds Through the Skin of Man. *Journal of Investigative Dermatology* **1970**, *51*, 399-404.
- 17) Keshary, P. R.; Chien, Y. W. Mechanisms of Transdermal Controlled Nitroglycerin Administration (I): Development of a Finite-Dosing Skin Permeation System. *Drug Development and Industrial Pharmacy* **1984**, *10*, 883-913.
- 18) Michaels, A. S.; Chandraskaren, S. K.; Shaw, J. E. Drug Permeation Through Human Skin: Theory and in Vitro Experimental Measurement. *AIChE Journal* **1975**, *21*, 985-996.
- 19) Flynn, G. L.; Yalkowsky, S. H. Correlation and Prediction of Mass Transport across Membranes I: Influence of Alkyl Chain Length on Flux-Determining Properties of Barrier and Diffusant. *Journal of Pharmaceutical Sciences* **1972**, *61*, 838-857.
- 20) Bronaugh, R. L.; Stewart, R. F. Methods for In Vitro Percutaneous Absorption Studies IV: the Flow-Through Diffusion Cell. *Journal of Pharmaceutical Sciences* **1985**, *74*, 64-67.
- 21) Squier, C. A.; Kremer, M.; Wertz, P. W. Continuous Flow Mucosal Cells for Measuring the in-Vitro Permeability of Small Tissue Samples. *Journal of Pharmaceutical Sciences* **1997**, *86*, 82-84.
- 22) Skoog, D. A.; Leary, J. J. *Principles of Instrumental Analysis*; fourth ed.; Saunders College Publishing: Fort Worth, 1992.
- 23) Pavia, D. L.; Lampman, G. M.; Kriz, G. S. *Introduction to Spectroscopy: A Guide for Students of Organic Chemistry*; second ed.; Saunders College Publishing: Fort Worth, 1996.
- 24) Scheuplein, R. J. Mechanism of Percutaneous Adsorption I. Routes of Penetration and the Influence of Solubility. *The Journal of Investigative Dermatology* **1965**, *45*, 334-346.

- 25) Scheuplein, R. J. Mechanism of Percutaneous Absorption II. Transient Diffusion and the Relative Importance of Various Routes of Skin Penetration. *The Journal of Investigative Dermatology* **1967**, *48*, 79-88.
- 26) Kasting, G. B.; Smith, R. L.; Cooper, E. R. Effect of Lipid Solubility and Molecular Size on Percutaneous Absorption. *Pharmacology of Skin* **1987**, *1*, 138-153.
- 27) Anderson, B. D.; Raykar, P. V. Solute Structure-Permeability Relationships in Human Stratum Corneum. *The Journal of Investigative Dermatology* **1989**, *93*, 280-286.
- 28) Anderson, B. D.; Higuchi, W. I.; Raykar, P. V. Heterogeneity Effects on Permeability-Partition Coefficient Relationships in Human Stratum Corneum. *Pharmaceutical Research* **1988**, *5*, 566-573.
- 29) Flynn, G. L. *Physicochemical Determinants of Skin Absorption*; Flynn, G. L., Ed.; Elsevier Science Publishing Co., Inc: New York, Amsterdam, London, 1990, pp 93-127.
- 30) Ackerman, C.; Flynn, G. L.; Smith, W. M. Ether-water Partitioning and Permeability Through Hairless Mouse Skin In Vitro. II. Hydrocortisone 21-n-alkyl Esters, Alkanols and Hydrophilic Compounds. *International Journal of Pharmaceutics* **1987**, *36*, 67-71.
- 31) Sloan, K. B. *Functional Group Considerations in the Development of Prodrug Approaches to Solving Topical Delivery Problems*; Sloan, K. B., Ed.; Marcel Dekker: New York, 1992, pp 17-116.
- 32) Abraham, M. H.; Martin, F.; Mitchell, R. C. Algorithms for Skin Permeability Using Hydrogen Bond Descriptors: the Problem of Steroids. *Journal of Pharmaceutics and Pharmacology* **1997**, *49*, 858-865.
- 33) Johnson, M. E.; Blankschtein, D.; Langer, R. Permeation of Steroids Through Human Skin. *Journal of Pharmaceutical Science* **1995**, *84*, 1144-1146.
- 34) Scheuplein, R. J.; Blank, I. H.; Brauner, M. D.; MacFarlane, D. J. Percutaneous Absorption of Steroids. *Journal of Investigative Dermatology* **1969**, *52*, 63-70.
- 35) Cronin, M. T. D.; Deardin, J. C.; Moss, G. P.; Murray-Dickeson, G. Investigation of the Mechanism of Flux Across Human Skin In Vitro by Quantitative Structure-Permeability Relationships. *European Journal of Pharmaceutical Science* **1999**, *7*, 325-330.
- 36) Cronin, M. T. D.; Dearden, J. C.; Gupta, R.; Moss, G. P. An Investigation of the Mechanism of flux Across Polydimethylsiloxane Membranes by use of Quantitative Structure-Permeability Relationships. *Journal of Pharmacy and Pharmacology* **1998**, *50*, 143-152.

- 37) Yamaguchi, Y.; Usami, T.; Natsume, H.; Aoyagi, T.; Nagase, Y.; Sugibayashi, K.; Morimoto, Y. Evaluation of Skin Permeability of Drugs by Newly Prepared Polymer Membranes. *Chem. Pharm. Bull.* **1997**, *45*, 537-541.
- 38) Hatanka, H.; Inuma, M.; Sugibayashi, K.; Morimoto, Y. Prediction of Skin Permeability of Drugs I. Comparison with Artificial Membrane. *Chem. Pharm. Bull.* **1990**, *38*, 3452-3459.
- 39) Twist, J. N.; Zatz, J. L. Influence of Solvents on Paraben Permeation Through Idealized Skin Model Membranes. *Journal of the Society of Cosmetic Chemists* **1986**, *37*, 429-444.
- 40) Zatz, J. L.; Dalvi, U. G. Evaluation of Solvent-Skin interaction in Percutaneous Absorption. *Journal of the Society of Cosmetic Chemists* **1983**, *34*, 327-334.
- 41) Zatz, J. L. *Modification of Skin Permeation by Surface-Active Agents*; Zatz, J. L., Ed.; Allured Publishing: Wheaton, IL, 1993, pp 149-162.
- 42) Zatz, J. L. *Modification of Skin Permeation by Solvents*; Zatz, J. L., Ed.; Allured Publishing: Wheaton, IL, 1993, pp 127-148.
- 43) Watson, J. T. *Introduction to Mass Spectrometry*; third ed.; Lippincott-Raven: Philadelphia, 1997.
- 44) Dass, C. *Principles and Practice of Biological Mass Spectrometry*; first ed.; John Wiley & Sons, Inc.: New York, 2001.
- 45) Heather, R. W. *LCQ MS Detector Hardware Manual*; Revision C ed.; Technical Publications, Finnigan Corporation: San Jose, 1997.
- 46) Windheuser, J. J.; Haslam, J. L.; Caldwell, L.; Shaffer, R. D. The Use of N, N-Diethyl-m-Toluamide to Enhance Dermal and Transdermal Delivery of Drugs. *Journal of Pharmaceutical Sciences* **1982**, *71*, 1211-1213.
- 47) Pozzo, A. D.; Pastori, N. Percutaneous Absorption of Parabens from Cosmetic Formulations. *International Journal of Cosmetic Sciences* **1996**, *18*, 55-66.
- 48) Twist, J. N.; Zatz, J. L. Membrane-Solvent-Solute Interaction in a Model Permeation System. *Journal of Pharmaceutical Sciences* **1988**, *77*, 536-540.
- 49) Twist, J. N.; Zatz, J. L. A Model for Alcohol-Enhanced Permeation through Polydimethylsiloxane Membranes. *Journal of Pharmaceutical Sciences* **1990**, *79*, 28-31.
- 50) Matheson, L. E.; Vayumhasuwan, P.; Moeckly, D. M. The Development of a predictive method for the Estimation of Flux Through Polydimethylsiloxane Membranes.

II. Derivation of a Diffusion Parameter and its Application to Multisubstituted Benzenes. *International Journal of Pharmaceutics* **1991**, *77*, 163-168.

51) Matheson, L. E.; Hu, M.-w. The Development of a Predictive Method for the Estimation of Flux Through Polydimethylsiloxane Membranes. IV. Applications to a Series of Substituted Quinolines. *Pharmaceutical Research* **1993**, *10*, 839-842.

52) Moeckly, D. M.; Matheson, L. E. The Development of a Predictive Method for the Estimation of Flux Through Polydimethylsiloxane Membranes: I. Identification of Critical Variables for a Series of Substituted Benzenes. *International Journal of Pharmaceutics* **1991**, *77*, 151-162.

53) Patel, D. C.; Fox, J. L.; Higuchi, W. I. Physical Model Approach in the Study of the Transport of Alkyl Amines Across a Silicone Rubber Membrane in a Two-Chamber Diffusion Cell. *Journal of Pharmaceutical Sciences* **1984**, *73*, 1028-1034.

54) Hu, M.-w.; Matheson, L. E. The Development of a Predictive Method for the Estimation of Flux Through Polydimethylsiloxane Membranes. III. Application to a Series of Substituted Pyridines. *Pharmaceutical Research* **1993**, *10*, 732-736.

55) Lopez-Avila, V.; Benedicto, J.; Prest, H.; Bauer, S. Automated MIMS for Direct Analysis of Organic Compounds in Water. *American Laboratory* **1999**, 32-37.

56) Sloan, K. B.; Koch, S. A. M.; Siver, K. G.; Flowers, F. P. The Use of Solubility Parameters of Drug and Vehicles to Predict Flux. *Journal of Investigative Dermatology* **1986**, *87*, 244-252.

57) Sloan, K. B.; Taylor, H. E.; Hamilton, J. C. Alcohol Flux and Effect on the Delivery of Theophylline from Propylene Glycol. *International Journal of Pharmaceutics* **1997**, *156*, 17-26.

58) Flynn, G. L.; Roseman, T. J. Membrane Diffusion II: Influence of Physical Adsorption on Molecular Flux through Heterogeneous Dimethylpolysiloxane Barriers. *Journal of Pharmaceutical Sciences* **1971**, *60*, 1788-1796.

59) Jetzer, W. E.; Huq, A. S.; Ho, N. F. H.; Flynn, G. L.; Duraiswamy, N.; Jr., L. C. Permeation of Mouse Skin and Silicone Rubber Membranes by Phenols: Relationship to In Vitro Partitioning. *Journal of Pharmaceutical Sciences* **1986**, *75*, 1098-1103.

60) Twist, J. N.; Zatz, J. L. *Interaction of Vehicles with Model Skin Membranes in the Permeation Process*; Twist, J. N.; Zatz, J. L., Ed., pp 147-173.

61) Greenwalt, C. C.; Voorhees, K. J.; Futrell, J. H. Transmission of Organic Molecules by a Silicone Membrane Gas Chromatography/Mass Spectrometer Interface. *Analytic Chemistry* **1983**, *55*, 468-472.



- 62) Giddings, J. C. *The Field Flow Fractionation Family: Underlying Principles*; first ed.; Giddings, J. C., Ed.; Wiley-Interscience: New York City, 2000, pp 3-30.
- 63) Hoy, J. B.; Cornell, J. A.; Karlix, J. L.; Schmidt, C. J.; Tebbett, I. R.; van-Haaren, F. Interactions of Pyridostigmine Bromide, DEET and Permethrin Alter Locomotor Behavior of Rats. *Vet-Hum-Toxicol* **2000**, *42*, 65-71.
- 64) Hoy, J. B.; Cornell, J. A.; Karlix, J. L.; Tebbett, I. R.; van-Haaren, F. Repeated Coadministrations of Pyridostigmine Bromide, DEET, and Permethrin Alter Locomotor Behavior of Rats. *Vet-Hum-Toxicol* **2000**, *42*, 72-76.
- 65) Abou-Donia, M. B.; Goldstein, L. B.; Jones, K. H.; Abdel-Rahman, A. A.; Damodaran, R. V.; Dechkovskaia, A. M.; Bullman, S. L.; Amir, B. E.; Kahn, W. A. Locomotor and Sensorimotor Performance Deficit in Rats following Exposure to Pyridostigmine Bromide, DEET, and Permethrin, Alone and in Combination. *Toxicological Sciences* **2001**, *60*, 305-314.
- 66) Abou-Donia, M. B.; Goldstein, L. B.; Dechkovskaia, A.; Bullman, S.; Jones, K. H.; Herrick, E. A.; Abdel-Rahman, A. A.; Kahn, W. A. Effects of Daily Dermal Application of DEET and Permethrin, Alone and in Combination, on Sensorimotor Performance, Blood-Brain Barrier and Blood-Testis Barrier in Rats. *Journal of Toxicology and Environmental Health Part A* **2001**, *62*, 523-541.
- 67) Franz, T. J.; Lehman, P. A.; Franz, S. F.; Guin, J. D. Comparative Percutaneous Absorption of Lindane and Permethrin. *Archives of Dermatology* **1996**, *132*, 901-905.
- 68) Sidon, E. W.; Moody, R. P.; Franklin, C. A. Percutaneous Absorption of Cis- and Trans-Permethrin in Rhesus Monkeys and Rats: Anatomic Site and Interspecies Variation. *Journal of Toxicology and Environmental Health* **1988**, *23*, 207-216.
- 69) Bast, G. E.; Kampffmeyer, H. G. No Effect of Albumin on the Dermal Absorption Rate of Hydrocortisone 21-Butyrate, Permethrin or Diflunisal in the Isolated, Single-Pass Perfused Rabbit Ear. *Skin Pharmacology* **1996**, *9*, 327-333.
- 70) Bast, G. E.; Taeschner, D.; Kampffmeyer, H. G. Permethrin Absorption Not Detected in Single Pass Perfused Rabbit Ear, and Absorption with Oxidation of 3-Phenoxybenzyl Alcohol. *Archives of Toxicology* **1997**, *71*, 179-186.
- 71) Baynes, R. E.; Brooks, J. D.; Abdullahi, A. R.; Wilkes, R.; Riviere, J. E. Influence of DEET and Pyridostigmine Bromide on Dermal Disposition of Permethrin. *The Toxicologist* **2001**, *60*, 128.
- 72) Baynes, R. E.; Halling, K. B.; Riviere, J. E. The Influence of Diethyl-m-toulamide (DEET) on the Percutaneous Absorption of Permethrin and Carbaryl. *Toxicology and Applied Pharmacology* **1997**, *144*, 332-339.

- 73) Abou-Donia, M. B.; Khan, W. A.; Suliman, H. B.; Abdel-Rahman, A. A.; Jensen, K. F. Combined Exposure to Pyridostigmine Bromide (PB), DEET, and Permethrin with Stress Increases the Blood-Brain Barrier (BBB) Permeability and Inhibits Acetylcholinesterase in Rats. *The Toxicologist* **2001**, *60*, 238.
- 74) Amir, B. E.; Abdel-Rahman, A. A.; Goldstein, L. B.; Jones, K. H.; Dechkovskaia, A. M.; Bullman, S. L.; Khan, W. A.; Abou-Donia, M. B. Exposure to Pyridostigmine Bromide, DEET, and Permethrin, Alone and in Combination Causes Sensorimotor Performance Deficit and Cholinergic Alterations in Rats. *The Toxicologist* **2001**, *60*, 376.
- 75) Kim, M. K.; Lee, C. H.; Kim, D. D. Skin Permeation of Testosterone and its Ester Derivatives in Rats. *Journal of Pharmaceutics and Pharmacology* **2000**, *52*, 369-375.
- 76) Kai, T.; Mak, V. H. W.; Potts, R. O.; Guy, R. H. Mechanism of Percutaneous Penetration Enhancement: Effect of n-Alkanols on the Permeability Barrier of Hairless Mouse Skin. *Journal of Controlled Release* **1990**, *12*, 103-112.

## BIOGRAPHICAL SKETCH

Lucas Utley was born August 26, 1971 in Dover, DE, to James and Dolores Utley. He and his family moved to Gainesville, FL, in 1975. Lucas attended public schools in Gainesville and graduated from Gainesville High School in 1989. He studied at Florida State University through his sophomore year before returning to the University of Florida. There, he met his wife Kristen in 1992 and they were married three years later. He graduated in 1993 with a Bachelor of Science in interdisciplinary studies/molecular biology. He returned to graduate school in 1995 as a student in the Medicinal Chemistry Department of the University of Florida's College of Pharmacy. He joined Ian Tebbett's lab a year later. Future plans for the Utleys include relocating to a cooler climate, and the starting of a family.